CREEP TESTING ON DIFFERENT SOILS TO BE USED AS FILL MATERIAL

by

İbrahim Burak Özgören

B.S., Civil Engineering, İstanbul Technical University, 1994

Submitted to the Institute for Graduate Studies in
Science and Engineering in partial fulfillment of
the requirements for the degree of
Master of Science

Graduate Program in Civil Engineering

Boğaziçi University

2010

ACKNOWLEDGEMENTS

I would like to express my sincere gratitude to my Professor Erol Güler for his invaluable guidance and help during the preparation and also for his encouragement prior to the presentation of my thesis. Many thanks to my thesis supervisor who gives me a chance to learn about the methods used in this thesis and of course about creep testing.

I would like to thank Dr. Özer Çinicioğlu and Dr. İsmail Hakkı Aksoy for their valuable advises for this study.

My thanks to my family, my mother Nezihe Özgören and my father A. Hamdi Özgören for their understanding and not disturbing me especially during the last period of the thesis preparation, which, I believe would not be formed but for their support and insistence.

I would also like to thank the Laboratory assistants, Hakkı Özhan, Elif Çiçek, Yusuf Eşidir, Cenk Erdurak, Tahir E. Öztürk, Arshiya Abadkon and Technicians Kadir Gündoğdu and Belgin Özgül for their help, support and discussions that made me think I am a part of the laboratory.

My special thanks to Anıl Yıldız, seeing his patience and determination on his own experiments he is handling, makes me believe I would finish this thesis at last, after all those years.

One last and a must acknowledgement I believe goes to BÜDAK and BÜMAK, and to my dear friends being affiliated with these clubs, who make me seize the day , Carpe diem as the saying goes. Without their aid and inner support I would not think of touching even the starting pages this thesis. I would like to thank to Arda Uruluer, Bahadır Sirkecioğlu and Adil Alibaş on behalf of my mountaineer, climber and cavern dweller friends for their enjoying of life aside me, and of course for having the club room at my disposal for three months along with the coldest days of 2009-2010 winter. Thanks guys, I love you all.

ABSTRACT

CREEP TESTING ON DIFFERENT SOILS TO BE USED AS FILL MATERIAL

The aim of this study is started with investigating the optimum backfill material to be used on a geosynthetic reinforced soil retaining structures by means of creep tests, where at some point it turns out to be understanding creep testing and by using the experimental data, investigating some of the properties of soil creep and some factors like time and stress levels which effects creep behaviour on different type of soils.

This study is dealt at laboratory under drained conditions on disturbed clays with high and low plasticity and also greywackes obtained from a construction site in İstanbul. For low plasticity soil kaolinite is used and for high plasticity soil kaolinite is mixed with bentonite under equal proportions to obtain samples. Soils that are compacted under their optimum water contents, consolidated for 28 days. Different loading is applied after the evalution of failure loads for each type of soils by breaking numerous samples on the same consolidation device. Daily data is recorded for vertical deformations and axial strain versus time curves are plotted in accordance with various ASTM standart test methods annexed in the thesis.

As a conclusion, rate of settlement of three different types of soils are investigated throughout creep tests and evaluations with comparisons are included within the results of the thesis.

ÖZET

DOLGU MALZEMESİ OLARAK KULLANILACAK DEĞİŞİK ZEMİNLERDE KRİP DENEYLERİ YAPILMASI

Bu çalışma başlangıçta geosentetik donatılı duvarlarda kullanılacak en uygun dolgu malzemesinin krip testleri vasıtasıyla araştırılması idi, fakat olay bir noktada krip testinin anlamlandırılması ve eldeki deneysel verilerin bazı krip özelliklerini ve değişik tipteki zeminlerde zaman ve gerilme seviyeleri gibi krip davranışına etki eden bazı faktörlerin incelenmesine dönmüştür.

Bu çalışma örselenmiş yüksek ve düşük plastisiteli killerle ve ayrıca İstanbul'da bir inşaat sahasından elde edilen grovaklarla laboratuvarda drenajlı olarak yürütülmüştür. Düşük plastisiteli zemin için kaolin kullanılmış, yüksek plastisiteli zemin için kaolin eşit miktarlarda bentonit ile karıştırılarak numune elde edilmiştir. Optimum su muhtevasında sıkıştırılan zeminler 28 gün boyunca konsolidasyona maruz bırakılmıştır. Her bir zemin için, aynı konsolidasyon aletinde oldukça numune kırılarak elde edilen maksimum yük miktarlarından sonra değişik yüklemeler uygulanmıştır. Düşey oturmaların günlük değerleri kaydedilerek bu tezin ekinde yer alan çeşitli ASTM standart deney metodlarına istinaden eksenel gerilme – zaman eğrileri çizilmiştir.

Sonuç olarak, üç değişik zeminin oturma hızları krip testleri vasıtasıyla incelenmiş ve karşılaştırmalı değerlendirmeler bu tezin sonuçları olarak gösterilmiştir.

TABLE OF CONTENTS

LIST OF FIGURES

LIST OF TABLES

LIST OF SYMBOLS / ABBREVIATIONS

A	Angstrom (10^{-10} m)
C_c	Compression index
C_r	Recompression index
C_v	Consolidation coefficient
C_α	Secondary compression coefficient
$C_{\alpha\varepsilon t}$	Tertiary compression ratio
D	Deviator stress
E	Experimental activation energy
f	Shear force acting on a flow unit
h	Planck's constant
K	Reaction rate constant
k_B	Boltzman constant
Ko	Coefficient of lateral earth pressure
m	Slope of the relationship between strain rate and time
N	Avogadro's Number
R	Universal gas constant
S	Number of flow units
T	Absolute temperature
t	Time
t_1	Reference time
X	Parameter relating activation frequency to strain rate
α	$\lambda / 4 S k_B T$
α'	$\lambda / 2 k_B T$
ΔF	Free Energy of Activation
ΔH	Activation enthalpy ($kJ.mol^{-1}$)
ΔS	Activation entropy ($J.mol^{-1} K^{-1}$)
ΔV	Volume change
∂	Partial differentiation
ε_R	Strain rate

κ	Gradient of swelling line
λ	Gradient of compression line
λ	Distance between equilibrium positions of flow units
μ	Critical state frictional constant
ν	Frequency of activation
B	Bentonite
K	Kaolinite
kN	Kilo Newton
kPa	Kilo Pascal
NE	North East
NW	North West
OCR	Over consolidation ratio
PI	Plasticity index
SE	South East
SW	South West

1. INTRODUCTION

Soil creep is the slowest form of mass movement. The expansion and contraction of the water within soil is the main cause of it. Wetting causes the soil to expand and to move downslope under the influence of gravity.

Creep can also be seen in areas that experience a constant alternation of wetting and drying periods which work in the same way as the freeze/thaw. Frost heave, thermal expansion and contraction of the surface, alternate wetting and drying of the soil can cause soil creep. The freeze lifts particles of soil and rocks and when there is a thaw, the particles are set back down, but not in the same place as before.

Soil creep is a very, very slow form of mass wasting. It's just a slow adjustment of soil and rocks that is so hard to notice unless you can see the effects of the movement. These effects would be things like fenceposts shifted out of alignment, or telephone poles tipping downslope. Another effect is the way a grass covered slope seems to ooze downhill forming little bulges in the soil. This heaving of the soil occurs in regions subjected to freeze-thaw conditions. Gravity always causes the rocks and soil to settle just a little farther downslope than where they started from. This is the slow movement that defines creep.

Soil creep is nearly imperceptible to the naked eye as it is the slowest of all types of mass movement. Soil creep generally occurs in the top few meters of the surface and is accomplished by expansion and contraction of the soil. For instance, when water in the soil freezes the ice pushes soil particles outward perpendicular to the slope. Upon warming, the ice melts and the soil is pulled down slope under the influence of gravity. Over many freeze-thaw cycles soil moves slowly down slope. In many cases one might not be able to tell that soil creep is occurring by just examining the surface. However, trees growing on surfaces undergoing creep will have curved trunks or roots that are curved. Broken retaining walls and curved railroad tracks also indicate creep in action.

Evidence of soil creep includes the formation of terracettes (steplike ridges along the hillside), leaning walls and telegraph poles, and trees that grow in a curve to counteract progressive leaning.

Monitoring is essentially done through observation of the effects of creep. Since the process is so slow, it can only be monitored in terms of flow over long periods of time.

Current methods for estimating the long-term settlement of shallow foundations on frozen soils are reviewed. It is found that, when the distortional creep is the main source of settlement there are some potentially good methods for its prediction.

Creep testing is used mostly for the determination of the stiffness parameters λ^* (gradient of compression line), κ^* (gradient of swelling line), μ^* (critical state frictional constant) and the initial OCR (over consolidation ratio) used in critical state soil mechanics. Especially since the creep behaviour depends on all four parameters, these parameters can be derived from a standard oedometer test, provided that the test has been performed for long enough after applying the load.

Rate Process Theory formulated by Henry Eyring at 1936 and fully explained within the next chapter of this thesis has been used worldwide to describe creep and consolidation behaviour of clays under stress.

2. SOIL CREEP AS RATE PROGRESS

2.1. The Theory of Absolute Reaction Rates and Eyring's Formula

The fundemantal equation of the theory of absolute reaction rates has been developed and adapted for use in the study of time-dependent soil deformations. The results of constant stress tests have established that the basic form of this equation is supported as regards the assumption of a thermally activated creep progress, the predicted relationship between experimental activation energy creep stress and the predicted stress dependence of creep rate. Some modification of the equation is needed, however, to account for the variation of creep rate with time.

The theory of absolute reaction rates, known more commonly as rate process theory, formulated originally by Eyring, 1941, has been used recently by several investigators to describe the creep and consolidation behaviour of clays under stress. Since this theory can be applied to any process involving the time-dependent rearrangement of matter it has the potential for providing a powerful tool for the description and prediction of soil behaviour. Basically Eyring's formula is as follows;

$$K = k_B T / h * \exp(\Delta S / R) * \exp(-\Delta H / RT) \qquad (2.1)$$

where K is the reaction rate constant, k_B is Boltzman constant, T is absolute temperature, h is Planck's constant, R is the universal gas constant, ΔS is the entropy of activation and ΔH is the enthalpy of activation.

According to this formula, a certain chemical reaction is performed at different temperatures and the reaction rate is determined. From the linear form of equation 2.1, the plot of ln (k / T) versus 1/T gives a straight line with slope $-\Delta H/R$ from which the enthalpy of activation can be derived and with the intercept ln (k_B / h) + ΔS/ R from which the entropy of activation is derived. A standart free energy diagram during hydrolysis of a chemical material is given in Figure 2.1 to show the activation entropy and enthalpy value applications on the curve. The dotted curve line gives the free energy of activation for the material.

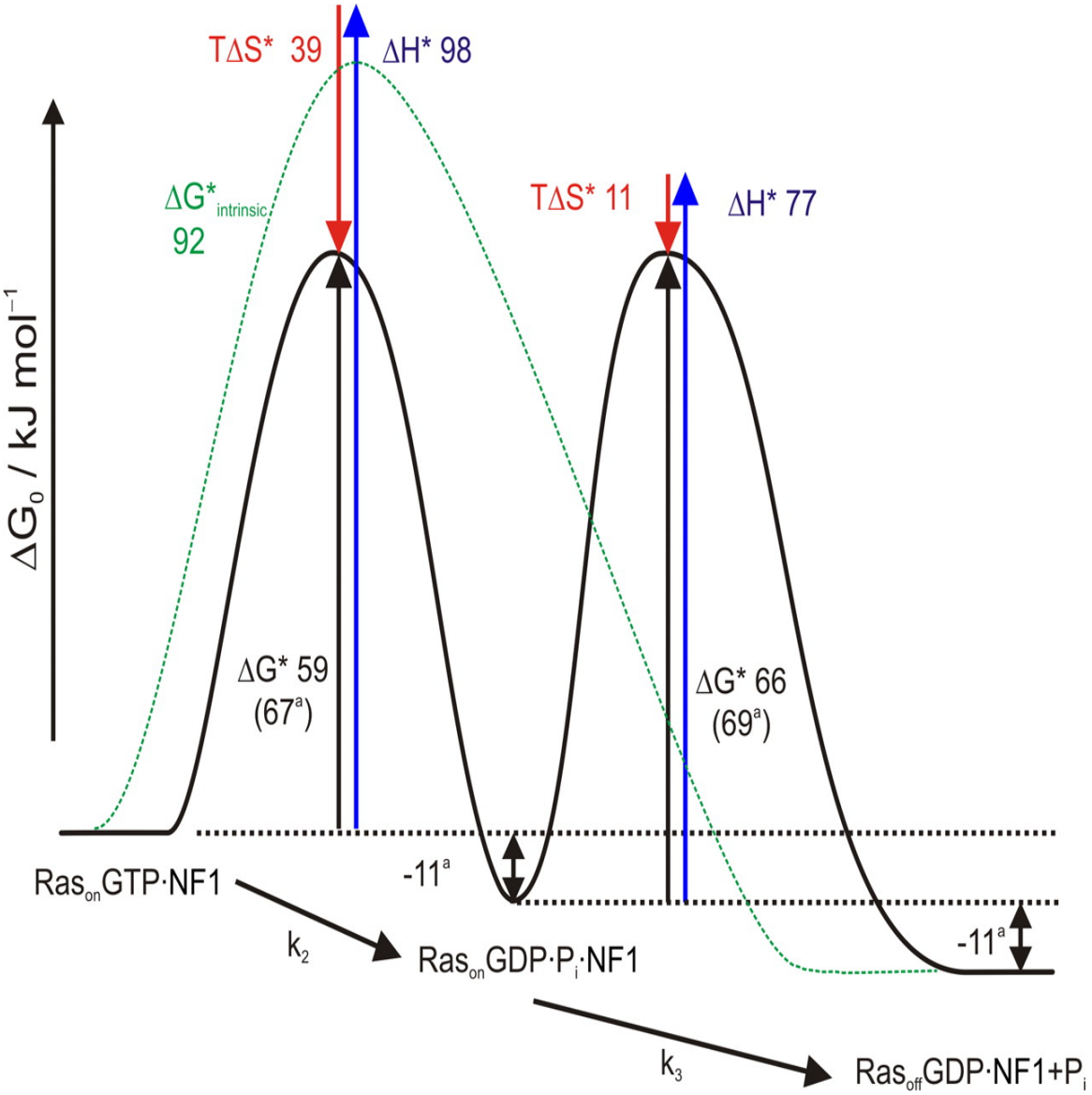

Figure 2.1. The sample free energy diagram for a chemical material

It should be noted, however that, thus far most investigations based on rate process theory have assumed a priori that the basic premises of this theory are valid when applied to soil masses. Rheologic models have been proposed (Murayama and Shibata, 1958, Christensen and Wu, 1964, Abdel-Hady and Herrin, 1966) incorporating dashpots whose parameters are developed from rate process theory, which give a reasonably accurate description of the creep, stress relaxation and consolidation behaviour of clays under some range of loadings. This has been taken as evidence that the basic premises of the theory are correct. Unfortunately, it is possible that the correlation may be due only to the mathematical consequences of the arbitrarily chosen arrangement of springs and dashpots.

The simple relationships found by Singh and Mitchell in 1967, and illustrated in Figures 2.2 and 2.3. for the creep behaviour of a variety of clays. These graphs represent results from constant stress creep tests on undisturbed San Fransisco bay mud. The findings of Singh and Mitchell further showed that the creep behaviour cannot be predicted using simple combinations of linear springs and non-linear dashpots derived from rate process theory.

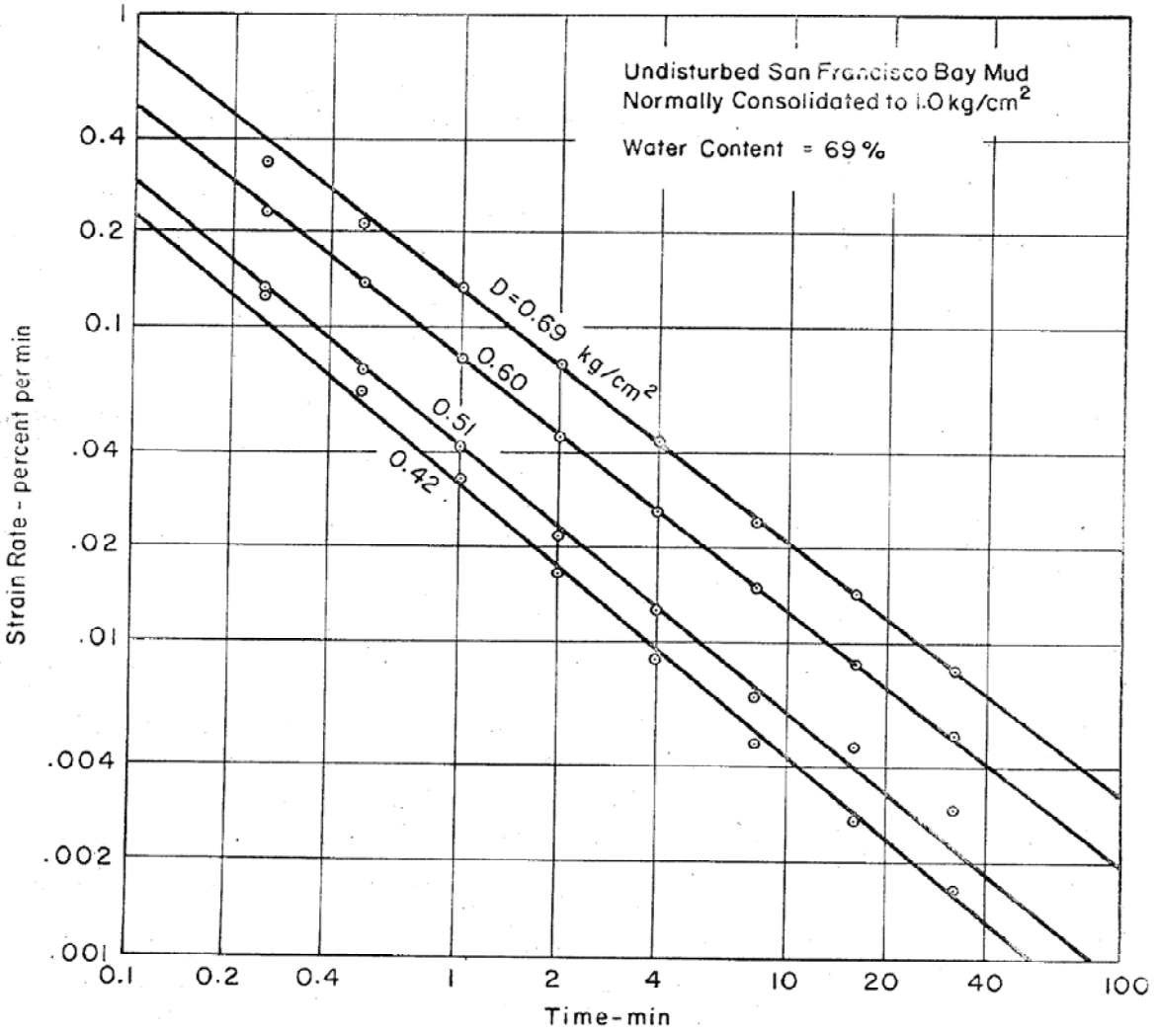

Figure 2.2. Strain rate versus time relationships during undrained creep of undisturbed San Fransisco bay mud

In Figure 2.2 we can see that the strain rate decreases with time, at all levels of applied deviator stresses. Non-linear dashpots are the data taken from triaxial creep tests and the linear springs are the calculated values of Eyring's formula which is adapted to soil

deformation and strain rates from energy calculations. Both in Figure 2.2 and Figure 2.3 we can see that the derived calculations from the formula are not exactly matching with the obtained data.

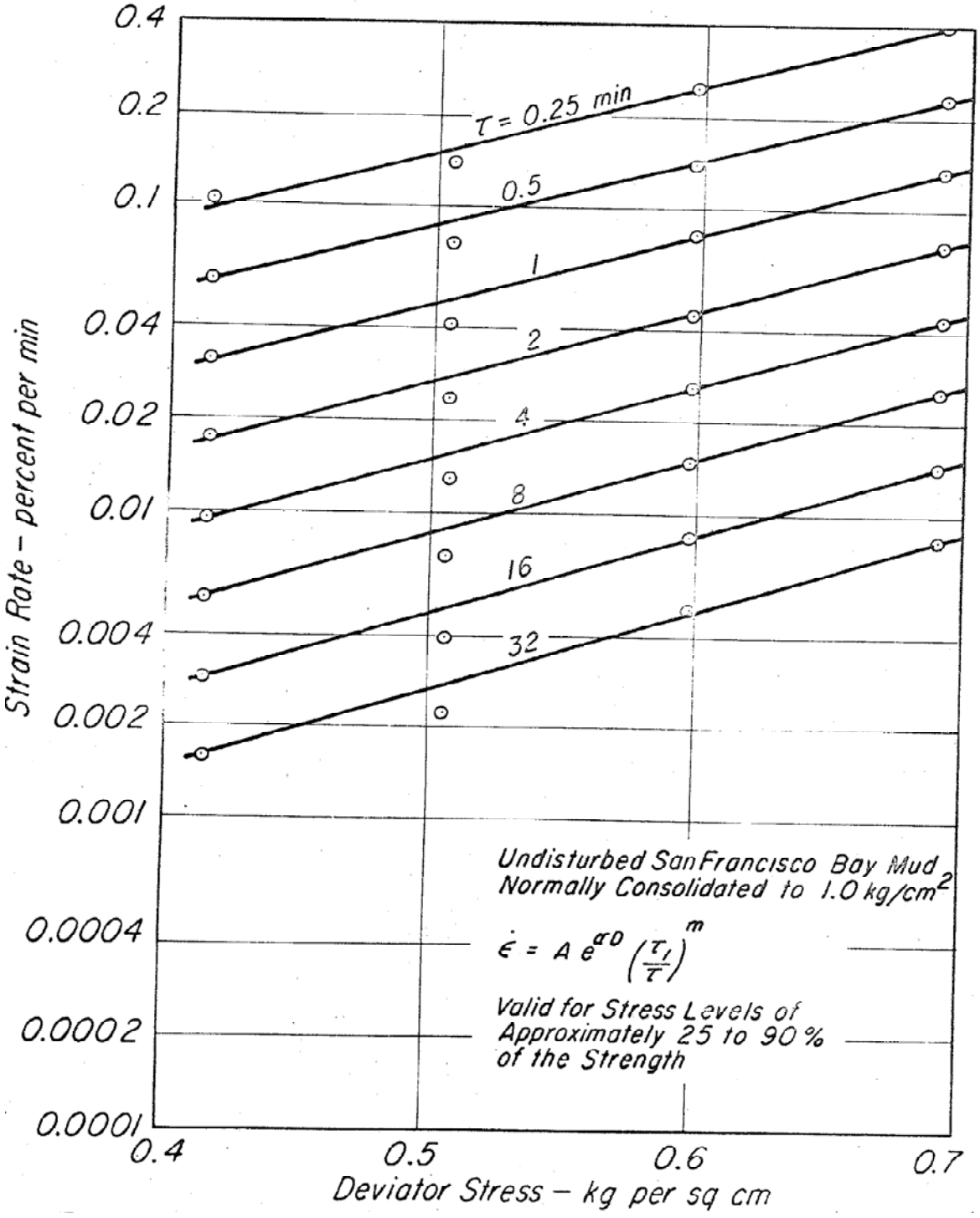

Figure 2.3. Strain rate versus stress relationships for undrained creep of undisturbed San Fransisco bay mud

2.2. Rate Process Theory Used in Creep Test Studies

Studies of the creep behaviour of soils have been in progress for some time at the University of California. The primary objective this work has been to develop information relating to the fundamental mechanisms of deformation and the nature of interparticle bonding in soils. Rate process theory has been used as the framework within much of the work that has been carried out. In the course of these studies data have been obtained which serve to lend confidence to the application of the theory to studies of deformation in soils.

If a parameter X, relating activation frequency to strain rate, is defined through Eyring's formula, which is a function of the number of flow units in the direction of deformation and the average component of displacement in the same direction due to a single surmounting of the barrier, then the total displacement per unit time will correspond to the rate of strain, $\varepsilon_{R.}$

$$\varepsilon_R = X\, k_B\, T/h * \exp\left(f \lambda /(2\, k_B\, T)\right) * \exp\left(-\Delta F/RT\right) \qquad (2.2)$$

where k_B is Boltzman constant, T is absolute temperature, h is Planck's constant, f is the shear force acting on a flow unit, λ is the distance between equilibrium positions of flow units, R is the universal gas constant, and ΔF is the free energy of activation.

Since this derived equation is adapted from the basic formula, it should have a similar energy diagram as shown in Figure 2.1. The basis of the relationship between equations (2.1) and (2.2) is that the atoms and molecules participationg in a deformation process are constrained from movement relative to each other by virtue of energy barriers separating adjacent equilibrium positions as shown as curve A in Figure 2.4. In the absence of applied potentials to the material, barriers will be crossed with equal frequency in all directions. If, for example, a shear stress is applied to the material, then the barrier heights become distorted as shown as curve B. Minimums in the energy curve are shown displaced a distance δ from their original positions. This represents elastic distortion of the material structure. The value E, shown on the graph is the experimental activation energy.

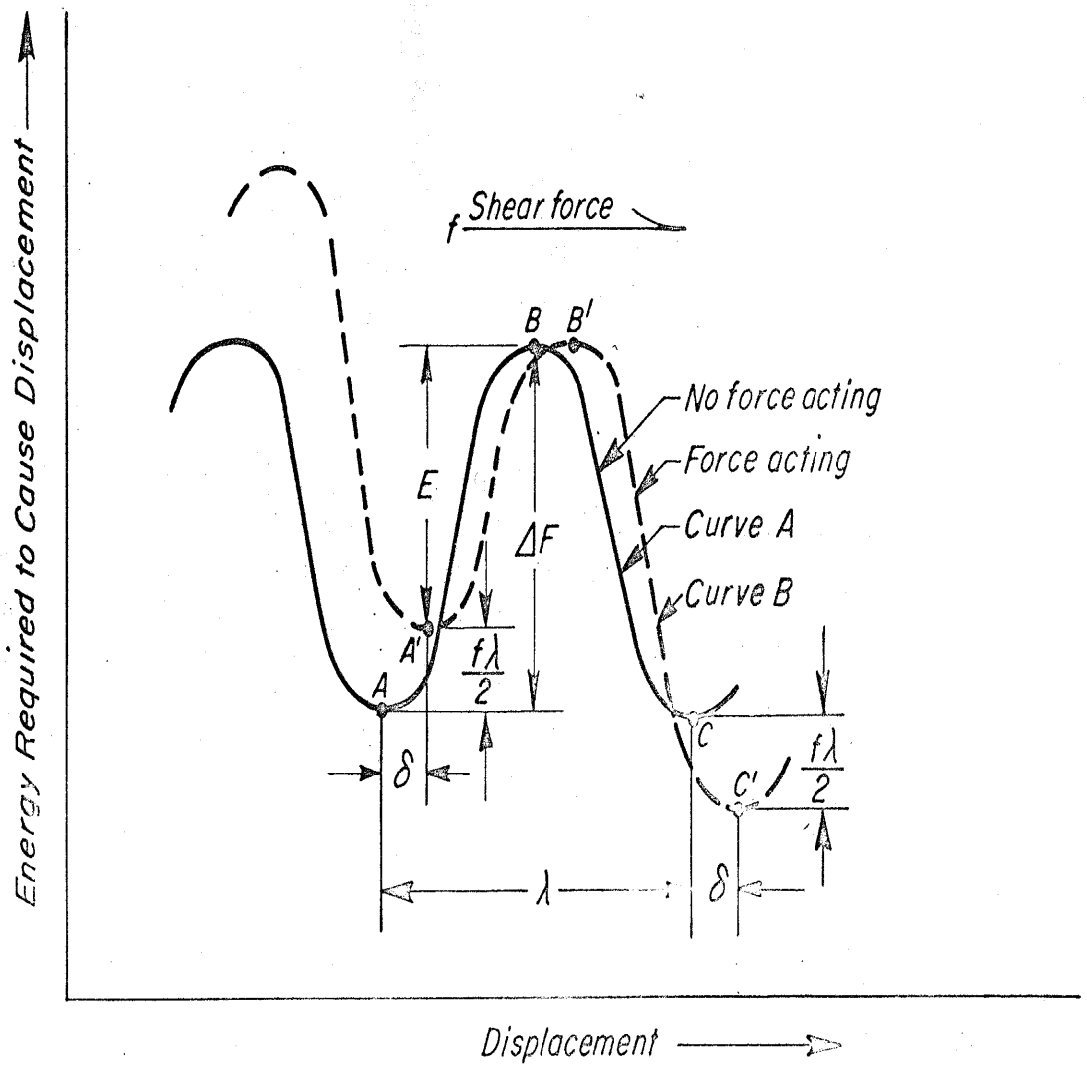

Figure 2.4. Representation of energy barriers separating equilibrium positions

It should be noted that the parameter X may be both time and structure dependent. It is possible to test separately different parts of equation (2.2) in order to determine its applicability to the study of deformation in soils. A number of relevant tests have been made and the test data have been examined directly to support evidence on this dependency.

2.3. Factors Effecting on Creep Behaviour

2.3.1. The Influence of Deviator Stress on Creep Rate

One test of the basic rate equation is possible through investigation of the influence of stress intensity on creep rate. According to equation (2.2) if all other parameters are constant the strain rate should vary with the average stress, f, per flow unit according to;

$$\varepsilon_R = K(t) * \sinh \alpha' f \qquad (2.3)$$

where

$$K = 2X(t)\, k_B\, T/h * \exp [-\Delta F(t)/RT] \qquad (2.4)$$

and

$$\alpha' = \lambda / 2\, k_B\, T \qquad (2.5)$$

Equations (2.3) and (2.4) are written to include the possibility that both X and ΔF may be time-dependent quantities. Although the basic mechanism of deformation may remain the same on an atomic scale, throughout the creep process, it is reasonable to expect that changes in soil structure due to changes in particle orientations and interparticle forces may cause variations in the activation energy, ΔF, and the parameter X.

Figure 2.5 shows the variation of the strain rate to logarithmic scale as a function of deviator stress intensity for unconfined undrained triaxial creep tests on remolded illite. For these tests identical specimens were consolidated isotropically under a stress of 2.0 kg per sq. cm., or about 82% of the compressive strength at the start of the creep test, and for any given time after the start of creep, that the variation between creep rate and deviator stress agrees well in form with the prediction of equation (2.3). At values of deviator stress greater than 1.4 kg per sq. cm. the creep rate increases more rapidly with increase in stress than predicted by equation (2.3). Physical limitations on the strength of the material are responsible for this, since at these high stresses the clay is on the verge of failure and strain rates accelerate rapidly.

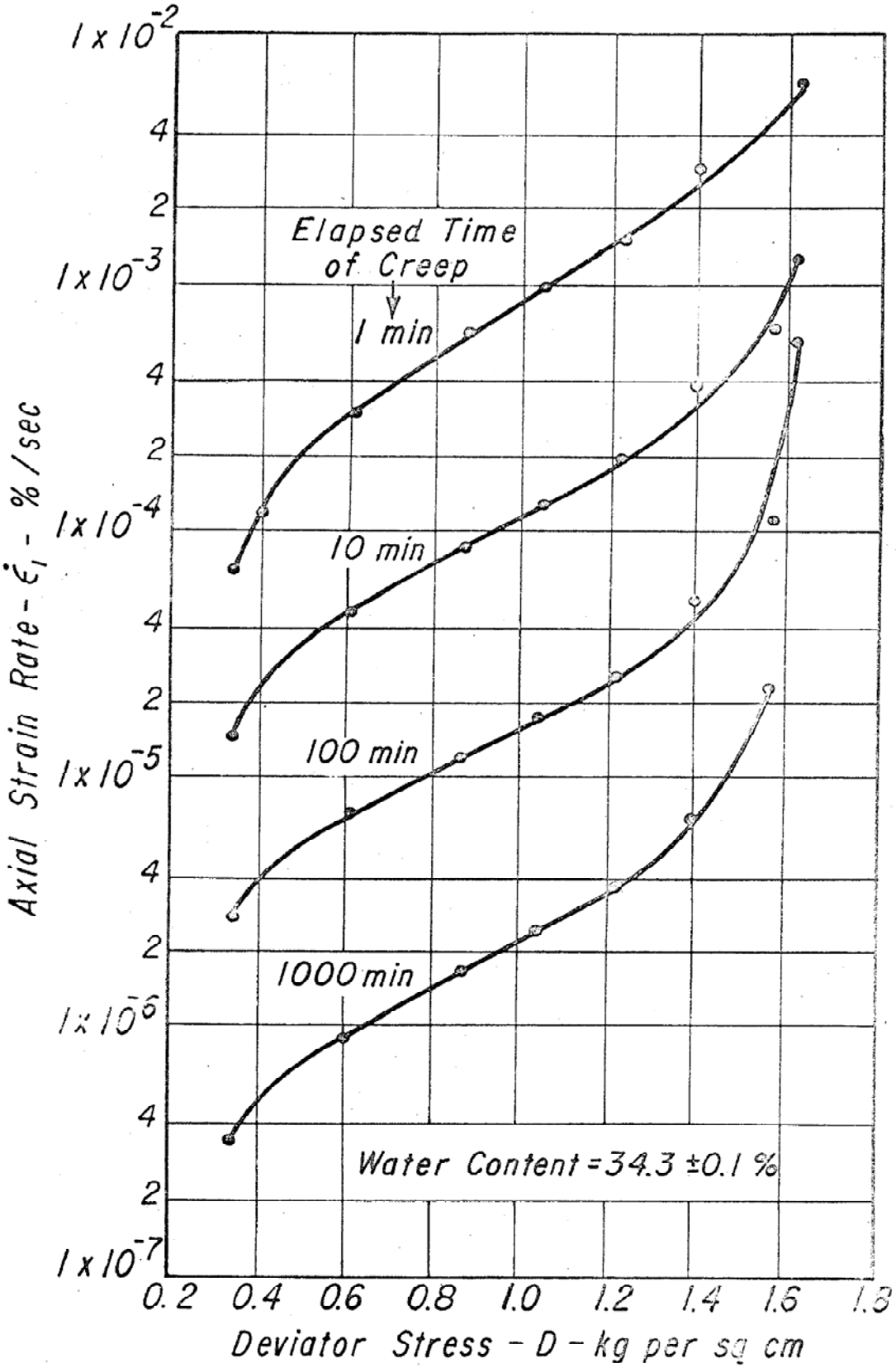

Figure 2.5. Variation of strain rate with deviator stress for undrained creep of illite

In addition to the data for saturated illite shown in Figure 2.5., similar relationships for dry illite, undisturbed normally consolidated (Fig. 2.3.) and overconsolidated San Francisco bay mud, and for remolded San Francisco bay mud have been found, all tested in undrained creep. Figure 2.6 presents the results of triaxial creep tests on undisturbed Osaka alluvial clay (Murayama and Shibata, 1958) and the results of drained triaxial creep tests on undisturbed London clay (Bishop, 1966) are shown in Figure 2.7. Also Andersland and Akili have also observed a linear relationship between logarithm of strain rate and creep stress for frozen soils at high stresses.

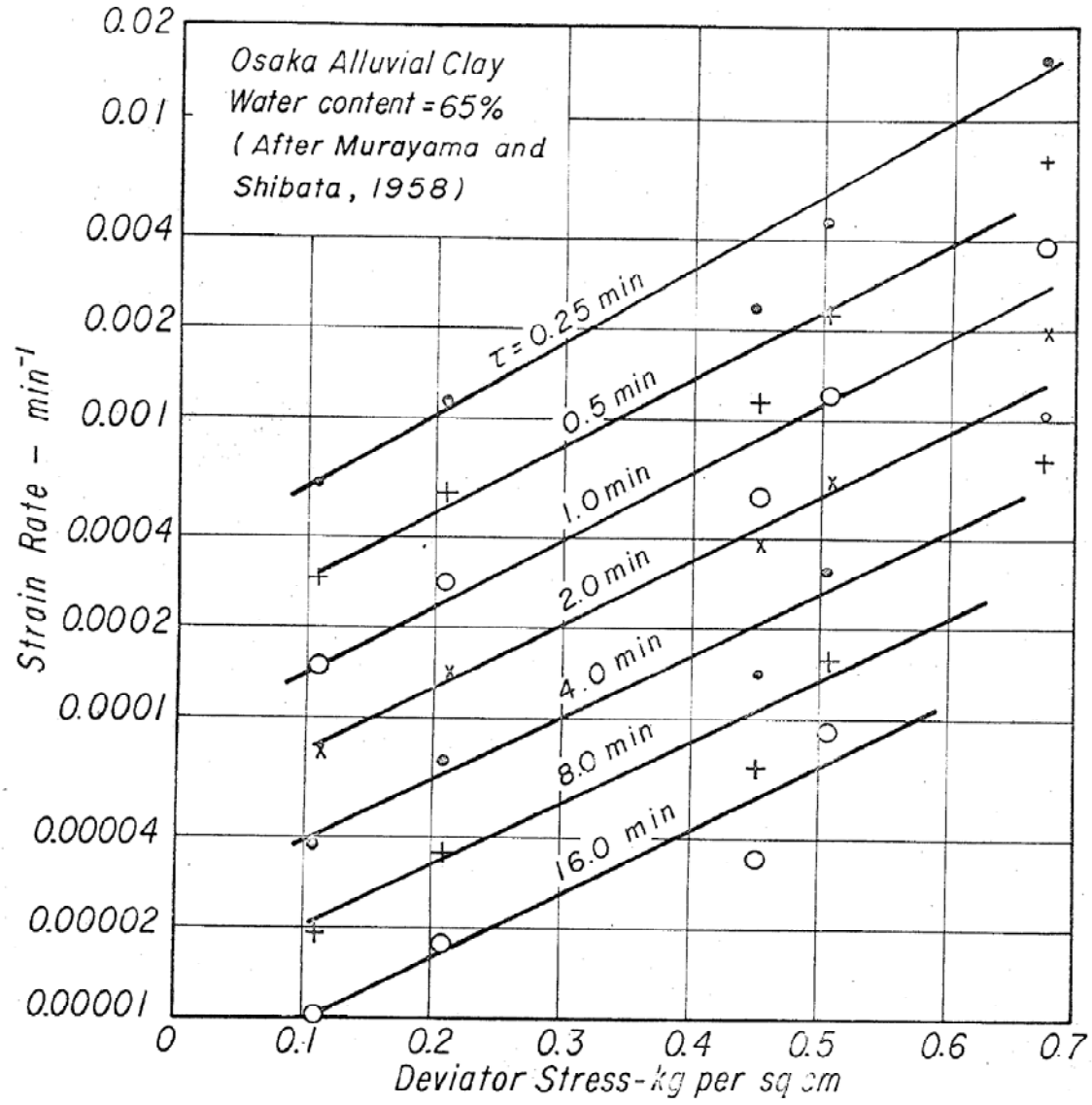

Figure 2.6. Influence of stress level on strain rate during creep of Osaka clay

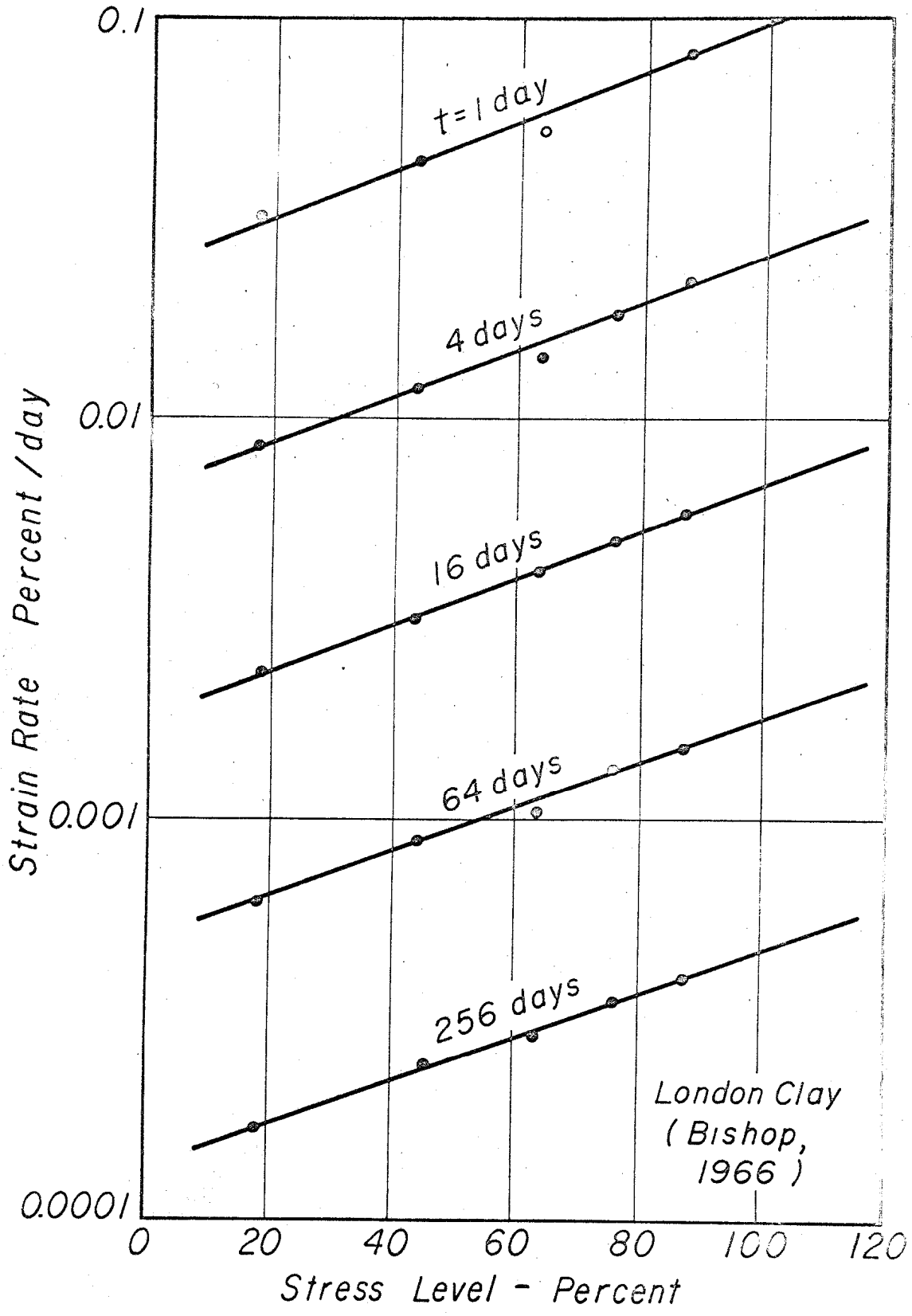

Figure 2.7. Influence of stress level on strain rate during creep of London clay

2.3.2. The Time Dependence of Creep Rate

The time-independent character of the dependence of creep rate on stress is clearly shown by Figures 2.3., 2.5., 2.6. and 2.7. The data show, however, that at any given stress the creep rate decreases in a regular manner with time. The nature of this relationship is more clearly shown by Figure 2.8., which gives the variation of strain rate with time for creep of illite, where they were consolidated isotropically under a stress of 2.0 kg per sq. cm., or about 82% of their failure loading. Thus the shown deviator stresses are between 20% and 60% of their failure loading. The regular nature of relationships of the type shown by Figures 2.5 and 2.8 has been discussed in detail by Singh and Mitchell, 1967, and phenomenological equations have been proposed for the description of creep deformation over the range of stresses of engineering interest.

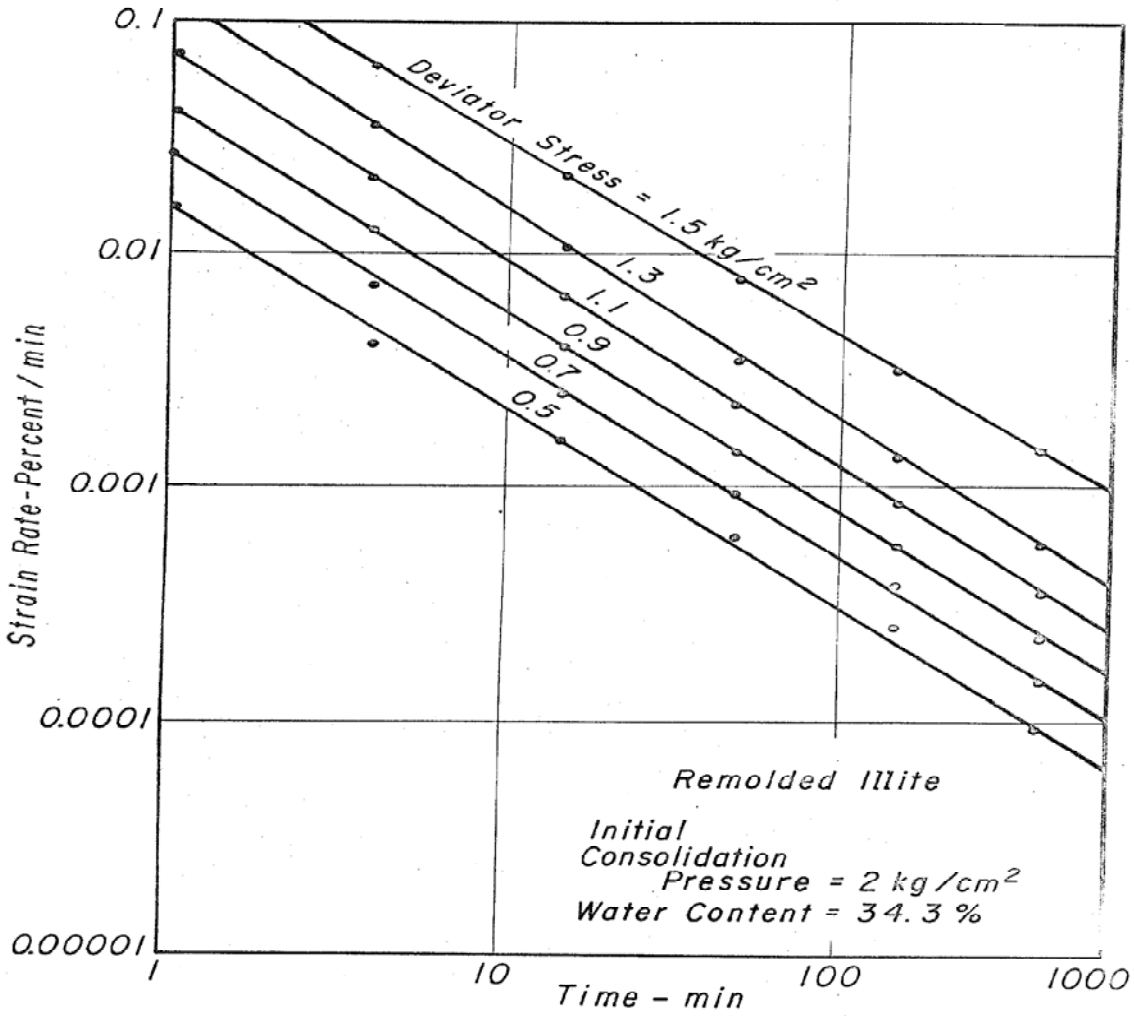

Figure 2.8. Influence of time on strain rate during creep of remolded illite

The basic form of equation (2.2) as regards the assumption of a thermally activated creep process, the relationship between experimental activation energy and deviator stress and the predicted stress dependence of the creep rate would appear to be supported by the data presented above. It is clear however that equation (2.2) cannot properly describe creep behaviour unless it is modified to account for the regular decrease in creep rate with time according to equation (2.4) as shown below,

$$K(t) / 2 = X(t)\, k_B\, T/h * \exp [-\Delta F(t)/RT] \qquad (2.6)$$

It may be deduced from plots of the type shown in Figures 2.5. through 2.8. that K(t) / 2 may be given by (Singh and Mitchell, 1967)

$$K(t) / 2 = A(t_1 / t)^m \qquad (2.7)$$

where A is the strain rate at some arbitrarily chosen reference time t1 and D=0 (deviator stress) and m is the negative of slope of the relationship between logarithm of strain rate and logarithm of time. It has been found for all data examined thus far that $0.75 < m < 1.0$.

Unfortunately it has not yet been possible to account completely for this time-dependence of the creep rate in quantitative physical terms relating to the rate process model for behaviour. It is reasonable to conclude, however, that it is a function of changes in the microstructure which influence the parameters X and ΔF as creep proceeds. Further discussion is given by Mitchell, Singh and Campanella (1967). Thus for the study of general relationship between stress, creep strain rate and time and for the study of the parameter α it would be appropriate to use the following equation,

$$K(t) / 2 = A(t_1 / t)^m \qquad (2.8)$$

where α is defined as,

$$\alpha = \lambda / 4\, S\, k_B\, T \qquad (2.9)$$

2.3.3. The Effect of Temperature on Soil Creep

An additional test of equation (2.2) is to examine the response of the creep rate of a soil to variations in temperature. Noting that the universal gas constant, R, and Boltzmann's constant, k_B, are related according to,

$$k_B = R / N \tag{2.10}$$

Where N is Avogadro's number (6.02×10^{23}), equation (2.2) can be written as,

$$\varepsilon_R = X\, k_B\, T/h * \exp\left[-(\Delta F - f\lambda N/2)/RT\right] \tag{2.11}$$

or can be simplified as,

$$\varepsilon_R = X\, k_B\, T/h * \exp\left(-E/RT\right) \tag{2.12}$$

where E is the experimental activation energy, given by,

$$E = \Delta F - \frac{f\lambda N}{2} \tag{2.13}$$

If X and E are independent of temperature, then from equation (2.12),

$$\left[\partial \ln (\varepsilon_R / T)\right] / \partial (1/T) = - E / R \tag{2.14}$$

Thus if identical specimens are subjected to creep tests under the same stress intensity but at different temperatures, then there should be a linear variation between (ε_R/T) and (1/T) having a slope of –E/R. In order to test this prediction a series of constant stress creep tests were run on identical samples using the controlled-temperature triaxial apparatus described by Mitchell and Campanella (1964). An obvious procedure might be able to test identical specimens under the same creep stress but at different temperatures. This type of tests is impratical, however, for the following reasons.

Since strain rates change rapidly with time after the start of creep it is likely that structure and effective stresses also change rapidly, and these variations may be different for different temperatures. Thus identical structures are only likely to exist at the the instant creep process is initiated, and even in this case there is some question that samples having different temperatures could have the same structure. Furthermore strain rates are very difficult to determine accurately at the instant of load application.

In order to overcome these difficulties and to enable determination of creep rates at two temperatures under conditions of essentially the same structure, thus minimizing effects of variations in X and E itself with time of creep, Dorn's method was used. This method was originally proposed for the determination of the activation energy for creep of metals (Tietz and Dorn, 1956). By this procedure the specimen is permitted to creep under a constant deviator stress at temperature T_1. The temperature is then increased rapidly to T_2 while the deviator stress is maintained constant. The strain versus time behaviour for this type of test is shown in Figure 2.9. and a comparison can be made between the strain rates ε_{R1} and ε_{R2} pertaining to temperatures T_1 and T_2, at the instant of temperature change.

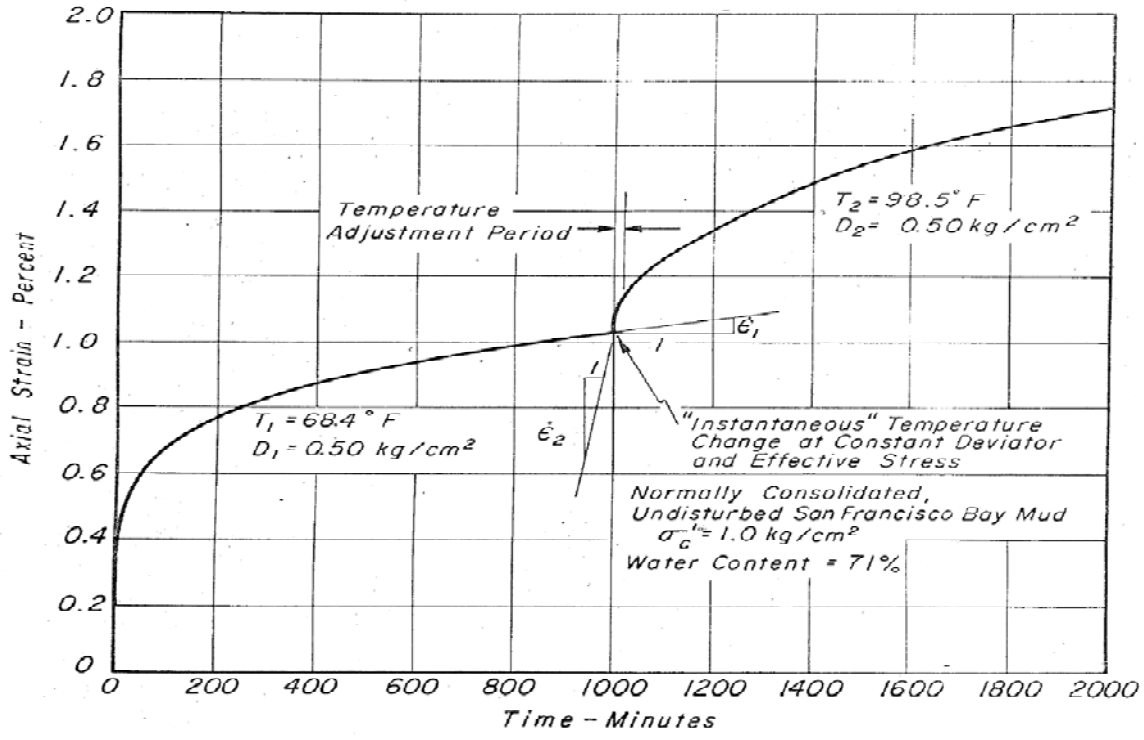

Figure 2.9. Axial strain rate versus time for creep test with rapid temperature change of undisturbed San Fransisco bay mud

Another aspect of importance in connection with tests of this type is that it is impossible to change the temperature of clay without causing either a volume change or an effective stress change (Campanella and Mitchell, 1967).

Tests have shown, e.g., Mitchell and Campanella, 1964, that during undrained creep of a fully saturated clay the application of the creep stress causes an immediate increase in pore water pressure but that after a relatively short time further changes in pore pressure with creep are very small. Thus the test was started under undrained conditions until the pore water pressure was essentially constant with time, and then converted to drained conditions. A typical result from this type of test is shown in Figure 2.10.

It may be seen from Figure 2.10. that when the temperature change was made under undrained conditions the pore pressure approximately doubled. On the other hand for the drained test the temperature change resulted in a volume change of only about less than 0.6% of the sample volume of 90cc. The considerably greater amount of creep observed for the undrained specimen after the temperature change would be expected because of the greatly reduced effective stress caused by the large pore water pressure increase. The factors influencing the magnitudes of pore pressure and volume change associated with temperature changes are discussed in detail by Campanella and Mitchell, 1967.

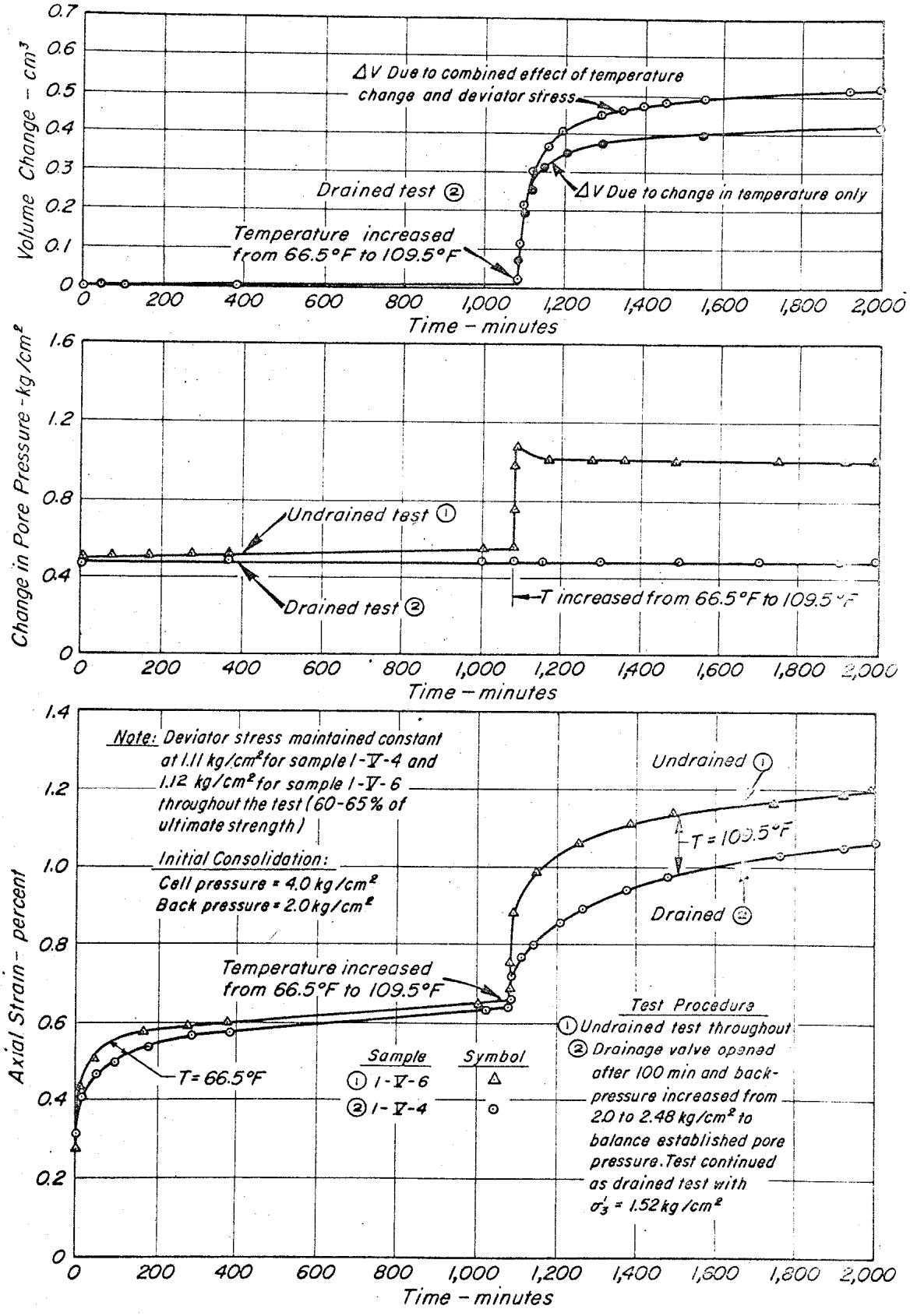

Figure 2.10. The effect of temperature on the creep behaviour of saturated remolded specimens of illite tested under drained and undrained conditions

3. CLAY

3.1. Clay Definition

Clay is used as a rock term and also as a particle-size term in the mechanical analyses of sedimentary rocks, rocks, etc. In general the term clay implies a natural, earthy, fine-grained material which develops plasticity when mixed with a limited amount of water. By plasticity, it is meant that the property of the moistened material to be deformed under pressure application, with the deformed shape being retained when the deforming pressure is removed. Chemical analyses of clays show them to be essentially silica, alumina and water, frequently with quantities of iron, alkalies and alkaline earths.

As a particle-size term, the clay fraction is that size fraction composed of the smallest particles. The maximum size of the particles in the clay size grade is defined differently in deifferent disciplines. In geology the tendency has been to follow the Wentworth 1922, scale and to define the clay grade as material finer than about 4 microns. In soil investigations, the tendency is to use 2 microns as the upper limit of the clay size grade. Although there is no sharp universal boundary between the particle size of the clay minerals and nonclay minerals in argillaceous sediments, a large number of analyses have shown that there is a general tendency for the clay minerals to be concentrated in a size less than 2 microns, or that naturally occurring larger clay-mineral particles break down easily to the size when the clay is slaked in water. Also such analyses have shown that the nonclay minerals usually are not present in particles much smaller than 1 to 2 microns. A separation at 2 microns is frequently about the optimum size for the best split of the clay-mineral and nonclay-mineral components of natural materials. There is, therefore, a fundamental reason for placing the upper limit of the clay size grade at 2 microns.

Clays contain varying percentages of clay-grade material and therefore, varying relative amounts of nonclay-mineral and clay-mineral components. Many materials are called clays in which the clay grade and clay-mineral component make up considerably less then half the total rock. In such materials the nonclay is frequently not much coarser than the maximum for the clay grade, and the clay-mineral fraction may be particularly

potent in causing plasticity. In general fine-grade materials have been called clay so long as they had distinct plasticity and insufficient amounts of coarser material to warrant the appellations silt or sand. If particle size analyses are made, the term clay would be reserved for a material in which the clay grade dominates. However, names have been and are applied most frequently solely on the basis of the appearance and bulk properties like plasticity of the sample.

3.2. Factors Controlling the Properties of Clay Materials

The factors which control the properties of clay materials or the attributes which must be known to characterize completely a clay material may be classified as follows:

3.2.1. Clay Mineral Composition

This refers to the identity and relative abundance of all the clay-mineral components. Since certain clay minerals which may be present in very small amounts may exert a tremendous influence on the attributes of a clay material, it is not adequate to determine only the major clay-mineral components. Thus only a 5% amount of montmorillonite in a clay is likely to provide a material very different from another clay with the same composition in all other ways except montmorillonite. In order to make complete clay-mineral determinations, it is frequently necessary to fractionate the clay grade to concentrate minor constituents so that adequate analytical data can be obtained. Fortunately such a concentration can often be attained because the various clay minerals frequently occur in particles of different sizes or break down easily in water to particles of different size. Also the clay minerals must be determined in their natural state. For example, care must be taken that the analysis will reveal the natural hydration state of the mineral and their ion exchange composition.

3.2.2. Nonclay Mineral Composition

This refers to the identity of the nonclay minerals, their relative abundance, and the

particle-size distribution of the individual species. Calcite, dolomite, large flakes of mica, pyrite, feldspar, gibbsite and other minerals are very abundant in some clay materials.

Nonclay minerals in clay materials tend generally to be concentrated in particles coarser than about 2 microns. There are, however, materials in which they are much finer grained. Many clay materials contain fine iron oxide or hydroxide, which acts as a pigment.

3.2.3. Organic Material

This refers to the kind and amount of organic material contained in clay material. In general the organic material occurs in clay materials in two ways: it may be present as discrete particles of wood, leaf matter, spores, etc., or it may be present as organic molecules absorbed on the surface of the clay-mineral particles. The discrete particles may be present in any size from large chunks easily visible to naked eye to particles of colloidal size which act as a pigment in the clay-mineral material.

Total amount of organic material can be determined simply by readily available standard analytical procedures. Values may be obtained from the difference between total loss on ignition and determination of loss of water, sulphure and other inorganic volatiles which are not precise but are usually adequate. Differential thermal analyses provide a crude determination of amount of organic material gives a dark gray or black color and organic content. A very small amount of organic material may have a very large pigmenting effect.

3.2.4. Exchangeable Ions and Soluble Salts

Some clay materials contain water-soluble salts which may have been entrained in the clay at the time of accumulation or may have developed subsequently as a consequence of weathering or alteration processes, as in the oxidation of pyrite to produce sulfates. It is frequently necessary to wash out the soluble salts before other attributes of the material are studied. Some salts may act to flocculate the clay, so that it cannot be dispersed for particle-size analyses or for fractionation preliminary to clay-mineral analyses until the

salts are washed out. Common water-soluble salts found in clay materials are chlorides, sulphates and carbonates of alkalies, alkaline earths, aluminum and iron.

Clay minerals and some of the organic material found in clay materials have significant ion-exchange capacity. The ion-exchange capacity of the clay minerals and the organic components, as well as the identity and relative abundance of the exchangeable ions, is extremely important attributes of clay materials.

3.2.5. Texture

The textural factor refers to the particle-size distribution of the constituent particles, the shape of the particles, the orientation of the particles in space and with respect to each other and the forces tending to bind the particles together.

Some knowledge of the particle-size distribution of the coarser grains can be obtained quickly by microscopic examinations and detailed determinations can be made by sieving and wet sedimentation methods. Fine-grained particles require wet methods and this applies to the clay-mineral fraction.

3.3. Clay-Water System and Nature of Adsorbed Water

The nature of the low-temperature water and the factors that control its characteristics are of great importance since they largely determine the plasticity, bonding, compaction, suspension and other properties of clay materials, which in turn frequently control their commercial utilization. Thus, an understanding of this low-temperature water in relation to clay minerals must precede an understanding of the plasticity and many other properties of clay materials.

The water holds directly on the surfaces of the clay particles is in a physical state different from that of liquid water. It has frequently been considered to be denser and more viscous than ordinary liquid water. Specific characteristics of this water which delimit it from ordinary water would probably be restricted ordinarily to relatively short distances

from the clay-particle surfaces, distances generally of the order of three to ten molecular layers of water, i.e., 8 to 28 A. The possible thickness of the non-ordinary water can vary a good deal even for a given clay mineral and the transition from non-ordinary water to ordinary water can be abrupt or gradual, depending on factors that will be considered presently.

It appears certain that the possible thickness of the non-ordinary or so-called nonliquid, water is relatively small on irregular surfaces, such as those around the edges of clay-mineral particles, and relatively large on the flat surfaces of clay minerals. The film of non-ordinary water is best developed and appears to reach its greatest thickness on the basal plane surfaces of the expanding-lattice minerals of the montmorillonite group. It follows that the water forming only a thin film on the surface of the pores and where adjacent clay-mineral particles come together.

The initially absorbed water on the basis of the dipole character of the water molecule; the latter possesses positive and negative charges, the centers of which do not coincide. Since the surface of the clay particle is normally negatively charged, the positive ends of the water molecules are considered to lie initial layer of water is believed to consist of water molecules all oriented in the same direction. According to this concept, the first layer of oriented-dipole water molecules forms another surface of negative charges on which can be built another layer of completely oriented water molecules. This process of building up layers could be continued indefinitely were it not for the fact that the water molecules possess thermal energy and tend to be in a state of continuous motion. In accordance with classical concepts of colloidal theory, the motion due to thermal energy will oppose the regular orientation. Therefore, at any given instant and at a certain distance from the surface, some of the molecules will be oriented at right angles to the surface. An instant later these molecules will have moved, but others will have become oriented in their place. At the actual clay-mineral surface the molecules will be highly oriented and the degree of orientation will decrease going outward, as the relative effect of thermal movement becomes greater. Macey 1941, has pointed out difficulties encountered by this concept, particularly in view of the facts that the clay-mineral surface is not uniformly charged plane and that the water molecules strictly do not act as little rods with positive and negative ends.

Earlier investigations, mainly by Bernal and Fowler, 1933 and Bernal and Megaw, 1935, of the hydrogen bond and of the distribution of charges about a water molecule led Hendricks and Jefferson, 1938, to a concept of the nature of the initially absorbed water that is based on an orientation of water molecules with a structure tied to the configuration of the oxygens or hydroxyls in the basl surface layers of the unit cells of clay minerals. In the language of Hendricks and Jefferson, 1938, a water layer is composed of water molecules joined into hexagonal groups of an extended hexagonal net. This arrangement is partly a result of a tetrahedral distribution of charge about a water molecule; two corners of tetrahedron being occupied by hydrogen atoms and the other two corners by an excess of electrons.

Each side of the hexagon must correspond to a hydroxyl bond, the hydrogen bond of one water molecule being directed toward the negative charge of a neighboring molecule. One-fourth of the hydrogen atoms or a hydrogen atom of half of the water molecules are not involved in bonding within the net. The net is tied to surface of the clay minerals by the attraction between those hydrogen atoms not involved in bonding within the net and the surface oxygen layer of the clay-mineral unit. When the surface of the clay mineral contains hydroxyl groups like halloysite and kaolinite, part of the hydroxyls are free for bonding through hydrogen to oxygen atoms in the water layer.

Stability of the layer of water molecules arises from the geometrical relationship to the oxygen atoms or hydroxyl groups of the silicate frame-work. Presence of the first layer would favor the formation of a second layer, and the water structure would thus be propagated away from the clay-mineral surface. At some distance from the surface dissociation pressure of successive layers, considerede as hydrates, would finally approach the vapor pressure of water at the temperature of observation and the oriented water net would cease to develop.

In the Hendricks and Jefferson, 1938, configuration every other water molecule lies about over the oxygen of the surface layer of the three layer clay minerals. Since half of the water molecules have hydrogen available for vertical bonding, the directly superimposed oxygens and water molecules may be assumed to be tied together through these hydrogen bonds. As successive molecule layers develop, the exterior layer can be tied to the layer

next below by a hydrogen from every other water molecule. According to this scheme no hydrogens would be available for tying together series of water layers growing outward from two neighboring clay-mineral surfaces, unless the directly adjacent water layers of two water envelopes were tied together by relatively fewer bonds. A plane or planes of relatively weakly bonded water molecules would exist, therefore, at the junction of two water envelopes.

Hendricks and Jefferson, 1938, concept of structure of the adsorbed water has been criticized by Hoffmann and Hausdorf, 1942, Mackenzie, 1950, and Walker, 1949, because it neglects the probable influence of adsorbed cations, which in many cases are to be found directly on or at least very close to the oxygen surface on which the water configuration develops. Further, some of these cations are hydrated and, therefore, would probably significantly influence the arrangement of the water molecules directly adjacent to them. Mackenzie, 1950, has particularly emphasized this point and has indicated that the matter of cation hydration would be particularly important in the part of the adsorbed water net closest to the clay-mineral surfaces. In the case of montmorillonite, there would be about one monovalent cation for each two hexagonal configurations of water in the first molecular water layer. According to Mackenzie, there is a space problem in fitting such a number of ions into the water net. Mackenzie presents computations of the energy of hydration of the sheet surface of montmorillonite carrying various ions; these data are in accord with his suggestion that, at low water contents, water adsorption depends primarily on the exchangeable ion present, the sheet surface being of subsidiary importance. Others, notably Williamson, 1951, have objected to Hendricks and Jefferson, 1938 concept, because of their feeling that the adsorption forces are strong enough to cause a dense packing of at least, the initially adsorbed water molecules.

Macey, 1941, arguing from the similarity between the structure of ice and of the oxygen atoms exposed at a sheet surface of the layer clay minerals, has postulated that the initially adsorbed water has the structure of ice. Macey considers that it fits on top of the oxygen net of the basal plane of the three-layer clay minerals. The fit of the water molecules with the oxygen net as suggested by Macey is different from that suggested by Hendricks and Jefferson. According to the Macey concept, the distance between oxygens in the water layer would be 4.52 A, and the packing would be even looser than that

suggested by Hendricks and Jefferson, 1938. There would be three molecules of water per unit cell per molecular layer. Such loose packing of water in a given layer would be predicated on hydrogen binding to additional water not in the layer under consideration. In the structure of ice, other water molecules would be just out of the plane in contact with the silicate structure and there is no epitaxial arrangement between them and the silicate surface. In Hendricks and Jefferson concept, the ice structure is stretched so that the offset water molecules come into the same plane and there is no change in the hydrogen binding. Also the stretch permits a complete epitaxial arrangement of all the water molecules and the silicate surface. The same objections raised against Hendricks and Jefferson structure can be raised against Macey structure. However, the space problem caused by the presence of adsorbed cations might be less acute. Forslind, 1948, has reported electron-diffraction data which seem to indicate a structure at least similar to ice in the initially adsorbed water of montmorillonite. Very recently DeWit and Arens, 1950, have published some density measurements that seem to be in agreement with the Macey concept.

Barshad, 1949, has very recently suggested another concept of the nature of the adsorbed water on the basis of careful dehydration determinations. According to him, at very low states of hydration for montmorillonite, the water molecules tend to form tetrahedrons of the lattice. This type of packing would give rise to hexagonal rings of water molecules which are similar to the hexagonal rings of oxygens of the vertices of the linked silica tetrahedrons of the individual silicate sheets. The packing in this configuration would be loose, as there would be only four molecules of water per unit cell per molecular layer and the height added for a single layer of water molecules would be 1.78 A according to Barshad.

3.4. Overconsolidated Clays

Many soils have been subject to high stresses at some stage in their depositional history. Such stresses cause the porosity of the soil to decrease. Later, these high stresses may be alleviated or entirely removed through the erosion of overlying later sediments. This process is termed ‘overconsolidation’ and is an early stage in the lithification of sediment. The terms ‘soil’ and ‘rock’ are used here in quite a different manner from that in

which they are used in the pure geological sciences. For an engineer, geological materials are soil until they become so hard that they must be excavated with special tools, wedges, picks, pneumatic and hydraulic drills or blasted with explosives. The overconsolidated clays, silty clays and clay-shales, therefore count as soils, not rocks, in this classification. Yet they are clearly different from the soft sediments of recent age. This kind of soils would be classified as 'normally consolidated' if they had never experienced higher stresses than those to which they are presently subjected.

One major difference between the normally consolidated and overconsolidated soils, apart from consistency or undrained strength, is the presence of fissures in overconsolidated soils. Terzaghi has suggested that clays may be divided into two categories, fissured clays and intact clays. Very stiff clays invariably contain fissures that are filled with small joints or cracks. These stiff clays have such high shearing strength that questions seldom arise regarding to adequacy of their strength to prevent failure. The real problems in such clays occur when water enters the cracks. They have been opened slightly by additional stresses imposed by a change of loading and this leads to slaking and formation of a soft clay matrix within the joint system. Intact clays may be defined as clays which are free of joints and fissures (Taylor, 1948). The occurrence of fissures, which are after all only one category in a wide variety of different discontinuity surfaces in the soil mass, is related to the stress relief element of overconsolidation process. Their genesis is by no means understood, but is no doubt due in some way to differential strains during the initial consolidation and the later swelling as stress is removed. Fissures have a bearing on the shear strength of the soil.

A second major difference is the presence of higher lateral stresses in the ground, which are left 'locked in' as vertical stresses are released. These then give greater stress relief effects if excavations are opened up in the ground.

In addition, the overconsolidated soils inevitably have lower porosities than their normally consolidated counterparts. This leads to their having a stiffer behaviour in respect of deformations under applied load and more dilatant behaviour under shear because of the denser packing of the particles.

Overconsolidation is normally caused by the removal of later sediments but can be caused in other ways, which are overconsolidation by the weight of overlying ice and desiccation. Salt-marsh deposits and river alluvium on the flood plain can be overconsolidated by the strong suction of normal evaporation and these may be supplemented by influence of plant roots. Rapidly accreting sediments may then have several lightly or even strongly overconsolidated horizons in an otherwise normally consolidated profile.

3.5. Grouping and Types of Clays

Depending on the academic source, there are three or four main groups of clays: kaolinite, montmorillonite-smectite, illite and chlorite. Chlorites are not always considered a clay, sometimes being classified as a separate group within the phyllosilicates. There are approximately 30 different types of "pure" clays in these categories, but most "natural" clays are mixtures of these different types, along with other weathered minerals. Since the tests done within the scope of this thesis includes only 2 types of clay, it will be enough to briefly define here these 2 clay minerals only.

3.5.1. Kaolinite

Kaolinite is a clay mineral with the chemical composition $Al_2Si_2O_5(OH)_4$. It is a layered silicate mineral, with one tetrahedral sheet linked through oxygen atoms to one octahedral sheet of alumina octahedra. Rocks that are rich in kaolinite are known as china clay, white clay, or kaolin. The name is derived from Gaoling or Kao-Ling in Jingdezhen, Jiangxi province, China. Kaolinite was first described as a mineral species in 1867 for an occurrence in the Jari River basin of Brazil.

Kaolinite has a low shrink-swell capacity and a low cation exchange capacity (1-15 meq/100g.) It is a soft, earthy, usually white mineral (dioctahedral phyllosilicate clay), produced by the chemical weathering of aluminium silicate minerals like feldspar. In many parts of the world, it is colored pink-orange-red by iron oxide, giving it a distinct rust hue. Lighter concentrations yield white, yellow or light orange colours.

3.5.2. Bentonite

Bentonite is an absorbent aluminium phyllosilicate, generally impure clay consisting mostly of montmorillonite. There are a few types of bentonites and their names depend on the dominant elements, such as potassium, sodium, calcium, and aluminium. As noted in several places in the geologic literature, there are some nomenclatorial problems with the classification of bentonite clays. Bentonite usually forms from weathering of volcanic ash, most often in the presence of water. However, the term bentonite, as well as a similar clay called tonstein, have been used for clay beds of uncertain origin. For industrial purposes, two main classes of bentonite exist: sodium bentonite and calcium bentonite. In stratigraphy and tephrochronology, completely devitrified (weathered volcanic glass) ash-fall beds are commonly referred to as K-bentonites when the dominant clay species is illite.

Much of bentonite's usefulness in the drilling and geotechnical engineering industry comes from its unique rheological properties. Relatively small quantities of bentonite suspended in water form a viscous, shear thinning material. Most often, bentonite suspensions are also thixotropic, although rare cases of rheopectic behavior have also been reported. At high enough concentrations (~60 grams of bentonite per litre of suspension), bentonite suspensions begin to take on the characteristics of a gel (a fluid with a minimum yield strength required to make it move). For these reasons it is a common component of drilling mud used to curtail drilling fluid invasion by its propensity for aiding in the formation of mud cake.

4. GREYWACKES

4.1. Greywacke Definition

Greywacke or Graywacke (German ‘grauwacke’, signifying a grey, earthy rock) is a variety of sandstone generally characterized by its hardness, dark color, and poorly-sorted, angular grains of quartz, feldspar, and small rock fragments or lithic fragments set in a compact, clay-fine matrix. It is a texturally-immature sedimentary rock generally found in Palaeozoic strata. The larger grains can be sand-to-gravel-sized, and matrix materials generally constitute more than 15% of the rock by volume. The term 'Greywacke' can be confusing, since it can refer to either the immature (rock fragment) aspect of the rock or the fine-grained (clay) component of the rock.

The origin of greywacke was problematic prior to the understanding of turbidity currents and turbidites since, according to the normal laws of sedimentation, gravel, sand and mud should not be laid down together. Currently geologists attribute its formation to submarine avalanches or strong turbidity currents. These actions churn sediment and cause mixed-sediment slurries to occur. When this is the case, the rocks may exhibit a variety of sedimentary features. Support for the turbidity current origin is the fact that deposits of greywacke are found on the edges of the continental shelves, at the bottoms of oceanic trenches, and at the bases of mountain formational areas. It also occurs in association with black shales of deep sea origin.

4.2. Greywacke Mineral Composition

Greywackes are mostly grey, brown, yellow or black, dull-colored, sandy rocks which may occur in thick or thin beds along with slates and limestones. They can contain a very great variety of minerals, the principal ones being quartz, orthoclase and plagioclase feldspars, calcite, iron oxides and graphitic, carbonaceous matters, together with (in the coarser kinds) fragments of such rocks as felsite, chert, slate, gneiss, various schists, and quartzite. Among other minerals found in them are biotite and chlorite, tourmaline,

epidote, apatite, garnet, hornblende and augite, sphene, pyrites. The cementing material may be siliceous or argillaceous, and is sometimes calcareous.

As a rule greywackes are not fossiliferous, but organic remains may be common in the finer beds associated with them. Their component particles are usually not very rounded or polished, and the rocks have often been considerably indurated by recrystallization, such as the introduction of interstitial silica. In some districts the greywackes are cleaved, but they show phenomena of this kind much less perfectly than the slates. Some varieties include feldspathic greywacke, which is rich in feldspar, and lithic greywacke, which is rich in tiny rock fragments.

Although the group is so diverse that it is difficult to characterize mineralogically, it has a well-established place in petrographical classifications because these peculiar composite arenaceous deposits are very frequent among Silurian and Cambrian rocks, and are less common in Mesozoic or Cenozoic strata. Their essential features are their gritty character and their complex composition. By increasing metamorphism, greywackes frequently pass into mica-schists, chloritic schists and sedimentary gneisses.

4.3. The Engineering Geological Characteristics of İstanbul Greywackes

Throughout the deep excavations of high-rise buildings located along the axis of Büyükdere Avenue in the city of İstanbul, typically soft rock greywacke, locally known as Trakya formation, is encountered. The Trakya formation is commonly exposed in the European side of İstanbul, especially in İkitelli, Cebeciköy, Şişli, Beşiktaş, Levent and Gaziosmanpaşa.

The term greywacke is used for dark gray, firmly indurated, coarse grained, lithologicaly alternating sandstone, siltstone and claystones, that consist of poorly sorted, angular to sub-angular grains of quartz and feldspar, with a variety of rock and mineral fragments embedded in compact clayey matrix and containing an abundance of very fine grained illite, sericite and chlorite minerals (Eroskay, 1985).

The interrelationships of primary textual characteristics, such as grain size, shape (form, roundness, surface texture), and fabric (grain orientation and grain-to-grain relations) control other properties such as density, porosity, etc. (Boggs, 1987). The relationship between petrographical, mineralogical, chemical and geomechanical properties of this type of rock has been studied by many investigators. They reported significant correlations between geological and geomechanical characterictics of different types of sandstones.

Trakya formation, greywackes, consists of intercalated sequences of sandstone, shale, siltstone and claystone. They are typically dark grey-green or grayish-brown due to weathering. Sandstone is the most abundant rock type in this formation and limestone and conglomerate interbeds or lenses are found between layers. The thickness of the Trakya formation varies between 600-1700 metres (Eroskay, 1985). Greywackes are generally of marine origin and believed to have been deposited by submarine turbidity currents (Pettijohn, 1972). Greenish brown colored andesite dykes, up to 10 m thick, are common in the city and generally follow a NW-SE direction. When they were fresh, they could be easily identified in the field. But in the highly weathered conditions, dykes which were yellowish brown colored could only be differentiated with difficulty from the greywackes (Eroskay, 1985).

The Trakya formation is very intensely folded, faulted, fractured and is also weathered which is well developed along discontinuities. The major structural features of the area are NW-SE and NE-SW trending faults. Dense crack surface developments are observed and rock masses are completely fractured from place to place. Usually, three or four clearly defined major sets of joints are found. Minor sets or random joints also occur in study area. The strike directions of joints are almost NW-SE and NE-SW (Tuğrul and Ündül, 2006).

Petrographical and mineralogical analyses have been used to document the fabric and mineralogical properties of both unweathered and weathered greywackes. Generally coarse and medium grained greywacke sandstones are dominated by angular and sub-angular grains of quartz, and a lesser amount of feldspars (orthoclase and plagioclase), muscovite, chlorite and hematite with a variety of dark rock and mineral fragments. The

quartz grains range from 60% to 75%. The rock fragments are between 8-15%; the muscovite is more than 3%. The cemented materials consisted mainly of clay (sericite, chlorite and illite) and sometimes hematite. They are generally poorly cemented, but have been firmly lithified by compaction and close packing of the sand-size grains (Tuğrul and Ündül, 2006). The above petrographic characteristics classify the rock as lithic wacke according to Dott, 1964. Based on the Wentworth, 1922, scale size classes, the greywackes range from very coarse to coarse sandstone.

The extension of weathering and fracturing controls the physical and mechanical properties of greywacke formations. Weathering of the greywackes decreases gradually and progressively with increasing depth. Physical properties of İstanbul greywackes are given in Table 4.1. Both porosity and water absorption increase and dry unit weight decreases with the increasing weathering grade.

Pore size distribution could be determined using the mercury intrusion technique as the mercury is forced in the specimen and its volume is determined from the displaced fluid volume. During the test, mercury fills up the large pores under low pressure and the small ones under high pressure. The effective porosity values of weathered samples are generally higher than unweathered samples. Changes in pore geometry are caused by the dissolution of some minerals and increase in microfracture density by progression of weathering and new mineral formation (Tuğrul, 1995). The strength of the unweathered and weathered greywackes could be determined on sample cores using the uniaxial compression test. Results of laboratory tests at different locations in İstanbul are given in Table 4.2. The mechanical properties of the greywackes, i.e. strength and modulus, decrease considerably with weathering.

Table 4.1. Physical properties of greywackes in different locations in İstanbul

Weathering	Location	Dry unit weight (kN/m3)	Water absorption (by weight) wa (%)	Total porosity (%)	References
Weathered	Levent (Deep Excavation)	25.6-26.1	3.23-4.12	-	Tuğrul and Ündül (2006)
	Eminönü (Boreholes)	25.8-26.6	3.14-3.73	8.47-10.23	Zarif and Tuğrul (2002)
	Eyüp Tunnel	26.0	2.8	8.0	Erguvanlı (1985)
	Haliç Tunnel	25.9	1.9	-	Erguvanlı (1985)
	Average	**26**	**3.0**	**8.9**	
Unweathered	Levent (Deep Excavation)	26.4-27.3	0.22-1.06	-	Tuğrul and Ündül (2006)
	Eminönü (Boreholes)	26.5-27.7	0.39-1.49	0.95-3.66	Zarif and Tuğrul (2002)
	Eyüp Tunnel	27.2	0.22	2.0	Erguvanlı (1985)
	Dolmabahçe-Baltalimanı	26.5	0.97	-	Erguvanlı et al.(1987)
	Average	**26.9**	**0.7**	**2.2**	

Table 4.2. Mechanical properties of greywackes in different locations in İstanbul

Weathering	Location	Uniaxial Comp. Strength, UCS (MPa)	Compression Modulus, E (103 MPa)	Total porosity (%)	References
Weathered	Levent (Deep Excavation)	38-62	4-36	-	Tuğrul and Ündül (2006)
	Eminönü (Boreholes)	14.1-43.3	33.9-47.3	0.16-0.33	Zarif and Tuğrul (2002)
	Eyüp Tunnel	35-60.5	4.1-9.6	0.22-0.24	Erguvanlı (1985)
	Dolmabahçe-Baltalimanı	36-62.1	1.6-18	-	Erguvanlı et al.(1987)
	Average	**43.9**	**19.3**	**0.24**	
Unweathered	Levent (Deep Excavation)	58-64.7	10.8-48.2	-	Tuğrul and Ündül (2006)
	Eminönü (Boreholes)	51.3-66.2	13.9-96.3	0.20-0.26	Zarif and Tuğrul (2002)
	Eyüp Tunnel	61-77.5	34.7-40.6	0.19-0.23	Erguvanlı (1985)
	Haliç Tunnel	66.9	37.5	0.19-0.21	Erguvanlı (1985)
	Dolmabahçe-Baltalimanı	118-121	22-31	-	Erguvanlı et al.(1987)
	Average	**76.1**	**37.2**	**0.21**	

5. METHODOLOGY

5.1. Universal Standard Methods for Creep Tests

Below are some standard methods that has been issued for creep testing and the tests done within this thesis are according to the procedures and highlights indicated in them. Detailed information about ASTM D4405 – 04 and ASTM D4406 – 04 and their complete definitions can be find at the annex pages of this thesis.

ASTM D4405 – 04 Standard Test Method for Creep of Soft Rock Core Specimens in Uniaxial Compression at Ambient or Elevated Temperature

ASTM D4406 – 04 Standard Test Method for Creep of Rock Core Specimens in Triaxial Compression at Ambient or Elevated Temperatures

ASTM D4341-93(1998) Standard Test Method for Creep of Cylindrical Hard Rock Core Specimens in Uniaxial Compression

ASTM D5202 - 08 Standard Test Method for Determining Triaxial Compression Creep Strength of Chemical Grouted Soils

ASTM D5520 - 94(2006)e1 Standard Test Method for Laboratory Determination of Creep Properties of Frozen Soil Samples by Uniaxial Compression

5.2. Selected Examples of Laboratory Tests on Creep

Mitchell and Campanella (1963) have shown that during undrained creep of saturated soil the application of the creep stress causes an immediate increase in pore water pressure but that after a relatively short time further changes in pore water pressure with creep are very small.

As reported by Murayama (1969), Dorn (1956) increase in temperature increases pore pressure but the effective stress decreases, as results, soil structure weakened. Due to change in soil structure creep rate increases and the stresses corresponding to specific values of strain decreases at higher temperature. The magnitude of creep strain rate may be small in sand, silt and dry soil. Time dependant deformations are more important at higher water content than at low.

Creep show significant variation with change in properties of pore fluid on undisturbed soil. Mc Gill University (1984) was found that creep change with Viscosity and Leaching of pore fluid.

The effect of creep on the value of K_0 (Coefficient of lateral earth pressure at rest) was evaluate by Yamamuro and Lade (1996) during one dimensional compression tests on the Cambria and Gypsum sand. Lacerda (1976) made similar observation of the effect of creep on the value of K_0 for normally consolidated soil. The experimental data presented by them suggests that even dense sands that are compressed in to essentially rock, undergo measurable amount of creep, which causes K_0 to increase even over a short period of time.

Çevikbilen, G. and Yılmaz, E. (2000) made some tests on secondary and tertiary consolidation behavior of Samsun - Carsamba blue clay with valuable results on about compression indexes. Liquid and plastic limit of the blue clay, which has been classified as high plasticity clay, is 73% and 29% respectively and its specific unit weight is 27,6 kN/m3. Accorrding to 2 conventional consolidation tests and 7 long term consolidation (creep) tests that lasted 3 to 8 months with undisturbed and remoulded samples at various stress levels ranging from 25 kPa to 400 kPa, remoulding increases the primary consolidation time, increases recompression index (C_r) and decreases compression index (C_c). At every stress level remoulding causes a decrease on consolidation coefficient (C_v) values for undisturbed and remoulded samples. Furthermore, remoulding decreases the ending of secondary compression or the initial time of tertiary compression. By remoulding the variation of secondary compression coefficient (C_α) and C_α / C_c ratio is negligible. For undisturbed samples as the effective stress increases, tertiary compression ratio ($C_{\alpha\varepsilon t}$) gradually increases whilst for remoulded samples the greater $C_{\alpha\varepsilon t}$ values at lower stress levels decreases.

Nanda, S. and Sadana, M. L. (2005) find some invaluable results on Varanasi soil with chemical showing the changes in strain rate vs deviator stress and during single loading creep tests. The creep observations, using a single loading, were made for soil sample subjected to undrained triaxial test conditions. Cylindrical soil samples measuring 38mm dia and 76mm in height were prepared through the statically compaction mould. For a given time interval and level of deviator stress, the strain rate decreases with increase in the confining pressure. This in turn suggests that with increase in the confining pressure, deformation modulus and strength of soil tend to increase. Likewise the total strain for a certain time interval and confining pressure increases with increase in deviator stress. The log strain rate versus log time relationship for different stress intensities corresponding to single loading creep tests are linear and parallel to each other, so strain decreases with time. Addition of lime produces changes in creep behaviour of soil.

Fodil, A. Aloulou, W. and Hicher, P. Y. (1997) made some experiments on soft clays taken from the foundations of 'Le Flumet' dam to study the influence of viscoplastic parameters. Liquid and plastic limits of the two clay materials taken from 9m and 12m depth are 38%-42% and 24%-30,5% respectively and their specific unit weight is 1.9g/cm^3 (19.0 kN/m^3). The existence of the viscosity aspect of the material was confirmed and characterized by stress-relaxation, creep and oedometric tests. It was found that the parameter m, which represents the capability in soil to be subjected to creep deformations, seems to quantify well the viscous behaviour on different stress and strain paths.

Horn, D. Chang, Y. and Chien, C. W. (2002) analysed time dependency on diaphgram wall displacement due to creep and presented a quantative method to evaluate this creep effect.

5.3. Soils to be Tested

Three types of soil are used on laboratory experiments. To determine the characteristics of these soils moisture content tests (ASTM D2216) and Atterberg limit tests (ASTM 4318) were conducted. To reach values for plastic limit, liquid limit and optimum water content values, more than one set of experiments were performed.

5.3.1. Kaolinite

Kaolinite (K401M - Balıkesir Gürbüz Madencilik origin) found in laboratory, with average plastic limit and liquid limit values of 20% and 29% respectively according to the results of Atterberg limit tests. Its optimum water content is found as 19,5% according to several proctor tests done and from calculations its average unit weight is found as 1,65 t/m3 (16,5kN/m3).

Figure 5.1. Kaolinite specimen after taken out of mold

Figure 5.2. Kaolinite found in laboratory is kept in sacks inside red plastic trolleys

5.3.2. Bentonite and Kaolinite Mixture

For high plastic clay samples bentonite and kaolinite mixture by 50-50% weight were used in the tests. Bentonite found in laboratory is originally from Mito-Çanakkale. Plastic limit and liquid limit values of the mixture is 22% and 56% respectively according to Atterberg limit tests. Proctor tests results show the mixture's average optimum water content around 27% and its unit weight is calculated as 1,33 t/m3 (13,3kN/m3).

Enough amount of dry mixture is prepared from bentonite and kaolinite at equal portions before the beginning of the tests.

Figure 5.3. Bentonite in the laboratory is kept in sacks inside green plastic trolleys

Figure 5.4. Bentonite and kaolinite mixture sample of size 3.3mm dia and 7.0mm height

5.3.3. Greywacke

Greywacke samples used for the tests are brought from İstanbul to the laboratory. Crushed Greywacke is taken from a construction site having sent in plastic bags with particle size distribution changing from rocks as big as human foot to micro clay particles. After sieved through 5mm opening size Proctor and Atterberg limit tests were conducted. According to tests its average optimum water content and liquid limit are found 17,2% and 25% respectively and its unit weight is calculated as 1,78 t/m3.

Figure 5.5. Greywackes seen prior to be sieved to operable size

5.4. Testing Process

5.4.1. Specimen Preparation

Creep observations were done on 3 different types of soil all having optimum water content. Cylindrical samples with 33mm diameter and 70mm height were prepared through Harvard miniature compaction mould seen in Fig. 5.7.

Figure 5.6. Specimen preparation inside porcelain plate

During preparation, adequate amount of soil mixture is produced by using precalculated amount of water and 100 grams of soil inside a plate, making one single cylindrical sample each time to ensure effective mixing, less waste and more homogenous samples.

Figure 5.7. Harvard miniature compaction mold with 240gr weight hammer inside

Cylindrical samples with 33mm diameter and 70mm height were prepared through Harvard miniature compaction mold. About 240 gram weight is dropped from 20 cm to the sample placed inside the compaction mould on three layers, 25 times for each layer. Cylindrical sample is taken out of the mould by pressing on top after placed inside a special apparatus shown on Fig. 5.8.

Figure 5.8. Special apparatus to take out specimens without breaking

All samples to be tested are wrapped with a flexible membrane as shown in Fig. 5.9. and tightly fixed from both ends before placing on the testing device. This is for maintaining the water content of samples at a constant value or at least to have the decreased amount within reasonable range for a long period of time during testing.

Figure 5.9. Flexible membrane used to wrap specimens

5.4.2. Equipment Used

Cylindrical samples are placed on the EL25-0402 oedometer apparatus shown in Fig. 5.10. and loaded for 14 days and/or 28 days. Settlement data is recorded from a dial indicator seen on top of the oedometer, with an accuracy of 1/100mm and a vertical range of 20 mm.

Loading device was the beam and weight mechanism capable of transmitting axial load to the specimen easily. The moment arm for the oedometer beam multiples the load by 10 times. The equipment was calibrated to ensure that the loads indicated were the ones actually applied to soil specimen.

Porous stones of 35mm diameter were used at both sides of the soil specimen to permit effective drainage. For routine testing, stones of medium porosity were satisfactory. The porous stones were cleaned after testing, preferably by boiling and flushing.

Figure 5.10. Oedometer EL25-0402 apparatus used for consolidation

To be easily used in the tests Greywacke particles are sieved through 5mm opening sized sieve then put into an oven for drying and kept in one day as all of the 3 soil types. Oven shown in Fig 5.12. is a standart one, its heating temperature value is adjusted to 100’C.

Other items used during testing process are balances, between 10g to 500g., cronometer for timing, filter papers, distilled water, flexible membranes, plactic clamps and metal caps.

Figure 5.11. Various sizes of sieves used in preparing greywacke samples

Figure 5.12. Oven inside the laboratory is used for drying soil samples

Figure 5.13. Metal caps are tightly fixed by rubber clamps from both ends of the flexible membrane before fitting in porous stones and the sample

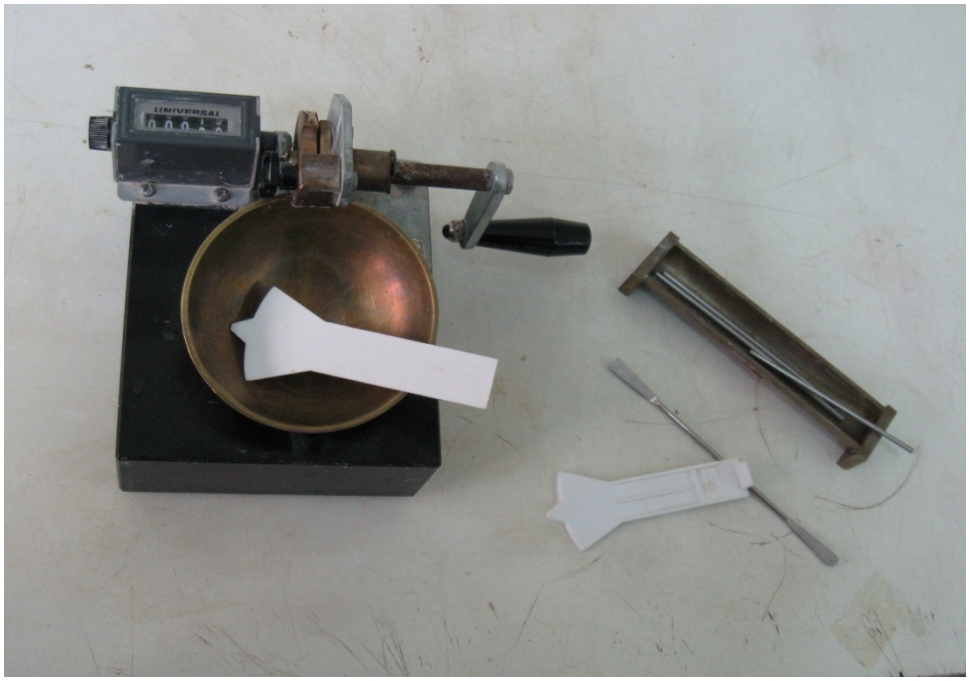

Figure 5.14. Equipment used to determine liquid and plastic limits of clays and greywacke particles

5.4.3. Optimum Water Content Determination

All dry soil mixtures, both clays and greywacke were mixed with distilled water to achieve the optimum water content. At first dry soil samples were poured in a plate and then water added by spraying over the samples. Water enriched samples were mixed and compacted with standard proctor tests inside miniature Harvard compaction mold and standard compaction mold. Through this test, the main aim was to identify the maximum dry unit weight of soil.

Optimum water content for kaolinite is determined by using standard compaction according to ASTM D1557. Proctor compaction tests were done twice on 6 samples each time starting with target water contents 14% and reaching up to 31% with 3,5% increaments on the first test and starting with 18% to 23,5% with 1% increaments on the second test.

For kaolinite, standard compaction molds were used with a calculated volume of 945,0 cm^3. After compacting three layers by 25 times on each layer, small amount of soil is taken from the top and bottom of the samples inside the mold and weighted before put inside oven for drying. After 24 hours they are taken out of the oven and weighted again to find out the water contents and their average is taken to calculate the dry unit weights at that water contents. The result of these calculations and water content – unit weight relationship curves are shown on figures and tables in the next chapter.

Optimum water content of bentonite and kaolinite mixture is determined inside miniature Harvard compaction mold weighted 134,28 grams with a calculated volume of 59,8 cm^3. Instead of taking a small amount of soil, the sample, which is taken out of the mold by a pressing device after the compaction, is weighted as a whole and then put inside oven and weighted again after taken out of oven one day later. The result of the dry unit weight calculations and water content – unit weight relationship curves are shown on figures and tables in the next chapter.

Optimum water content of greywacke is determined inside miniature Harvard compaction mold again. Prior to testing greywacke is sieved through 5mm opening sieve,

the particles that passed 5mm is used in the tests and the remaining larger particles are thrown away. So using the term greywacke could be misleading here since the tests are done on tiny greywacke particles with clay mixed inside rather than of large stones. Again after the compaction greywacke samples are weighted as a whole prior and after drying inside oven and the results are shown on figures and tables in the next chapter.

5.4.4. Atterberg Limits Determination Tests

Tests are done according to ASTM 4318 and the results shown on the table in the next chapter.

5.4.5. Finding out Failure Loads for the Specimens

At the beginning of tests automatic uniaxial compression device is used for breaking kaolinite samples and both the failure loads and the vertical displacement at that load is recorded accurately on the first 22 samples. But then a change on the calibration of the device and its being never fixed, enforces the usage of the mechanical EL25-0402 oedometer device for breaking the samples where it cannot be possible to find out the failure loads and the vertical displacement at that loads accurately. Over 30 samples are break through with trial and error methods before the evaluation of failure loads and deciding the weight to be used for creep testing. Maximum load to apply on the device for cylindrical kaolinite samples is evaluated as 0.85 kgf/cm2 – 84kPa, after several failures on loading between 700-750 gram scales. As the device has a moment arm of 10, scales should be multiplied accordingly to reach 7 to 7.5 kg loads applying to soil samples.

For Kaolinite-Bentonite mixture maximum loading of cylindrical samples is evaluated as about 750-800 grams (7,5 to 8 kgs applying to soil samples), which equals to 0,91 kgf/cm2 – 89 kPa. A total of 20 samples are broken by July 2009 to reach an approximate failure value by using 750 and 800 gram scales as loads. Another 20 are broken at the expected 90% of this failure load during September 2009 before successfully placing 3 samples on the oedometer device under 700 gram scales as loads. Still this does

not change the fact that these failure loads are evaluated through trial and error methods and could be subject to change.

For Greywacke samples maximum loading for 33 mm dia. 70 mm height cylindrical samples is evaluated as 500gram (5 kgs applying to the samples) which equals to 0,60 kgf/cm2 – 57kPa. Some 8 samples are broken to reach this evaluation and during the creep tests of 90% of this value, still 5 more samples are failed before the placing of 3 succesful samples on the device under 450 grams on November 2009.

5.4.6. Creep Testing for the Soil Types

25 days vertical deformation of kaolinite samples are recorded under 90% of the previously determined failure load value by using 650gr scales on July 2009. Testing on kaolinite samples gave out valuable information about mixture preparation and sample handling furthermore to wrapping them with membranes without disturbing and having the water contents on a reasonable range. The approach for creep testing methods like their duration and their data to be recorded and values to be used in calculations were established but unfortunately not much data is obtained in order to continue with bentonite-kaolinite mixture and greywacke samples, since there was limited time left.

After the failure load determination of kaolinite-bentonite mixture, their 14 and 28 days vertical deformation data is collected under 90%-80%-65%-60% and 40% of this evaluated load. Only 14 days long vertical deformation data is collected for 80%-65% and 60% of failure loading on August 2009. During September and October 2009 samples are tested for 28 days under 700 gram scales, which equals to 0,82 kgf/cm2 – 80kPa and 300gram scales, equals 0,35 kgf/cm2 – 34kPa.

After breaking at failure loads of greywacke samples, their 28 days vertical deformation data is collected under 90%-65% and 40% of this evaluated load by using 450-320 and 200 gram scales respectively during November-December 2009 and January 2010.

6. TEST RESULTS AND DISCUSSIONS

6.1. Proctor Compaction Test Results

6.1.1. Optimum Water Content for Kaolinite Samples

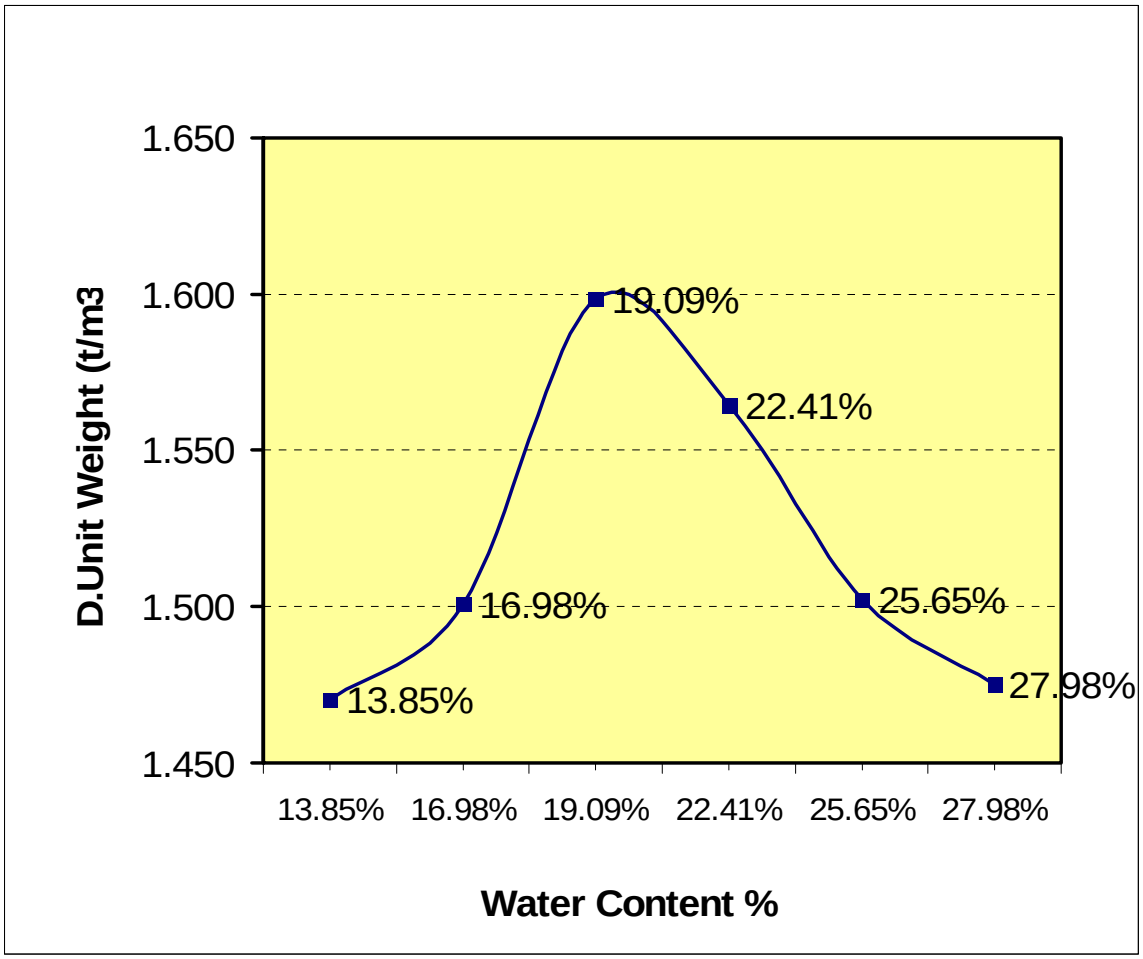

Figure 6.1 Water content - unit weight relationship curve for kaolinite samples

Figure 6.1. shows water content testing on a large range, starting with 14% target water content and reaching up to 31% having 3,5% increaments at each step. Calculated water contents in Table 6.1. shows a peak value of about 19%, where the dry unit weight of kaolinite sample is calculated as 1,60ton/m3 (16,0kN/m3) at that peak value.

Table 6.1. Dry unit weight calculations on kaolinite samples after standard proctor tests

Estimated Water Content	14.26%	17.74%	20.98%	24.89%	27.95%	31.06%
Can Weight (gram)	32,65-33,30	32,71-33,10	32,51-33,56	9,36-9,61	9,38-9,46	32,07-32,27
Wet Sample + Can	64,30-69,77	71,34-73,83	68,33-82,78	74,75-93,54	78,08-85,73	133,60-142,92
Dry Sample + Can	60,47-65,31	65,75-67,90	62,67-74,78	62,93-77,98	63,99-70,23	111,44-118,69
Water Weight (gram)	3,83-4,46	5,59-5,93	5,66-8,00	11,82-15,56	14,09-15,50	22,16-24,23
Dry Sample Weight	27,82-32,01	33,04-34,80	30,16-41,22	53,57-68,37	54,61-60,77	79,37-86,42
Calculated Water Content	13,77-13,93%	16,92-17,04%	18,77-19,41%	22,06-22,76%	25,80-25,50%	27,92-28,04%
Average Water Content	13.85%	16.98%	19.09%	22.41%	25.65%	27.98%
Sample Weight (gram)	1,582.0	1,659.0	1,799.0	1,810.0	1,784.0	1,784.0
Mold Volume (cm3)	945.0	945.0	945.0	945.0	945.0	945.0
Dry Unit Weight (ton/m3)	1.470	1.501	1.599	1.565	1.502	1.475

Table 6.2. Dry unit weight calculations on kaolinite samples after standard proctor tests

Estimated Water Content	18.05%	19.05%	20.11%	21.28%	22.24%	23.33%
Can Weight (gram)	32,73-33,56	32,26-33,31	32,63-33,11	32,49-32,04	9,31-9,46	9,39-9,60
Wet Sample + Can	78,83-86,70	60,21-60,60	74,63-83,33	72,57-71,94	48,73-67,72	83,03-94,91
Dry Sample + Can	71,99-78,77	55,99-56,44	67,99-75,22	66,15-65,28	42,36-58,09	70,69-80,38
Water Weight (gram)	6,84-7,93	4,22-4,16	6,64-8,11	6,42-6,66	6,37-9,63	12,34-14,53
Dry Sample Weight	39,26-45,21	23,73-23,13	35,36-42,11	33,66-33,24	33,05-48,63	61,30-70,78
Calculated Water Content	17,42-17,54%	17,78-17,98%	18,78-19,26%	19,07-20,03%	19,27-19,80%	20,13-20,53%
Average Water Content	17.48%	17.88%	19.02%	19.53%	19.54%	20.33%
Sample Weight (gram)	1,692.0	1,749.0	1,832.0	1,863.0	1,869.0	1,848.0
Mold Volume (cm3)	945.0	945.0	945.0	945.0	945.0	945.0
Dry Unit Weight (ton/m3)	1.524	1.570	1.629	1.649	1.654	1.625

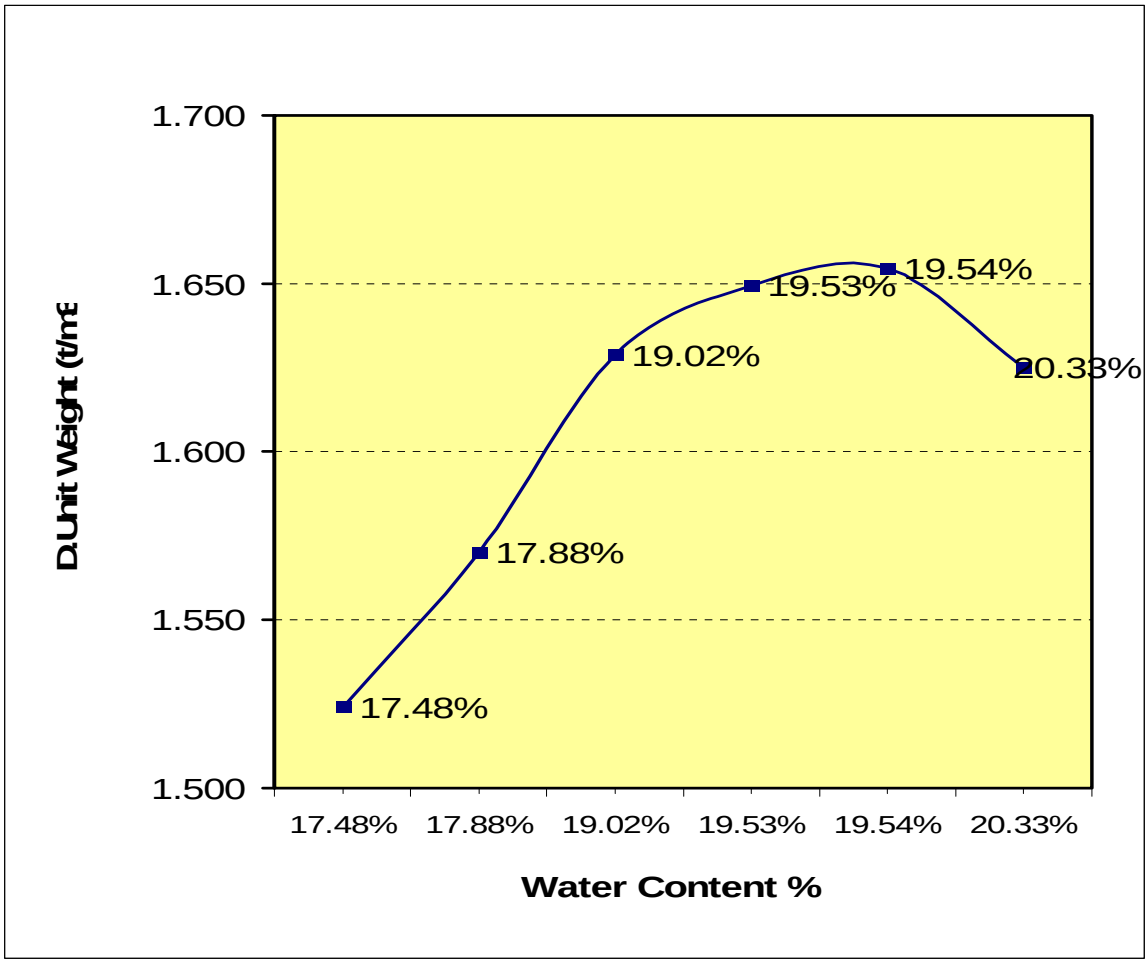

Figure 6.2 Water content - unit weight relationship curve for kaolinite samples

Figure 6.2. shows another water content testing on a different day having target water contents changing between 18% and 23,5% with 1% increments. Calculated water contents on Table 6.2. shows a peak value of about 19,5% where the unit weight of soil equals to 1,65ton/m3 (16,5kN/m3) at that value. Since this test is much detailed then the previous one, and both results are consistent, the result is accepted as the final value of kaolinite sample.

6.1.2. Optimum Water Content for Bentonite and Kaolinite Mixture

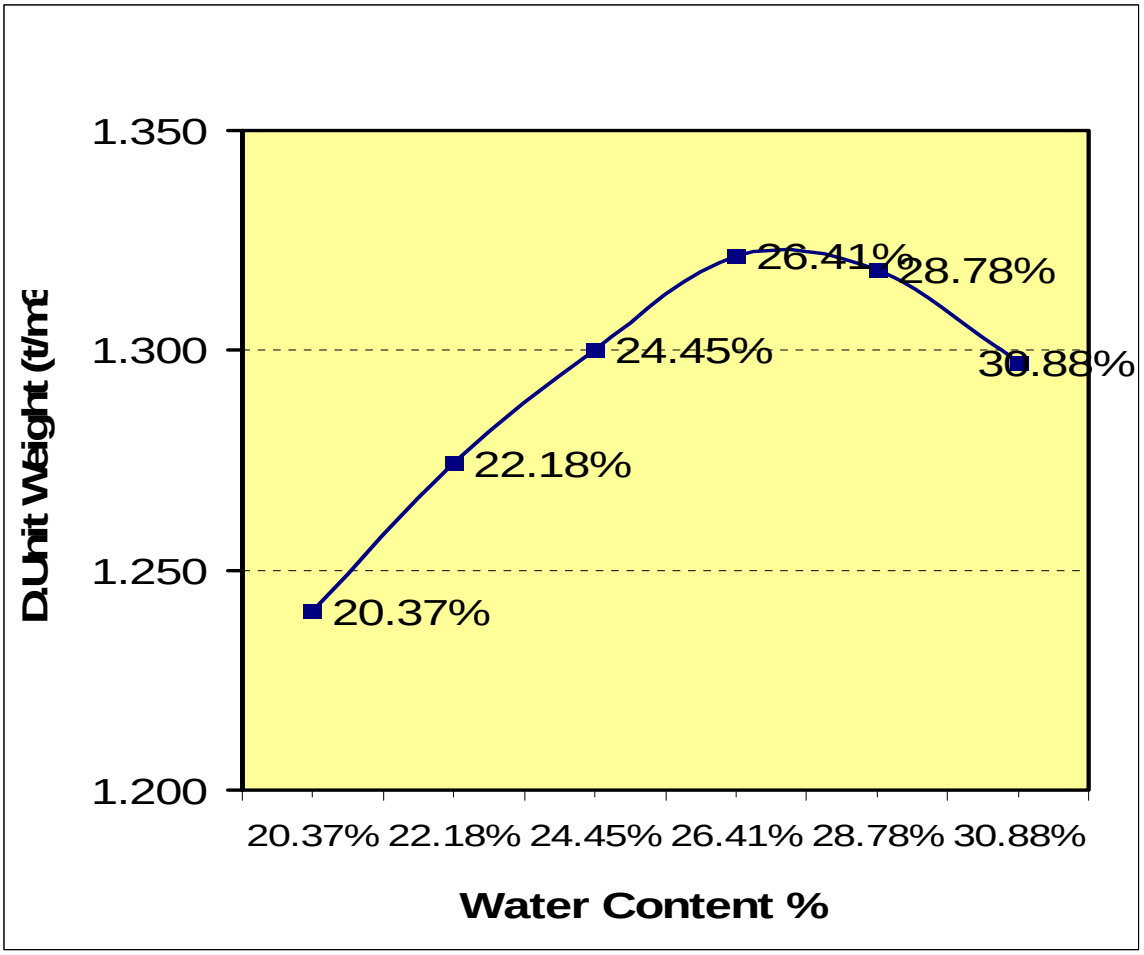

Figure 6.3 Water content - unit weight relationship curve for bentonite and kaolinite mixture samples

Figure 6.3. shows water content tests for bentonite and kaolinite mixture done on a large range. Target water contents beginning with 20% and reaches to 30% by 2% increments. Samples are weighted after 1 day of standby out of oven. All these weight values and calculations done are shown on Table 6.3., here we can see the peak value as 26,5% and the unit weight as 1,32ton/m3 (13,2kN/m3).

Table 6.3. Dry unit weight calculations on B and K mixture after standard proctor tests

Estimated Water Content	19.96%	21.97%	24.01%	26.00%	28.03%	29.98%
Can Weight (gram)	32.65	33.45	32.26	33.31	32.68	32.55
Wet Sample + Can	121.58	126.21	128.61	133.00	132.64	129.40
Dry Sample + Can	106.53	109.37	109.68	112.17	110.30	106.55
Water Weight (gram)	15.05	16.84	18.93	20.83	22.34	22.85
Dry Sample Weight	73.88	75.92	77.42	78.86	77.62	74.00
Calculated Water Content	20.37%	22.18%	24.45%	26.41%	28.78%	30.88%
Sample+Mold Weight (gram)	223.64	227.45	231.10	234.25	235.87	235.88
Mold Weight (gram)	134.28	134.28	134.28	134.28	134.28	134.28
Sample Weight (gram)	89.36	93.17	96.82	99.97	101.59	101.60
Mold Volume (cm3)	59.8	59.8	59.8	59.8	59.8	59.8
Dry Unit Weight (ton/m3)	1.241	1.274	1.300	1.322	1.318	1.297

Figure 6.4. shows tests done on bentonite and kaolinite mixture within tighter range of target (estimated) water content values between 20,5% and 25,5% with 1% increaments. These tests are done on a different day but their result shows similar values, where the peak of the mixture is about 27% and it's calculated unit weight equals to 1,33ton/m3 (13,3kN/m3) as seen on Table 6.4.

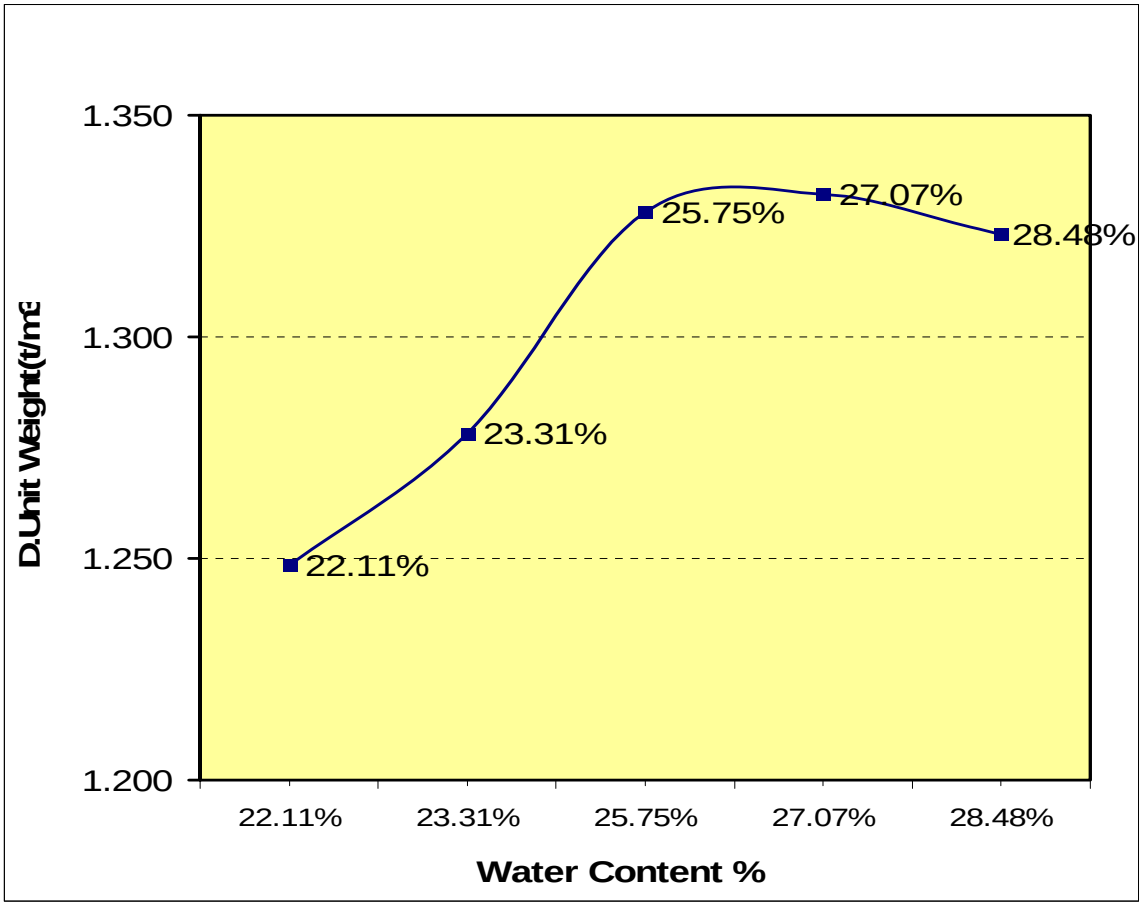

Figure 6.4. Water content - unit weight relationship curve for B and K mixture samples

Table 6.4. Dry unit weight calculations on B and K mixture after standard proctor tests

Estimated Water Content	20.47%	21.50%	23.55%	24.52%	25.62%
Can Weight (gram)	6.61	6.69	6.68	6.54	6.58
Wet Sample + Can	97.40	98.25	105.04	107.28	107.60
Dry Sample + Can	80.96	80.94	84.90	85.82	85.21
Water Weight (gram)	16.44	17.31	20.14	21.46	22.39
Dry Sample Weight	74.35	74.25	78.22	79.28	78.63
Calculated Water Content	22.11%	23.31%	25.75%	27.07%	28.48%
Sample Weight (gram)	91.24	94.32	99.94	101.30	101.72
Mold Volume (cm3)	59.8	59.8	59.8	59.8	59.8
Dry Unit Weight (ton/m3)	1.249	1.278	1.328	1.332	1.323

6.1.3. Optimum Water Content for Greywacke Samples

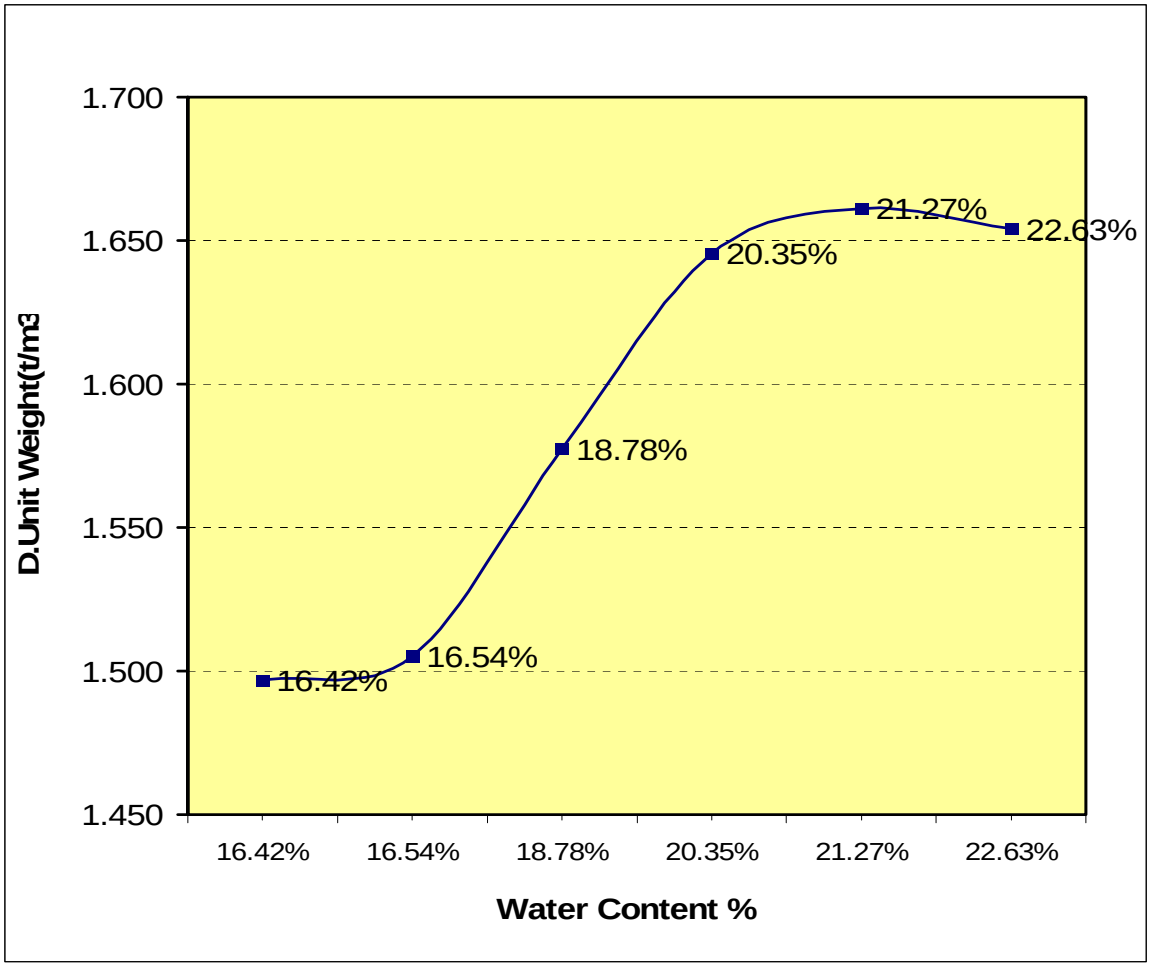

Figure 6.5. Water content - unit weight relationship curve for greywacke samples

Figure 6.5. shows water content measurement for greywacke samples done on a large scale basis. Target water contents were between 15% and 22%. Figure 6.6. shows much tighter range target water contents measured between 18,5% and 21,5%. From both graphs we can see the peak value as optimum water content, which is between 21,5% and 22,5% and the unit weight as 1,66ton/m3. Results of measurements and calculations are shown on Table 6.5.

Table 6.5. Dry unit weight calculations on greywacke samples after standard proctor tests

Estimated Water Content	15.04%	16.05%	17.96%	20.08%	19.98%	22.11%
Can Weight (gram)	32.51	32.26	33.03	33.43	33.31	32.62
Wet Sample + Can	136.76	134.19	145.21	151.76	153.51	153.17
Dry Sample + Can	122.06	119.72	127.47	131.75	132.43	130.92
Water Weight (gram)	14.70	14.47	17.74	20.01	21.08	22.25
Dry Sample Weight	89.55	87.46	94.44	98.32	99.12	98.30
Calculated Water Content	16.42%	16.54%	18.78%	20.35%	21.27%	22.63%
Sample Weight (gram)	104.27	104.97	112.13	118.52	120.54	121.38
Mold Volume (cm3)	59.8	59.8	59.8	59.8	59.8	59.8
Dry Unit Weight (ton/m3)	1.497	1.505	1.577	1.646	1.661	1.654

Table 6.6. Dry unit weight calculations on greywacke samples after standard proctor tests

Estimated Water Content	19.50%	20.00%	20.52%	21.02%	21.48%
Can Weight (gram)	32.50	33.30	32.26	33.44	32.62
Wet Sample + Can	150.64	152.87	154.14	155.70	153.91
Dry Sample + Can	129.40	131.30	131.65	132.66	130.52
Water Weight (gram)	21.24	21.57	22.49	23.04	23.39
Dry Sample Weight	96.90	98.00	99.39	99.22	97.90
Calculated Water Content	21.92%	22.01%	22.63%	23.22%	23.89%
Sample Weight (gram)	118.17	119.88	121.93	122.47	121.58
Mold Volume (cm3)	59.8	59.8	59.8	59.8	59.8
Dry Unit Weight (ton/m3)	1.620	1.642	1.662	1.661	1.640

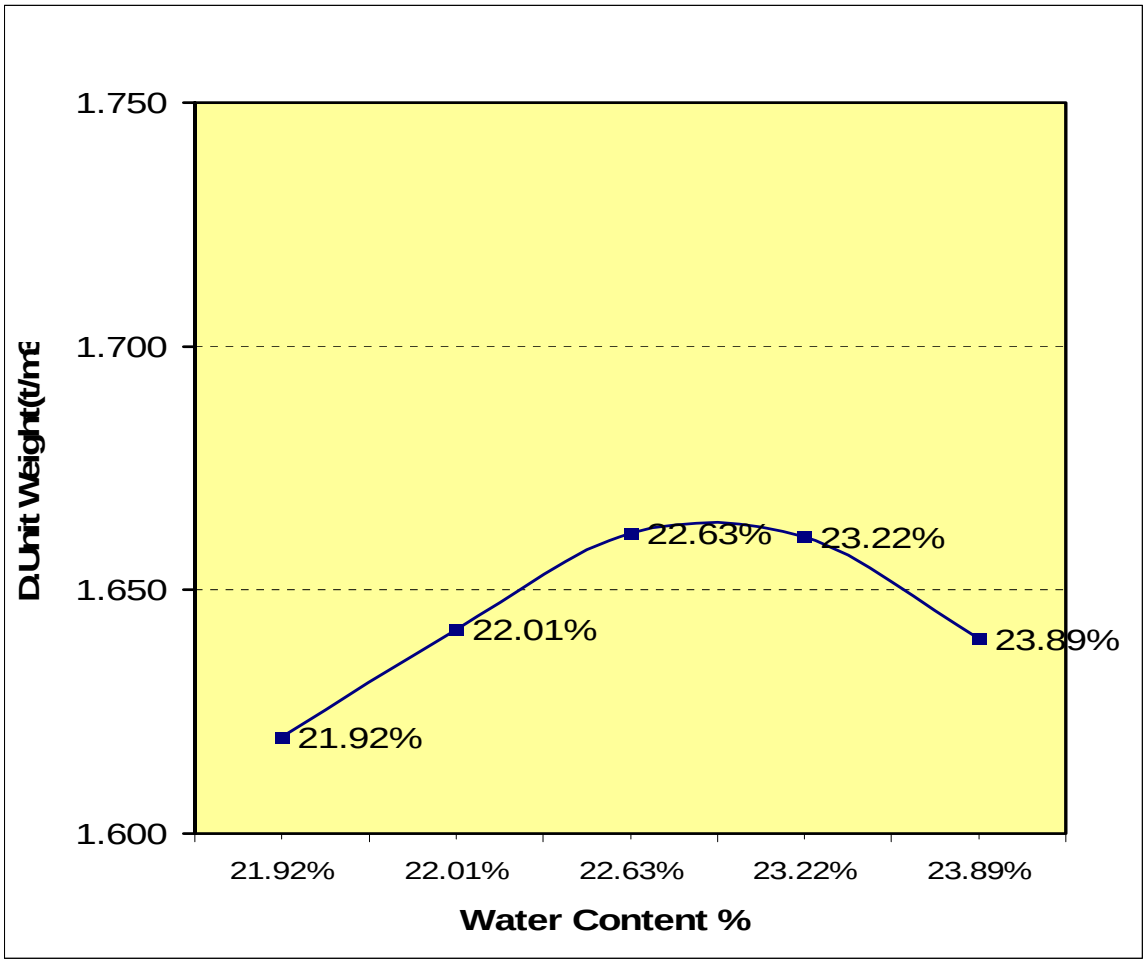

Figure 6.6. Water content - unit weight relationship curve for greywacke samples

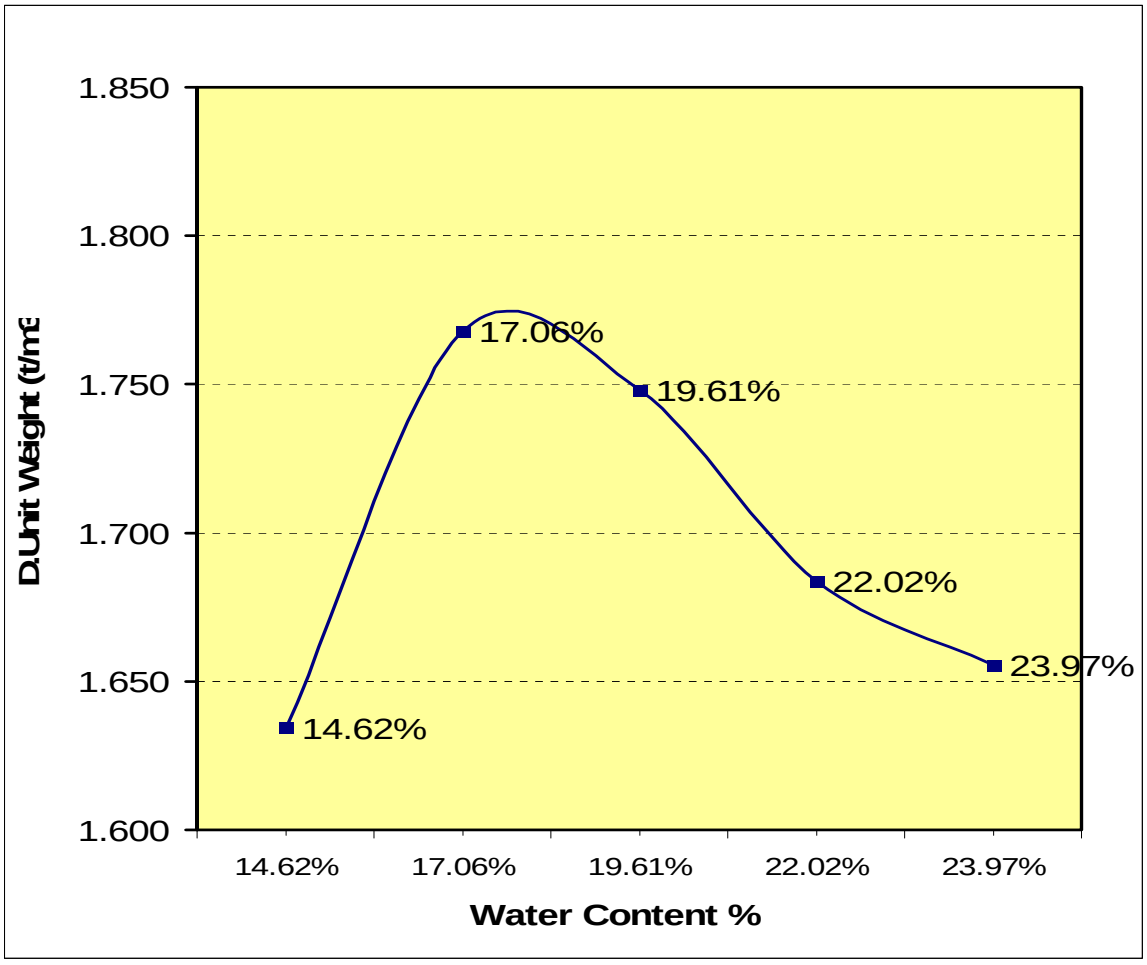

Figure 6.7. Water content - unit weight relationship curve for greywacke samples

After 2 months new water content analyses are made from sieved and prepared greywacke samples. Target values are between 12,5% and 22,5% with 2% increment on Figure 6.7. and between 14% - 18% with 1% increase on Figure 6.8. From both graphs and the measurements and calculations seen on Tables 6.7 and 6.8. we can say that water content measurement of the samples decreases by 2,5% against the previous values and peak value is about as 17,2% corresponding to a unit weight of 1,78 ton/m3 which can be due to a change in soil gradation during preparation.

Table 6.7. Dry unit weight calculations on greywacke samples after standard proctor tests

Estimated Water Content	12.47%	14.98%	17.50%	20.01%	22.47%
Can Weight (gram)	33.00	32.31	9.44	9.56	9.32
Wet Sample + Can	144.98	155.88	134.24	131.95	130.46
Dry Sample + Can	130.70	137.87	113.78	109.86	107.04
Water Weight (gram)	14.28	18.01	20.46	22.09	23.42
Dry Sample Weight	97.70	105.56	104.34	100.30	97.72
Calculated Water Content	14.62%	17.06%	19.61%	22.02%	23.97%
Sample Weight (gram)	112.10	123.85	125.11	122.95	122.81
Mold Volume (cm3)	59.8	59.8	59.8	59.8	59.8
Dry Unit Weight (ton/m3)	1.634	1.768	1.748	1.684	1.656

Table 6.8. Dry unit weight calculations on greywacke samples after standard proctor tests

Estimated Water Content	14.14%	15.02%	15.03%	16.66%	18.34%
Can Weight (gram)	9.55	32.25	9.43	33.03	9.42
Wet Sample + Can	129.59	156.76	132.62	156.88	133.81
Dry Sample + Can	112.84	138.46	114.40	137.31	112.86
Water Weight (gram)	16.75	18.30	18.22	19.57	20.95
Dry Sample Weight	103.29	106.21	104.97	104.28	103.44
Calculated Water Content	16.22%	17.23%	17.36%	18.77%	20.25%
Sample Weight (gram)	120.08	124.70	123.22	124.10	124.67
Mold Volume (cm3)	59.8	59.8	59.8	59.8	59.8
Dry Unit Weight (ton/m3)	1.727	1.778	1.755	1.746	1.732

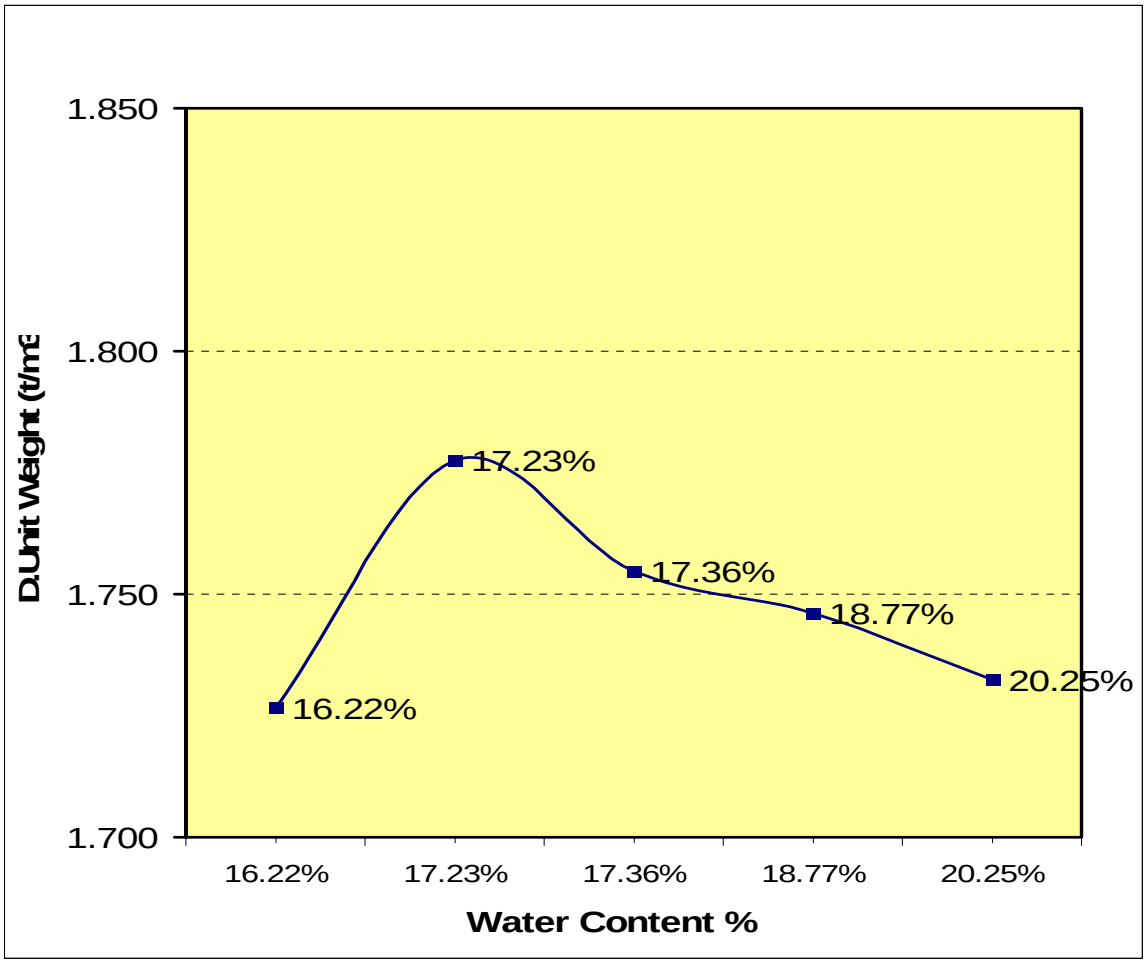

Figure 6.8. Water content - unit weight relationship curve for greywacke samples

6.2. Atterberg Limits Test Results

Table 6.9. Results of Atterberg limits tests on the tested soil types

SOIL TYPES	GREYWACKE	KAOLINITE	50%KAOLINITE-50%BENTONITE
LIQUID LIMIT VALUE	25	29	56
PLASTIC LIMIT VALUE	NA	20	22
PLASTICITY INDEX	NA	9	34
UNIT WEIGHT (TON/M3)	1.78	1.65	1.33

6.3. Creep Test Results

6.3.1. Vertical Deformations for Kaolinite Samples

Creep tests are started with kaolinite samples. At the beginning, the approach for creep testing, their durations and the loading were undecided. These parameters are established through a series of trial error testing and by the availability of the oedometer devices and mesuring gauges. So at first, 25 days of their vertical deformations are recorded under 90% of the previously determined failure load values by using 650gr scales on July 2009. Later on, when there was no apparent critical behaviour on the low plastic samples, it has been decided to conduct tests on high plastic clay samples. In Table 6.10 the deformations recorded for the Kaolinite samples are given.

Table 6.10. Recorded daily vertical deformation data for kaolinite samples under 90% of failure loads (650 grams)

DAYS	0,0hr	0.5hrs	1,0hr	2,0hrs	4,0hrs	1	2	3	4	5	6	7	8	9	10
DATE	6/25	6/25	6/25	6/25	6/25	6/26	6/27	6/28	6/29	6/30	7/1	7/2	7/3	7/4	7/5
SAMPLE #1	105.0	144.0	147.5	150.0	151.5	153.0	154.3	155.7	157.0	158.1	159.0	160.2	161.2	162.2	163.2
SAMPLE #2	95.0	146.0	151.0	155.0	157.0	161.2	162.5	163.7	165.0	166.0	167.0	168.8	170.0	171.1	172.2
SAMPLE #3	85.0	125.5	129.1	131.6	132.7	134.9	136.0	137.2	138.3	139.3	140.4	141.5	142.6	143.5	144.4

DAYS	11	12	13	14	15	16	17	18	19	20	21	22	23	24	25
DATE	7/6	7/7	7/8	7/9	7/10	7/11	7/12	7/13	7/14	7/15	7/16	7/17	7/18	7/19	7/20
SAMPLE #1	164.2	165.2	166.1	167.0	168.0	169.0	170.1	171.1	172.0	172.9	173.8	174.7	175.5	176.4	177.2
SAMPLE #2	173.3	174.3	175.6	176.9	178.3	179.6	180.9	182.2	183.5	184.7	185.7	186.5	187.4	188.3	189.2
SAMPLE #3	145.3	146.3	147.2	148.1	149.1	150.1	151.1	152.1	153.2	154.2	155.1	155.9	156.8	157.7	158.6

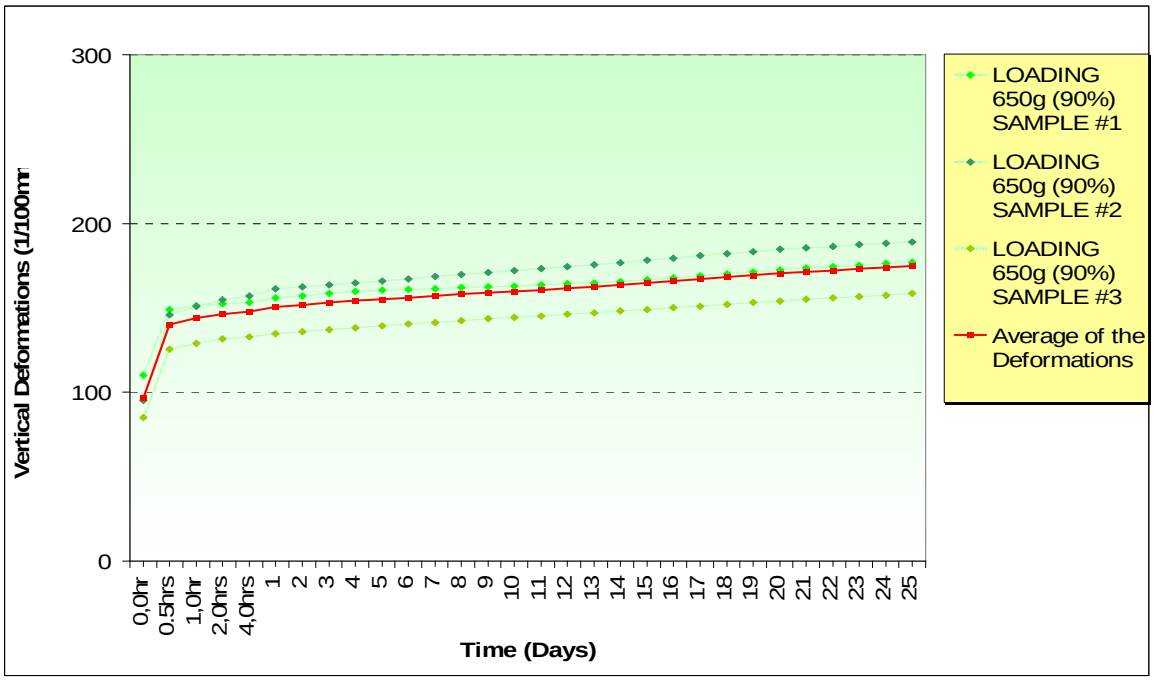

Figure 6.9. Vertical deformations – time curve for 3 kaolinite samples under 90% of failure loads (650 grams) and their average values

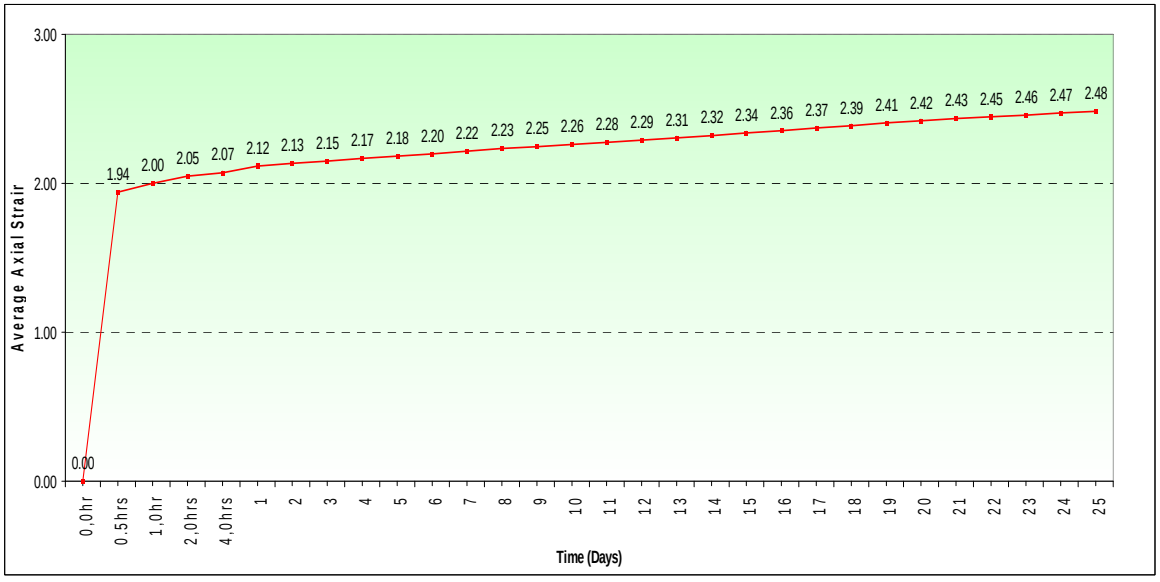

Figure 6.10. Axial strain – time relationship for kaolinite samples

According to ASTM standard methods for creep testing, it is essential to plot strain versus time curves for the axial and lateral directions but since lateral deformation data have not been recorded only axial strain values for kaolin samples are plotted on Figure 6.10.

Figure 6.11. Daily average rate of settlement versus time graph of kaolinite samples

Daily rate of settlement values which are seen on Figure 6.11. are calculated through the average of the daily vertical deformation differences. These calculated values are shown on Table 6.11 as well.

Table 6.11. Average of daily rate of settlement values for kaolinite samples

DAYS	0,0hr	0.5hrs	1,0hr	2,0hrs	4,0hrs	1	2	3	4
AVERAGE OF 650g (90%) LOADING	NA	435.00	40.33	30.00	20.67	20.00	12.56	12.56	12.56

DAYS	5	6	7	8	9	10	11	12	13
AVERAGE OF 650g (90%) LOADING	11.33	10.33	13.00	11.00	10.00	10.00	10.00	10.00	10.33

DAYS	14	15	16	17	18	19	20	21	22
AVERAGE OF 650g (90%) LOADING	10.33	11.33	11.22	11.22	11.22	10.67	10.33	9.33	9.00

DAYS	23	24	25						
AVERAGE OF 650g (90%) LOADING	8.57	8.57	8.57						

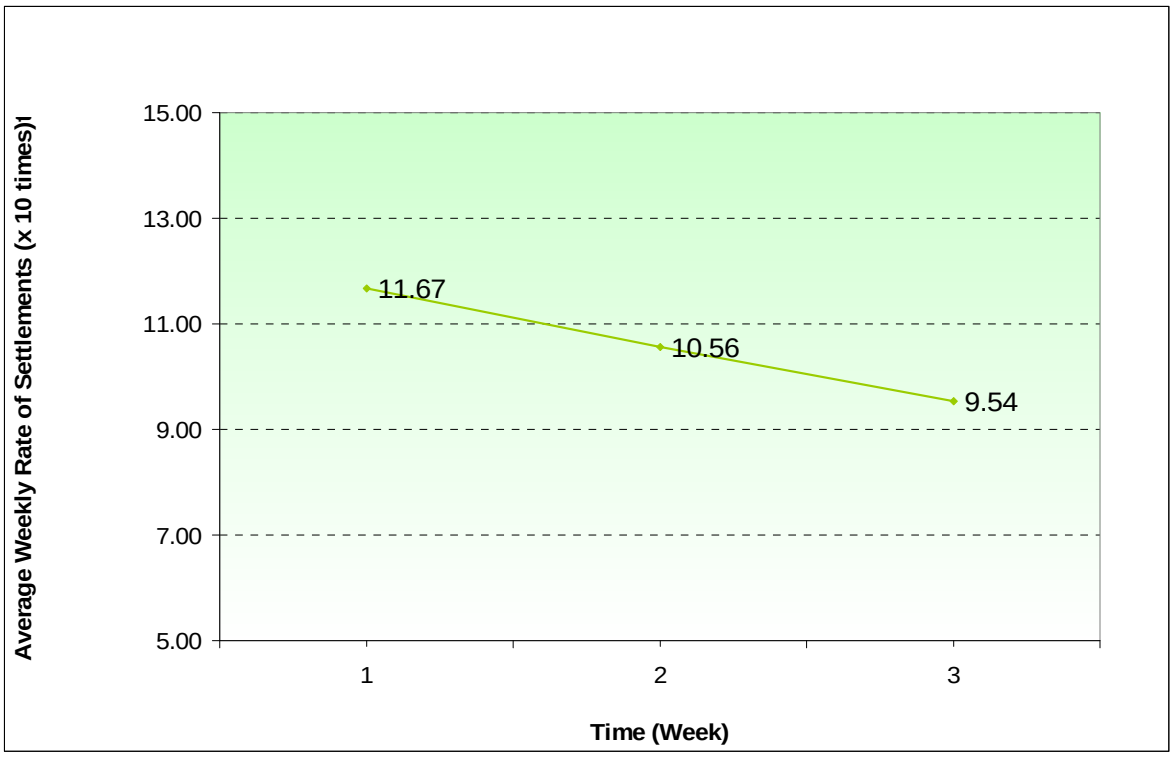

Figure 6.12. Average rate of settlement for kaolinite samples on each week

Values from Table 6.11 are divided into weekly averages, since the duration of the tests are only 25 days, valid 3 values calculated are plotted on Figure 6.12. As a conclusion, it can be stated that even under 90% of failure load, the deformations tend to decrease with time.

6.3.2. Vertical Deformations for Bentonite and Kaolinite Mixture Samples

To understand whether clays with higher plasticity will show a more critical behaviour during creep testing, bentonite is mixed with kaolinite by equal amounts in weight to be used in the study. After the failure load determination of kaolinite-bentonite mixture, their 14 and 28 days vertical deformation data is collected under 90%-80%-65%-60% and 40% of this evaluated load. Only 14 days long vertical deformation data is collected for 80%-65% and 60% of failure loading on August 2009. During September and October 2009 samples are tested for a duration of 28 days under 700 gram scales and 300gram scales.

Table 6.12. Recorded daily vertical deformation data for B and K mixture samples under 80% - 65% and 60% of failure loads

DAYS	0,0hr	0.5hrs	1,0hr	2,0hrs	1day	2	3	4	5
DATE	7/20	7/20	7/20	7/20	7/21	7/22	7/23	7/24	7/25
LOADING 600g (80%) SAMPLE #1	155.0	261.5	269.0	276.0	287.0	290.6	295.0	296.7	298.4
LOADING 600g (80%) SAMPLE #2	190.0	299.0	309.0	318.5	329.8	334.0	342.5	344.9	347.3
LOADING 600g (80%) SAMPLE #3	175.0	320.0	331.2	341.8	347.7	352.0	354.0	356.0	358.1
DATE	8/3	8/3	8/3	8/3	8/4	8/5	8/6	8/7	8/8
LOADING 500g (65%) SAMPLE #1	85.0	149.5	154.3	158.5	174.2	177.5	179.9	182.2	184.4
LOADING 500g (65%) SAMPLE #2	87.0	160.5	168.0	175.0	188.8	191.5	193.5	195.9	197.7
LOADING 500g (65%) SAMPLE #3	90.0	169.6	173.7	181.0	191.0	194.6	197.4	200.2	202.6
DATE	8/17	8/17	8/17	8/17	8/18	8/19	8/20	8/21	8/22
LOADING 450g (60%) SAMPLE #1	32.0	85.0	90.0	94.1	105.0	112.0	114.6	117.0	118.8
LOADING 450g (60%) SAMPLE #2	30.0	80.0	85.0	91.0	106.5	113.0	117.0	120.0	122.0
LOADING 450g (60%) SAMPLE #3	40.0	88.0	95.0	100.8	113.9	120.2	123.4	126.6	129.7

DAYS	6	7	8	9	10	11	12	13	14
DATE	7/26	7/27	7/28	7/29	7/30	7/31	8/1	8/2	8/3
LOADING 600g (80%) SAMPLE #1	300.0	301.7	303.0	304.2	305.5	306.7	307.9	309.0	310.2
LOADING 600g (80%) SAMPLE #2	349.6	352.0	353.7	355.5	357.2	358.9	360.5	362.0	363.6
LOADING 600g (80%) SAMPLE #3	360.1	362.1	364.2	366.3	368.3	370.4	372.0	373.6	375.2
DATE	8/9	8/10	8/11	8/12	8/13	8/14	8/15	8/16	8/17
LOADING 500g (65%) SAMPLE #1	186.6	188.8	190.9	193.0	195.1	197.0	198.8	200.7	202.5
LOADING 500g (65%) SAMPLE #2	199.4	201.2	203.0	204.7	206.4	208.1	209.8	211.5	213.2
LOADING 500g (65%) SAMPLE #3	205.0	207.4	209.8	212.2	214.6	217.0	219.4	221.7	224.1
DATE	8/23	8/24	8/25	8/26	8/27	8/28	8/29	8/30	8/31
LOADING 450g (60%) SAMPLE #1	120.7	122.5	125.0	127.1	128.6	130.1	131.6	133.1	134.6
LOADING 450g (60%) SAMPLE #2	124.0	126.0	128.3	130.0	131.8	133.6	135.1	136.6	138.1
LOADING 450g (60%) SAMPLE #3	132.9	136.0	139.1	142.0	144.7	147.4	149.9	152.5	155.0

14 days long vertical deformation data for 3 different load values on 3 different samples each are recorded on Table 6.12., then their average values are calculated and the results are shown on Table 6.13. All these values are plotted on the deformation-time curve seen at Figure 6.13. We can say from both the Table 6.13 and Figure 6.13 that the average values are representative of the obtained test data.

Table 6.13. Average vertical deformation values for B and K mixture samples under 80% - 65% and 60% of failure loads

DAYS	0,0hr	0.5hrs	1,0hr	2,0hrs	1day	2	3	4	5
AVERAGE OF 600g (80%) LOADING	173.3	293.5	303.1	312.1	321.5	325.5	330.5	332.5	334.6
AVERAGE OF 500g (65%) LOADING	87.3	159.9	165.4	171.5	184.7	187.9	190.3	192.8	194.9
AVERAGE OF 450g (60%) LOADING	34.0	84.3	90.0	95.3	108.5	115.1	118.3	121.2	123.5

DAYS	6	7	8	9	10	11	12	13	14
AVERAGE OF 600g (80%) LOADING	336.6	338.6	340.3	342.0	343.7	345.3	346.8	348.2	349.7
AVERAGE OF 500g (65%) LOADING	197.0	199.1	201.2	203.3	205.4	207.4	209.3	211.3	213.3
AVERAGE OF 450g (60%) LOADING	125.8	128.2	130.8	133.0	135.0	137.0	138.9	140.7	142.6

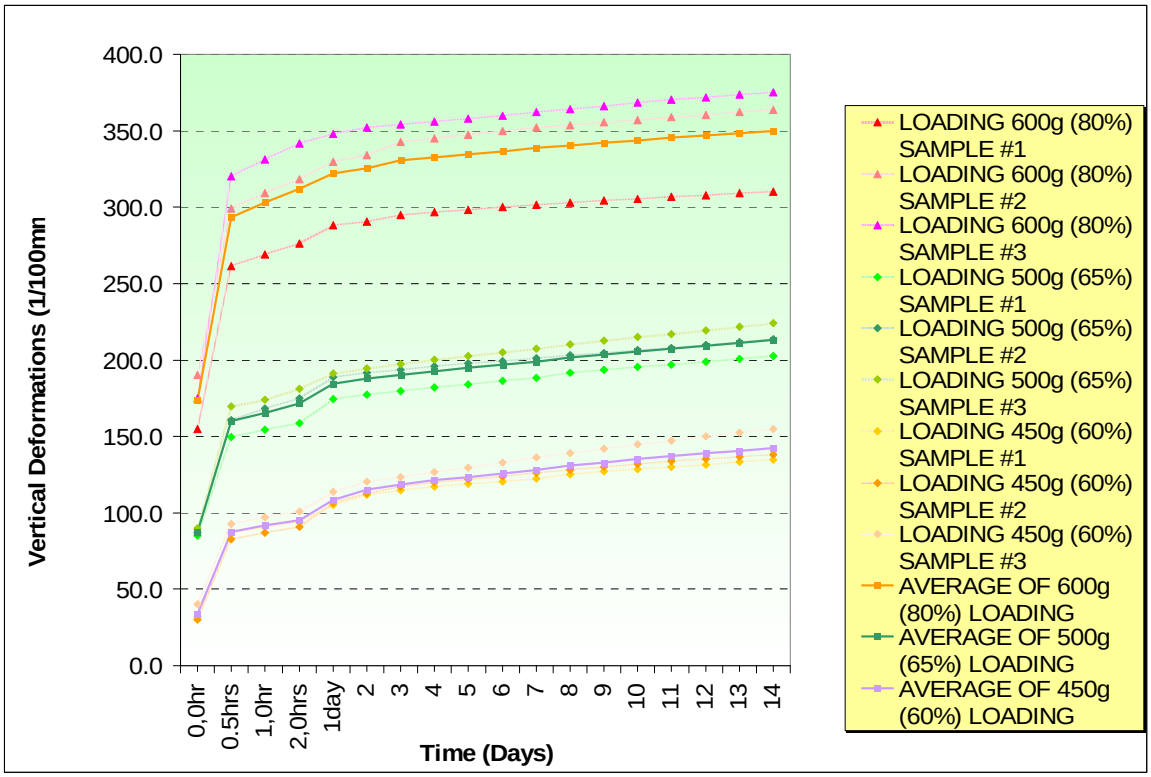

Figure 6.13. Vertical deformations – time curve for B and K mixture samples under 80% - 65% and 60% of failure loads and their average values

Axial strain and rate of settlement versus time graphs seen on Figures 6.14., 6.15. and 6.16. are plotted through the same calculation methods defined at the kaolinite samples part.

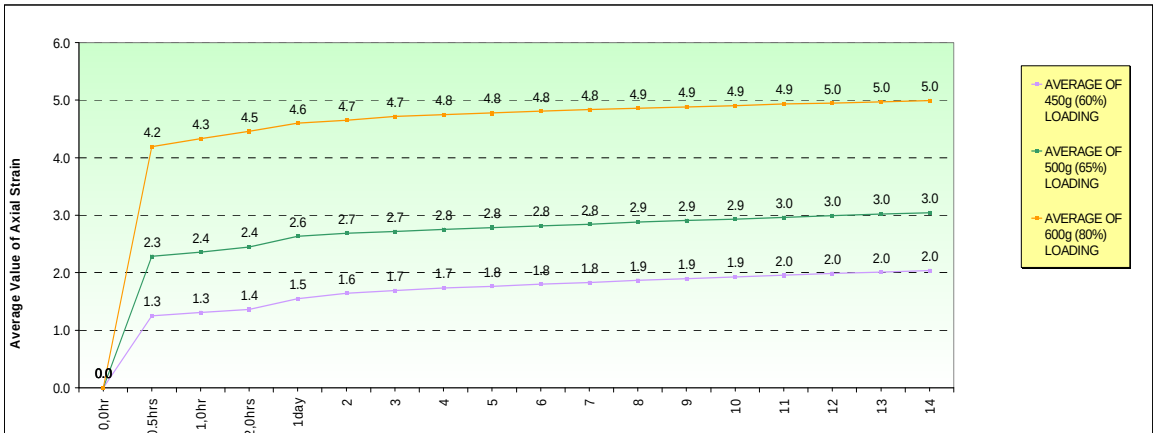

Figure 6.14. Axial strain – time relationship for B and K mixture samples under 80% - 65% and 60% of failure loads

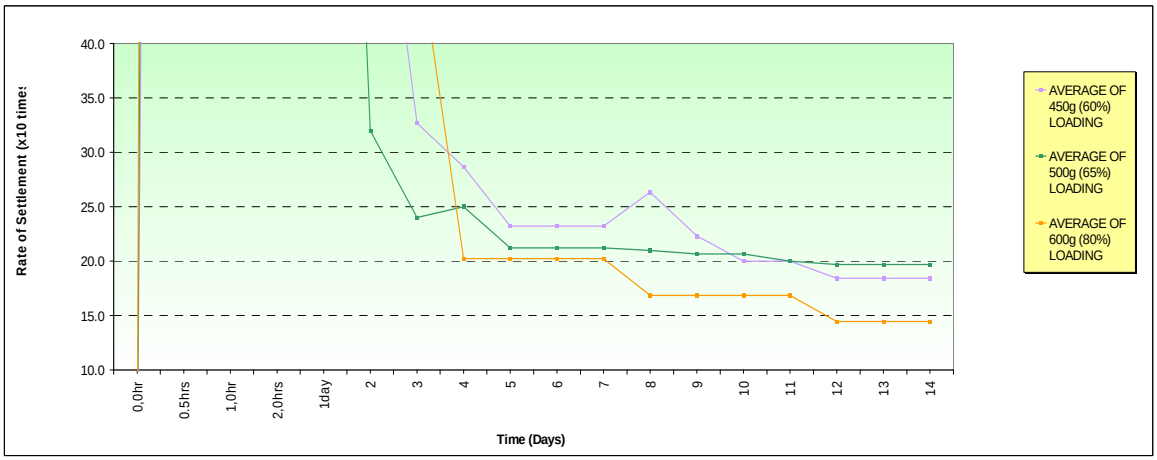

Figure 6.15. Daily rate of settlement values of B and K mixture samples under 80% - 65% and 60% of failure loads

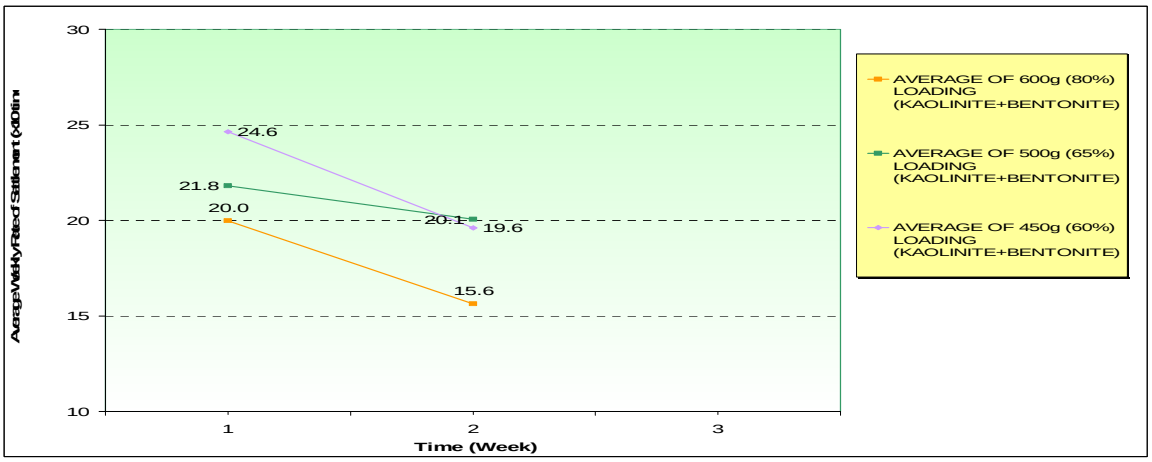

Figure 6.16. Weekly rate of settlement values of B and K mixture samples under 80% - 65% and 60% of failure loads

After these 14 days long creep tests, 28 days long testing are done with samples loaded under 90% and 40% of failure loads, which equals to 700 grams and 300 grams respectively. Their recorded data is shown in Table 6.14. and the various graphs plotted from this data can be seen through Figures 6.17. to 6.20.

Table 6.14. Recorded daily vertical deformation data for B and K mixture samples under 90% and 40% of failure loads

DAYS	0,0hr	0.5hrs	1,0hr	2,0hrs	1day	2	3	4	5	6	7
DATE	9/3	9/3	9/3	9/3	9/4	9/5	9/6	9/7	9/8	9/9	9/10
LOADING 700g (90%) SAMPLE #1	135.0	260.0	266.8	274.2	291.0	294.7	298.5	302.2	304.5	306.8	309.0
LOADING 700g (90%) SAMPLE #2	140.0	269.3	281.0	294.7	321.4	326.4	329.2	331.2	333.2	335.2	336.9
LOADING 700g (90%) SAMPLE #3	195.0	318.6	326.8	334.3	353.0	356.6	360.3	363.9	366.3	368.7	370.5
DATE	9/30	9/30	9/30	9/30	10/1	10/2	10/3	10/4	10/5	10/6	10/7
LOADING 300g (40%) SAMPLE #1	19.0	58.8	62.7	66.8	77.2	80.3	83.3	86.3	89.3	91.8	93.9
LOADING 300g (40%) SAMPLE #2	21.0	65.0	69.3	73.7	86.6	90.2	93.2	96.2	99.2	102.0	104.3
LOADING 300g (40%) SAMPLE #3	25.0	65.9	70.3	74.2	86.7	89.8	93.2	96.5	99.9	102.7	104.9

DAYS	8	9	10	11	12	13	14	15	16	17	18
DATE	9/11	9/12	9/13	9/14	9/15	9/16	9/17	9/18	9/19	9/20	9/21
LOADING 700g (90%) SAMPLE #1	311.1	312.8	314.5	316.2	317.8	319.1	320.3	322.2	323.4	324.7	325.9
LOADING 700g (90%) SAMPLE #2	338.6	340.3	342.0	343.4	344.9	346.3	347.8	349.3	350.8	352.3	353.6
LOADING 700g (90%) SAMPLE #3	372.2	373.9	375.5	377.2	378.5	379.9	381.2	382.5	383.8	385.0	386.3
DATE	10/8	10/9	10/10	10/11	10/12	10/13	10/14	10/15	10/16	10/17	10/18
LOADING 300g (40%) SAMPLE #1	96.2	98.9	101.0	103.0	105.1	107.2	109.3	111.6	113.7	115.4	117.0
LOADING 300g (40%) SAMPLE #2	107.2	109.6	111.8	114.0	116.2	118.4	120.5	122.7	124.8	126.4	128.0
LOADING 300g (40%) SAMPLE #3	108.1	110.5	112.7	114.8	117.0	119.0	121.6	124.0	126.0	127.6	129.1

DAYS	19	20	21	22	23	24	25	26	27	28	
DATE	9/22	9/23	9/24	9/25	9/26	9/27	9/28	9/29	9/30	10/1	
LOADING 700g (90%) SAMPLE #1	327.2	328.4	329.9	331.2	332.5	333.7	335.0	336.1	337.3	338.4	
LOADING 700g (90%) SAMPLE #2	354.7	355.8	356.8	357.9	359.0	360.1	361.2	362.2	363.3	364.4	
LOADING 700g (90%) SAMPLE #3	387.5	388.8	389.9	391.0	392.2	393.4	394.6	395.8	396.9	398.0	
DATE	10/19	10/20	10/21	10/22	10/23	10/24	10/25	10/26	10/27	10/28	
LOADING 300g (40%) SAMPLE #1	118.7	119.9	121.4	123.0	124.8	126.2	127.6	129.0	130.7	132.1	
LOADING 300g (40%) SAMPLE #2	129.6	131.2	132.8	134.6	136.1	137.5	138.8	140.2	141.8	143.1	
LOADING 300g (40%) SAMPLE #3	130.7	132.7	134.8	136.6	138.3	139.7	141.2	142.6	143.9	145.2	

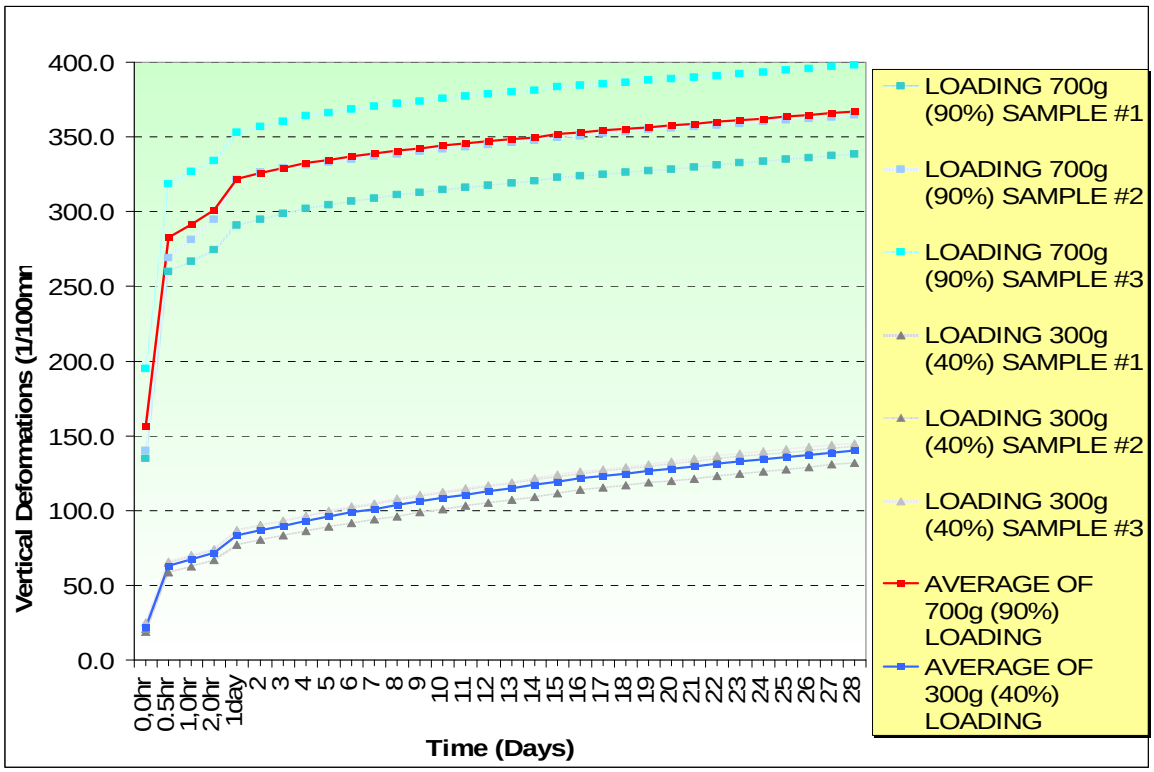

Figure 6.17. Vertical deformations – time curve for B and K mixture samples under 90% - and 40% of failure loads and their average values

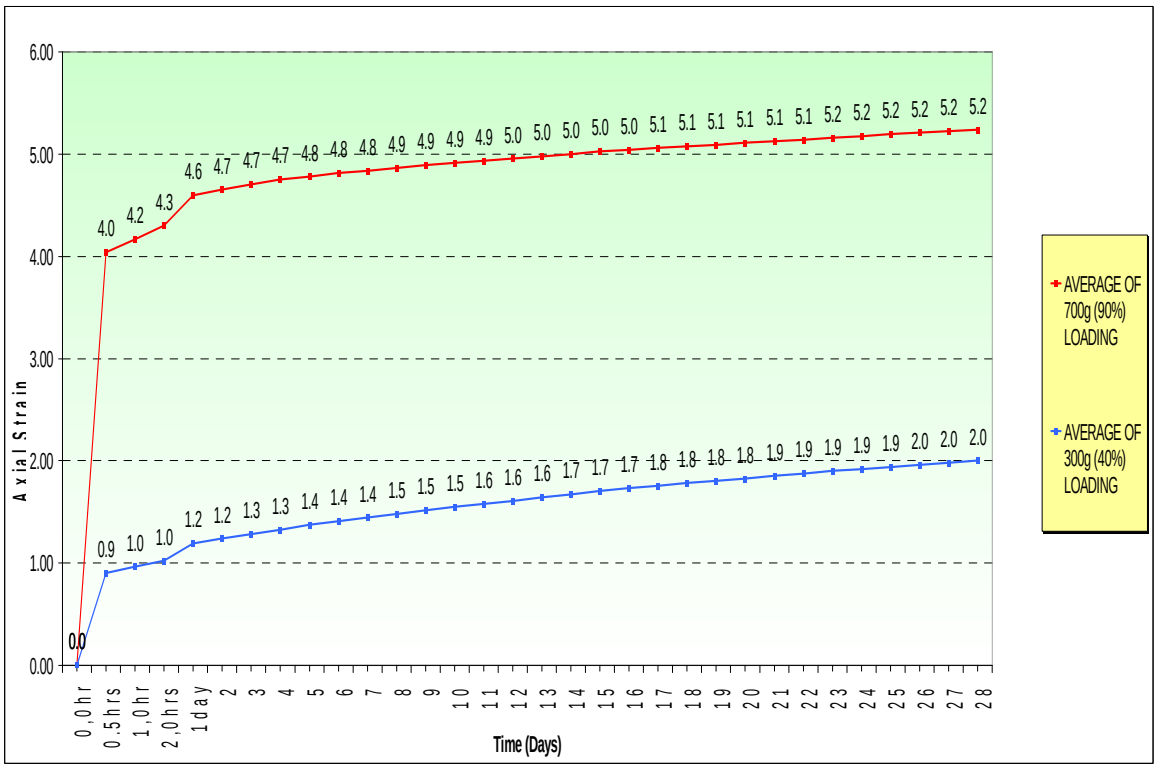

Figure 6.18. Axial strain – time relationship for B and K mixture samples under 90% and 40% of failure loads

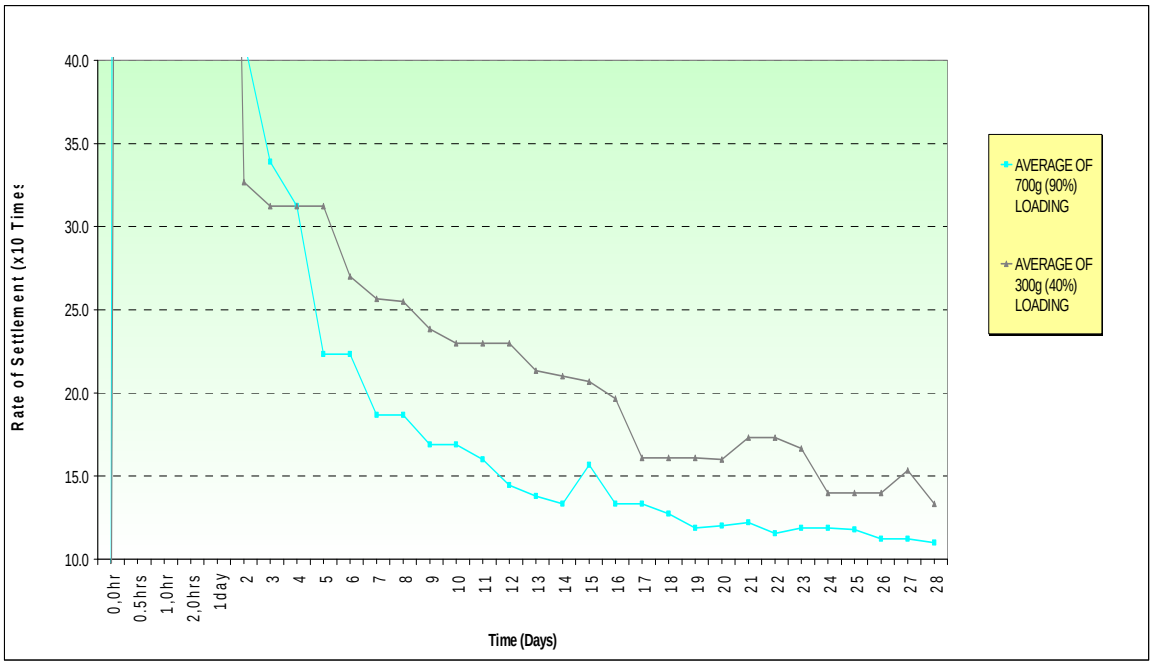

Figure 6.19. Daily rate of settlement values of B and K mixture samples under 90% and 40% of failure loads

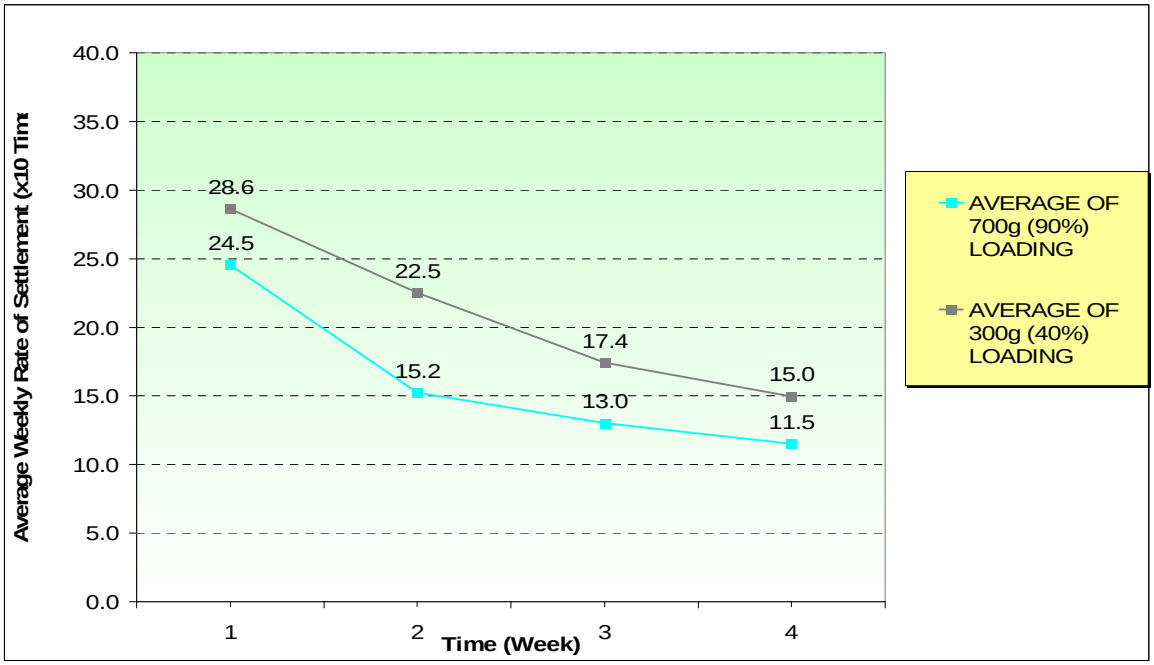

Figure 6.20. Average rate of settlement for B and K mixture samples under 90% and 40% of failure loads on each week

It can be seen from Figure 6.20. that different loading values do not affect the weekly settlement rate changes, both of the rate of settlement values for the 90% and the 40% of failure loads have a tendency to decrease to a future limit value.

6.3.3. Vertical Deformations for Greywacke Samples

Greywacke samples' 28 days vertical deformation data is collected under 90% and 65% of the evaluated failure load by using 450 and 320 gram scales respectively during November and December 2009. Totally 8 samples are failed to evaluate the maximum loading and during the creep tests of 90% of this value, still 5 more samples are failed before placing 3 succesful samples on the device under 450 grams.

Table 6.15. Recorded daily vertical deformation data for greywacke samples under 90% and 65% of failure loads

DAYS	0,0hr	0.5hrs	1,0hr	2,0hrs	4,0hrs	1day	2	3	4	5	6
DATE	11/5	11/5	11/5	11/5	11/5	11/6	11/7	11/8	11/9	11/10	11/11
LOADING 450g (90%) SAMPLE #1	960.0	1,134.3	1,139.0	1,142.0	1,145.0	1,148.0	1,149.6	1,151.2	1,152.8	1,154.4	1,155.9
LOADING 450g (90%) SAMPLE #2	1,150.0	1,338.7	1,345.0	1,348.1	1,349.7	1,351.3	1,352.8	1,354.3	1,355.8	1,357.3	1,358.7
LOADING 450g (90%) SAMPLE #3	1,200.0	1,484.0	1,490.5	1,493.5	1,496.5	1,499.5	1,500.9	1,502.3	1,503.7	1,505.0	1,506.2
DATE	12/3	12/3	12/3	12/3	12/3	12/4	12/5	12/6	12/7	12/8	12/9
LOADING 320g (65%) SAMPLE #1	500.0	713.9	717.9	731.2	753.0	758.0	759.4	760.9	762.3	763.7	765.1
LOADING 320g (65%) SAMPLE #2	640.0	850.0	857.6	866.8	875.6	881.0	882.3	883.5	884.8	886.2	887.5
LOADING 320g (65%) SAMPLE #3	740.0	935.2	943.0	955.1	957.9	962.0	963.2	964.4	965.6	966.7	967.8

DAYS	7	8	9	10	11	12	13	14	15	16	17
DATE	11/12	11/13	11/14	11/15	11/16	11/17	11/18	11/19	11/20	11/21	11/22
LOADING 450g (90%) SAMPLE #1	1,157.4	1,158.9	1,160.3	1,161.8	1,163.2	1,164.3	1,165.4	1,166.5	1,167.4	1,168.2	1,169.1
LOADING 450g (90%) SAMPLE #2	1,360.1	1,361.5	1,362.8	1,364.0	1,365.3	1,366.4	1,367.4	1,368.4	1,369.4	1,370.2	1,371.0
LOADING 450g (90%) SAMPLE #3	1,507.5	1,508.8	1,510.1	1,511.3	1,512.6	1,513.9	1,515.2	1,516.4	1,517.6	1,518.5	1,519.3
DATE	12/10	12/11	12/12	12/13	12/14	12/15	12/16	12/17	12/18	12/19	12/20
LOADING 320g (65%) SAMPLE #1	766.5	767.8	769.0	770.1	771.3	772.5	773.7	774.9	776.0	776.8	777.5
LOADING 320g (65%) SAMPLE #2	888.9	890.3	891.6	892.9	894.2	895.5	896.8	898.1	899.3	900.2	901.1
LOADING 320g (65%) SAMPLE #3	968.9	970.0	970.9	971.7	972.6	973.4	974.2	975.0	975.6	976.1	976.6

DAYS	18	19	20	21	22	23	24	25	26	27	28
DATE	11/23	11/24	11/25	11/26	11/27	11/28	11/29	11/30	12/1	12/2	12/3
LOADING 450g (90%) SAMPLE #1	1,169.9	1,170.7	1,171.5	1,172.3	1,173.1	1,173.9	1,174.6	1,175.4	1,176.1	1,176.8	1,177.5
LOADING 450g (90%) SAMPLE #2	1,371.8	1,372.6	1,373.4	1,374.2	1,375.0	1,375.8	1,376.5	1,377.3	1,378.0	1,378.7	1,379.4
LOADING 450g (90%) SAMPLE #3	1,520.2	1,521.0	1,521.8	1,522.6	1,523.4	1,524.2	1,524.9	1,525.7	1,526.4	1,527.1	1,527.8
DATE	12/21	12/22	12/23	12/24	12/25	12/26	12/27	12/28	12/29	12/30	12/31
LOADING 320g (65%) SAMPLE #1	778.3	778.9	779.5	780.0	780.5	781.0	781.5	782.0	782.5	782.9	783.3
LOADING 320g (65%) SAMPLE #2	902.0	902.6	903.2	903.8	904.4	905.0	905.5	906.1	906.7	907.2	907.7
LOADING 320g (65%) SAMPLE #3	977.1	977.6	978.0	978.4	978.9	979.3	979.7	980.1	980.5	980.8	981.2

Table 6.16. Average vertical deformation values for greywacke samples under 90% and 65% of failure loads

DAYS	0,0hr	0.5hrs	1,0hr	2,0hrs	4,0hrs	1day	2	3	4	5	6
AVERAGE OF 450g (90%) LOADING	1,103.3	1,319.0	1,324.8	1,327.9	1,330.4	1,332.9	1,334.4	1,335.9	1,337.4	1,338.9	1,340.3
AVERAGE OF 320g (65%) LOADING	626.7	833.0	839.5	851.0	862.2	867.0	868.3	869.6	870.9	872.2	873.5

DAYS	7	8	9	10	11	12	13	14	15	16	17
AVERAGE OF 450g (90%) LOADING	1,341.7	1,343.1	1,344.4	1,345.7	1,347.0	1,348.2	1,349.3	1,350.4	1,351.5	1,352.3	1,353.1
AVERAGE OF 320g (65%) LOADING	874.8	876.0	877.1	878.3	879.4	880.5	881.6	882.7	883.6	884.4	885.1

DAYS	18	19	20	21	22	23	24	25	26	27	28
AVERAGE OF 450g (90%) LOADING	1,354.0	1,354.8	1,355.6	1,356.4	1,357.2	1,357.9	1,358.7	1,359.5	1,360.2	1,360.9	1,361.6
AVERAGE OF 320g (65%) LOADING	885.8	886.4	886.9	887.4	887.9	888.4	888.9	889.4	889.9	890.3	890.7

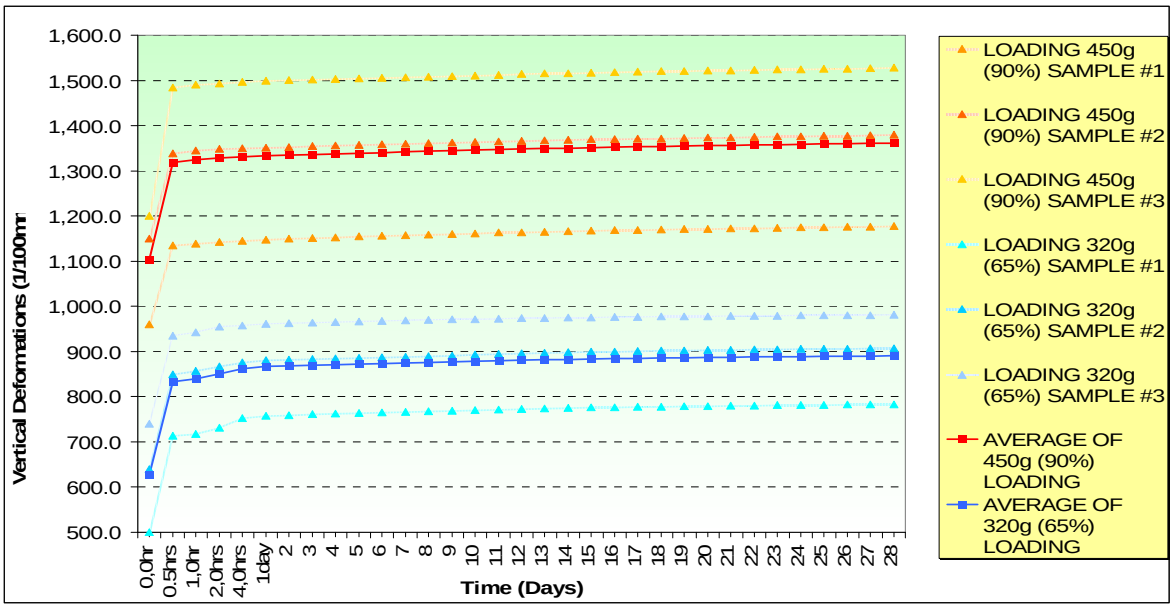

Figure 6.21. Vertical deformations – time curves for greywacke samples under 90% and 65% of failure loads and their average values

During November and December 2009, 28 days long creep tests are done on 6 greywacke samples loaded under 90% and 65% of failure loads respectively. Their recorded data and calculated average values are shown in Tables 6.15. and 6.16. Average values shown in Figure 6.21. are representative, though a little more scattered at higher loads than the lower ones as well as clay average values as can be seen and compared from Figure 6.17.

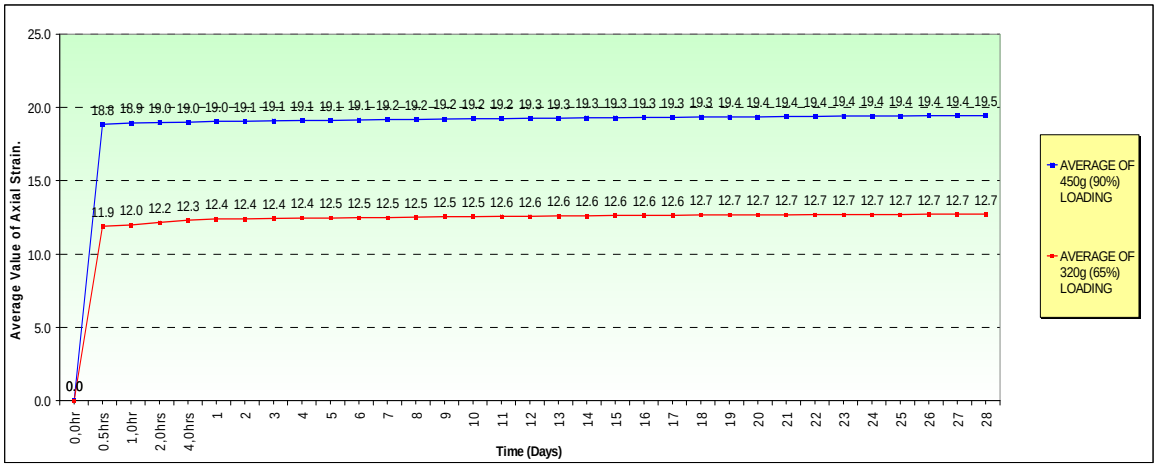

Figure 6.22. Axial strain – time relationship curves for greywacke samples under 90% and 65% of failure loads

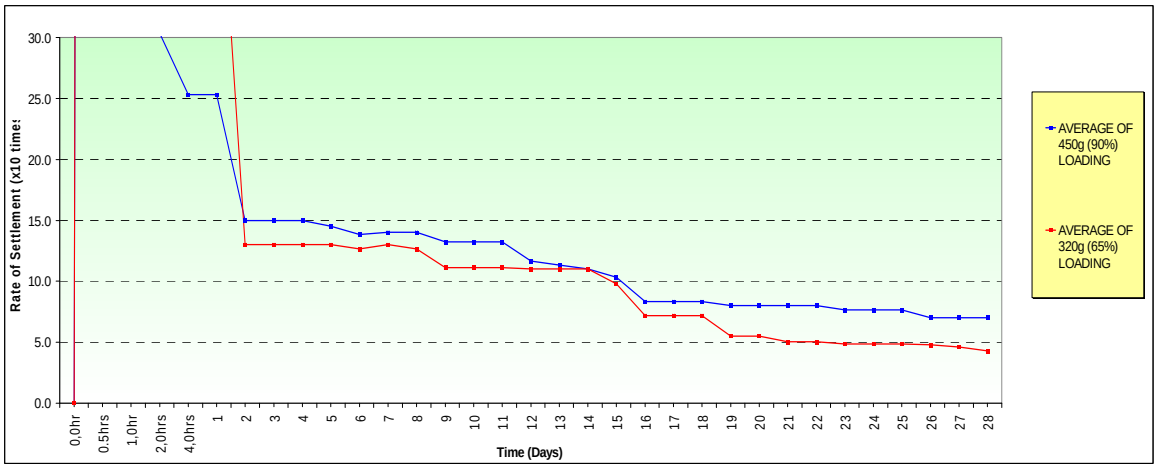

Figure 6.23. Daily rate of settlement values for greywacke samples under 90% and 65% of failure loads

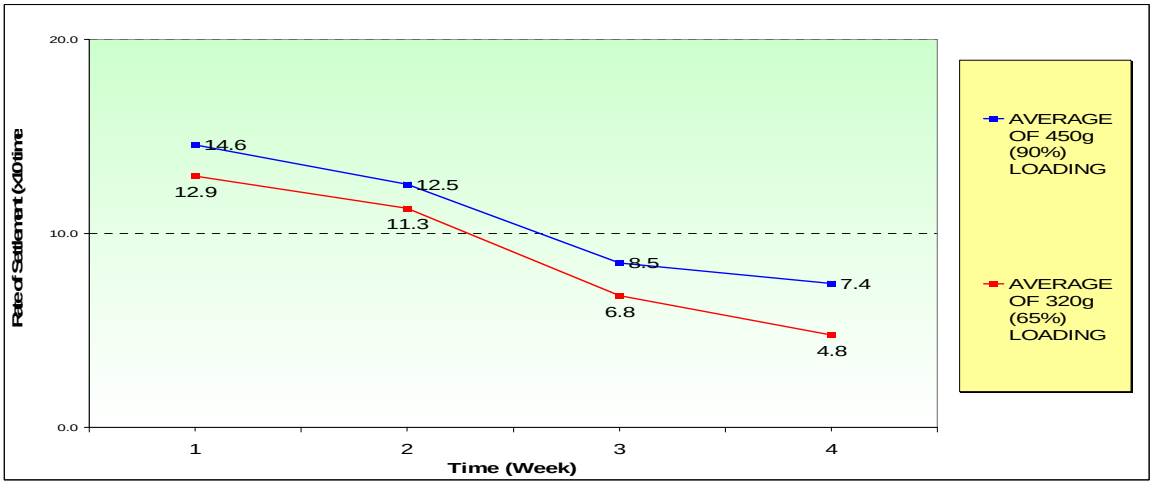

Figure 6.24. Weekly rate of settlement values for greywacke samples under 90% and 65% of failure loads

Table 6.17. Vertical deformation values for greywacke samples under 40% of failure loads

DAYS	0,0hr	0.5hrs	1,0hr	2,0hrs	4,0hrs	1day	2	3	4	5	6
LOADING 200g (40%) SAMPLE #1	25.0	59.0	63.1	67.2	71.3	81.0	83.6	86.1	88.7	91.2	93.8
LOADING 200g (40%) SAMPLE #2	22.0	44.6	47.1	49.7	52.8	67.2	74.2	76.9	79.6	82.3	85.2

DAYS	7	8	9	10	11	12	13	14	15	16	17
LOADING 200g (40%) SAMPLE #1	96.3	98.8	101.3	103.8	106.3	108.8	111.3	113.8	116.2	118.6	120.9
LOADING 200g (40%) SAMPLE #2	88.1	91.0	94.0	97.0	100.1	103.1	106.0	109.0			

DAYS	18	19	20	21	22	23	24	25	26	27	28
LOADING 200g (40%) SAMPLE #1	123.3	125.6	127.9	130.4	132.9	135.4	137.9	140.4	142.7	145.0	147.2
LOADING 200g (40%) SAMPLE #2											

On January 2010, 28 day long creep tests started on two greywacke samples, under 40% of their failure loads. Their recorded data is shown in Table 6.17 and vertical deformations plotted in Figure 6.25. The reason for using only 2 samples was the unavailability of the oedemeter devices and even after 14 days, one of the sample was taken out of the device without my knowledge so its data have not been obtained for the last 14 days, leaving only a sample to plot the necessary curves seen between Figures 6.25. to 6.28.

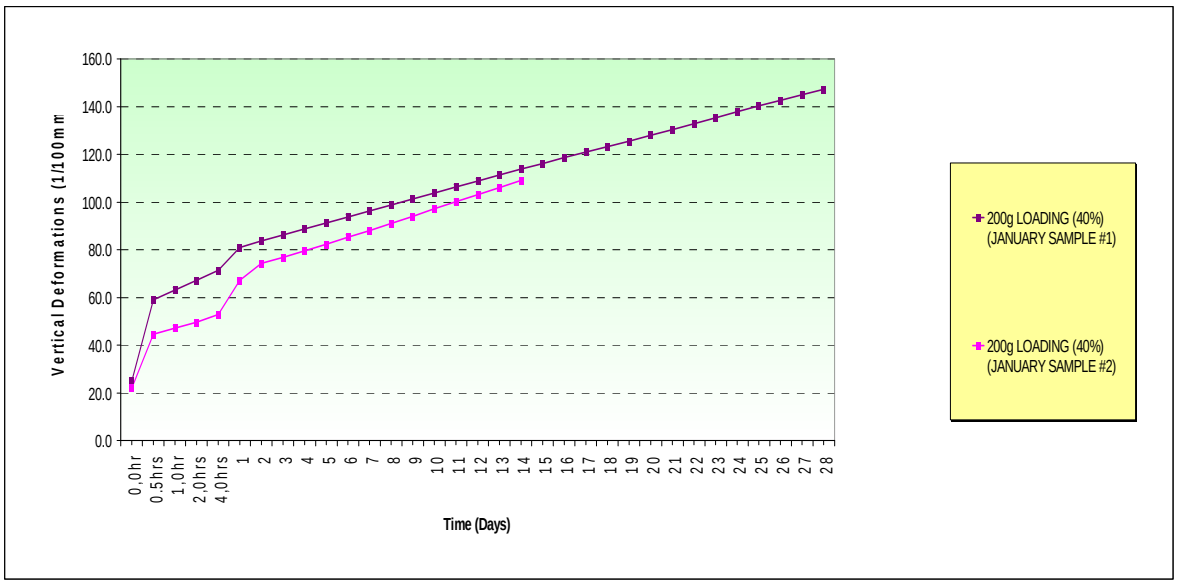

Figure 6.25. Vertical deformations – time curves for 2 greywacke samples under 40% of the failure loads – Tests done on January

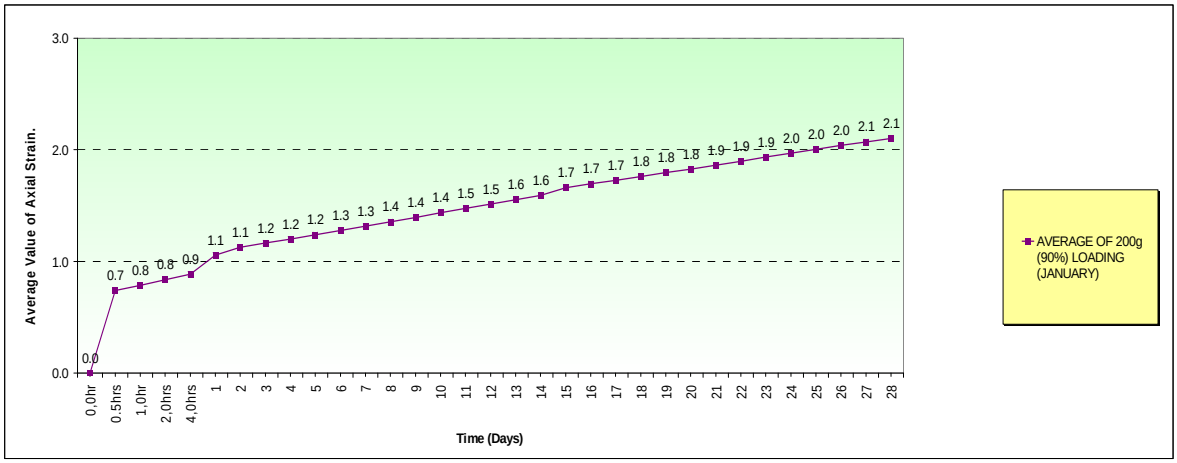

Figure 6.26. Axial strain – time relationship curve for greywacke sample under 40% of the failure loads – Tests done on January

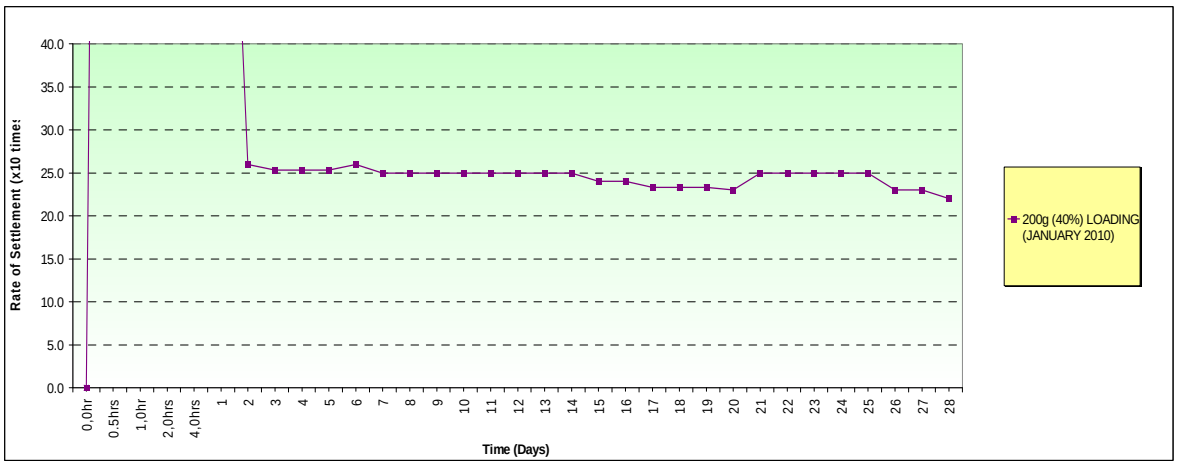

Figure 6.27. Daily rate of settlement values for greywacke sample under 40% of the failure loads – Tests done on January

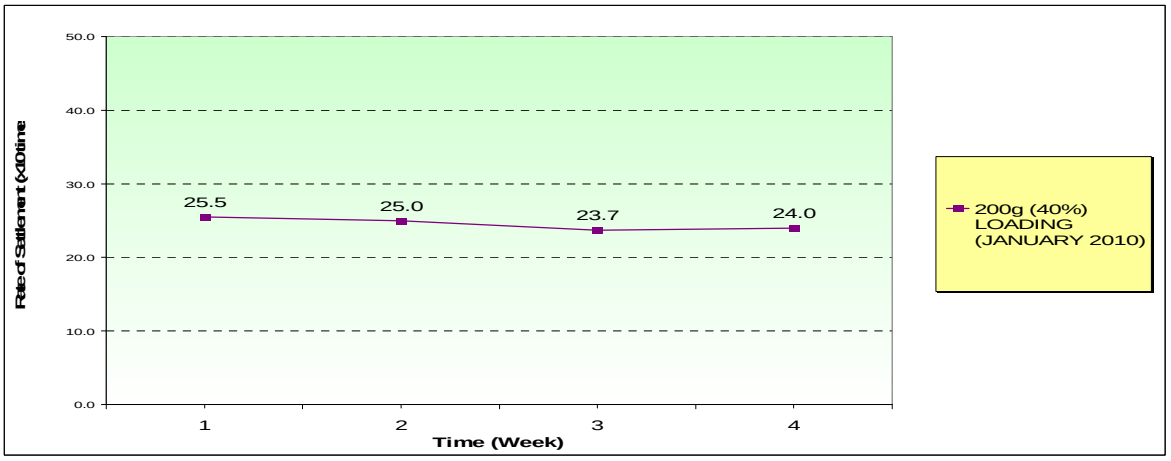

Figure 6.28. Weekly rate of settlement values for greywacke sample under 40% of the failure loads – Tests done on January

Table 6.18. Vertical deformation values for greywacke samples under 90% and 40% of failure loads

DAYS	0,0hr	0.5hrs	1,0hr	2,0hrs	4,0hrs	1day	2	3	4	5	6
450g (90%) LOADING	600.0	920.0	930.0	937.0	942.0	946.4	947.9	949.4	950.9	952.3	953.9
200g (40%) LOADING	50.0	90.0	96.0	101.0	106.0	111.0	114.8	118.6	122.4	126.0	129.7

DAYS	7	8	9	10	11	12	13	14	15	16	17
450g (90%) LOADING	955.5	956.9	958.2	959.4	960.7	962.0	963.3	964.7	965.9	967.2	968.5
200g (40%) LOADING	133.7	137.3	141.1	144.9	148.7	152.2	155.7	159.6	163.5	166.9	170.3

DAYS	18	19	20	21	22	23	24	25	26	27	28
450g (90%) LOADING	969.8	971.0	972.2	973.8	975.1	976.4	977.6	978.9	980.0	981.1	982.3
200g (40%) LOADING	173.7	176.7	179.8	183.2	186.3	189.0	191.8	194.5	197.1	199.7	202.4

Another problem encountered by the end of December was the consuming of all the prepared greywacke material during previous tests. So water content analyses are made from newly sieved and prepared greywacke samples and as mentioned at the optimum water content tests results, a change in the water content and the unit weight values was seen. In order to check the reliability of the loading and whether this newly prepared greywacke sample behaves likewise, 2 more creep tests done on February 2010. Samples are loaded, one with 40% of its failure load and the other with 90% of its failure load, for 28 days. Their recorded data is shown in Table 6.18 and the curves were plotted through Figures 6.29. to 6.32.

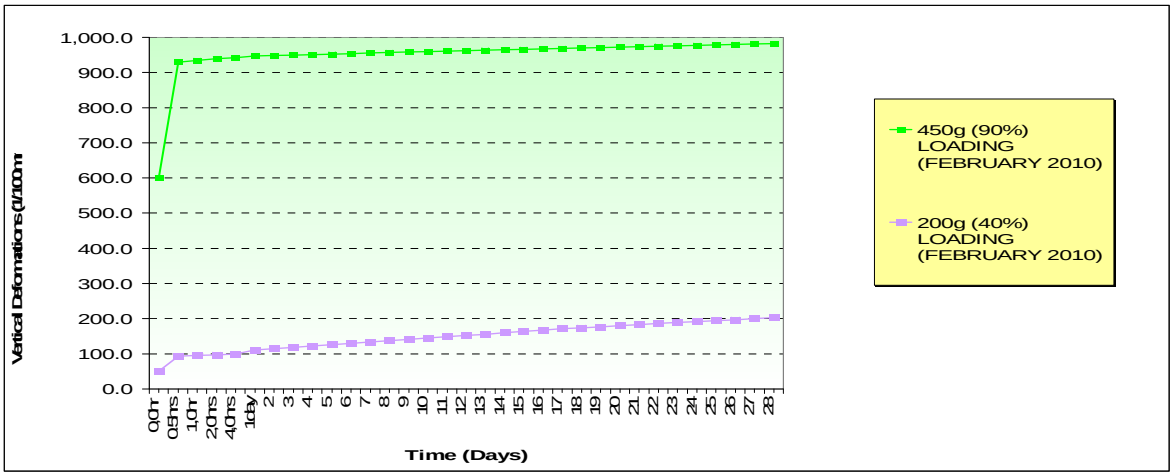

Figure 6.29. Vertical deformations – time curves for 2 greywacke samples under 90% and 40% of failure loads

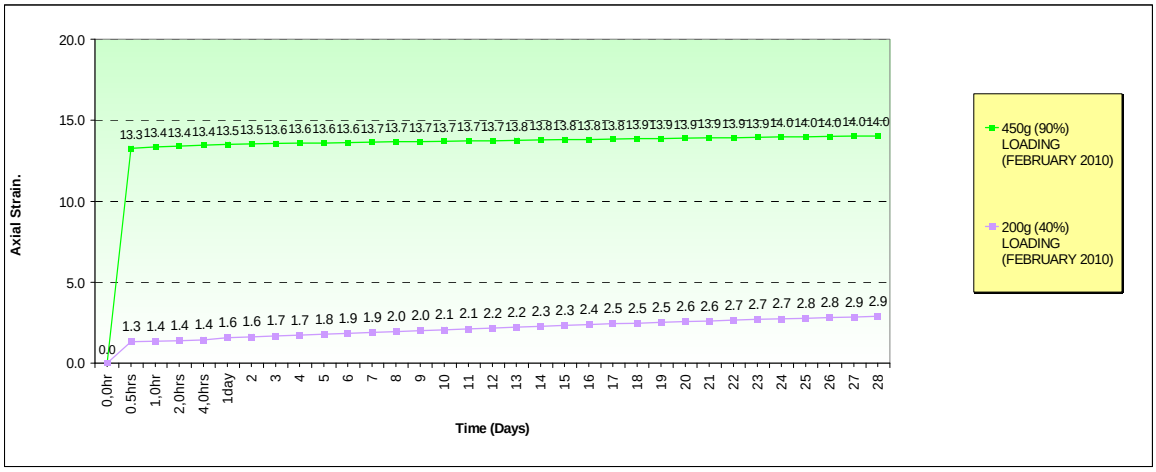

Figure 6.30. Axial strain – time relationship curves for 2 greywacke samples under 90% and 40% of their failure loads – Tests done on February

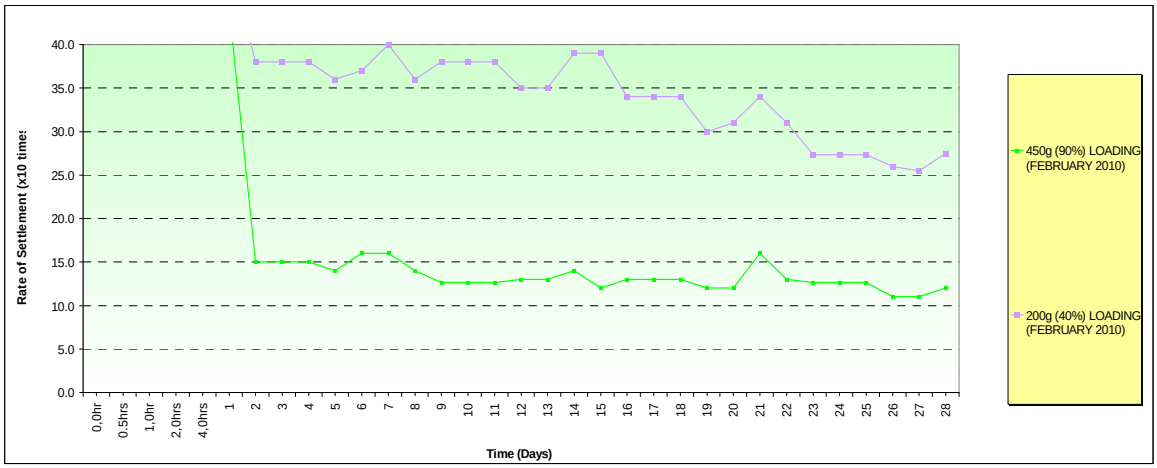

Figure 6.31. Daily rate of settlement values for 2 greywacke samples under 90% and 40% of their failure loads – Tests done on February

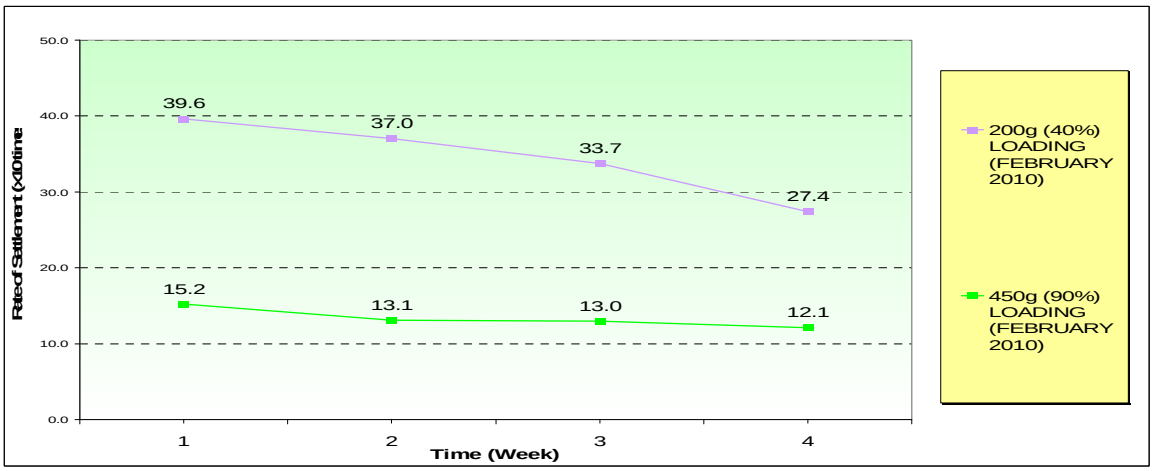

Figure 6.32. Weekly rate of settlement values for 2 greywacke samples under 90% and 40% of their failure loads – Tests done on February

For comparison, all tested greywacke samples' daily and weekly rate of settlement time relationship graphs are shown on Figures 6.33. and 6.34.

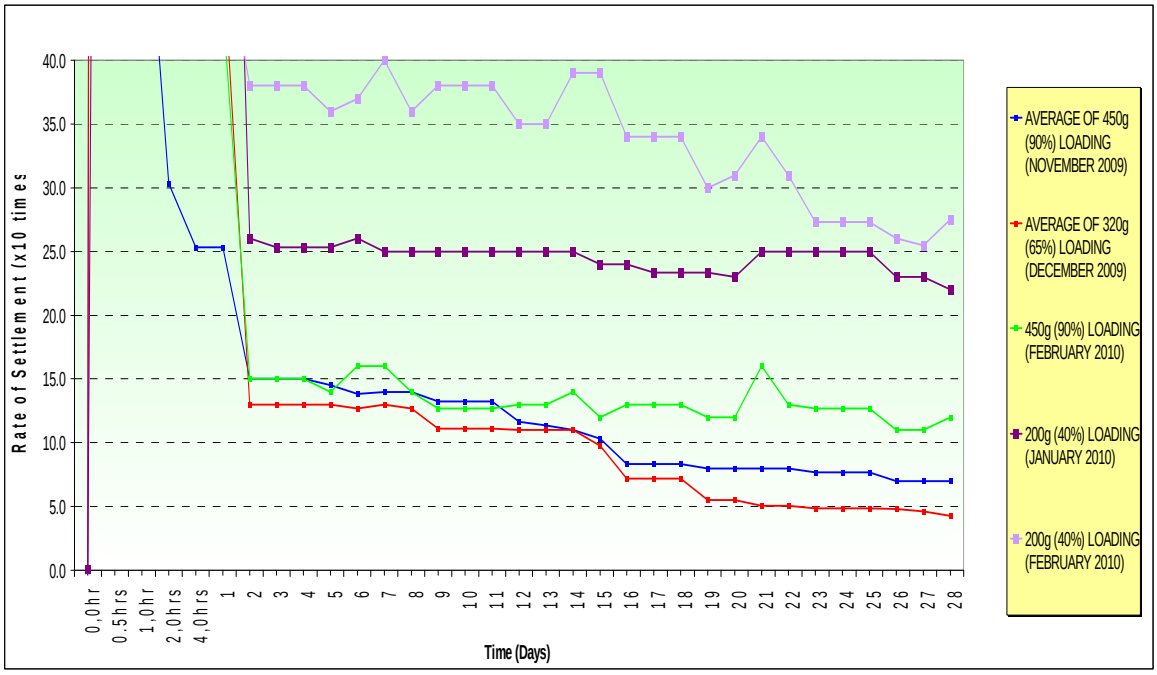

Figure 6.33. Daily rate of settlement values for greywacke samples under 90% - 65% and 40% of their failure loads

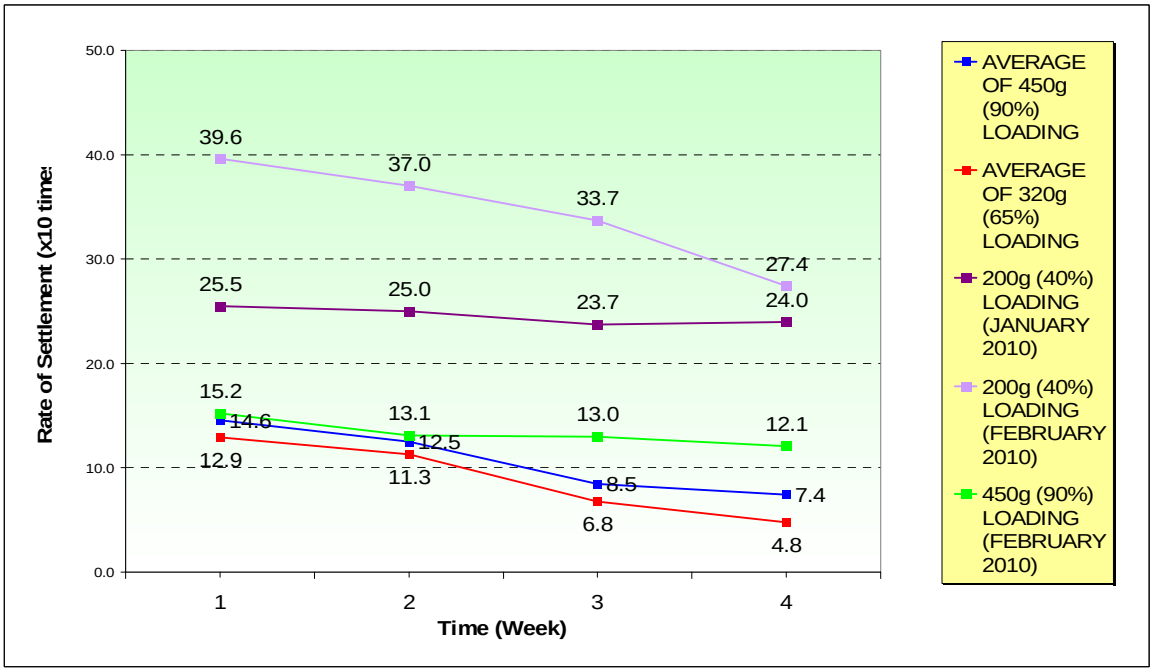

Figure 6.34. Weekly rate of settlement values for greywacke samples under 90% - 65% and 40% of their failure loads

6.4. Comparisons and Test Result Discussions

In order to understand the difference between the behaviour of kaolinite and bentonite-kaolinite mixture samples, their rate of settlement data is plotted on the same graph in Figure 6.35.

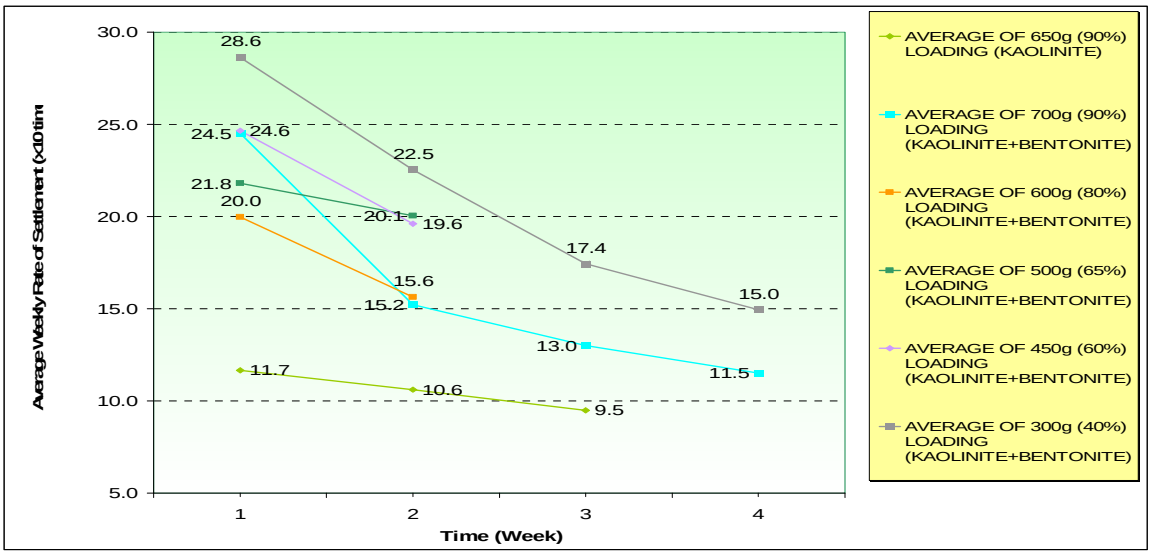

Figure 6.35. Comparing weekly rate of settlements of high and low plasticity clays (Kaolinite vs. B and K mixture)

Seen in Figure 6.36. below are the data for the high plastic clay and greywacke samples plotted together on the same graph.

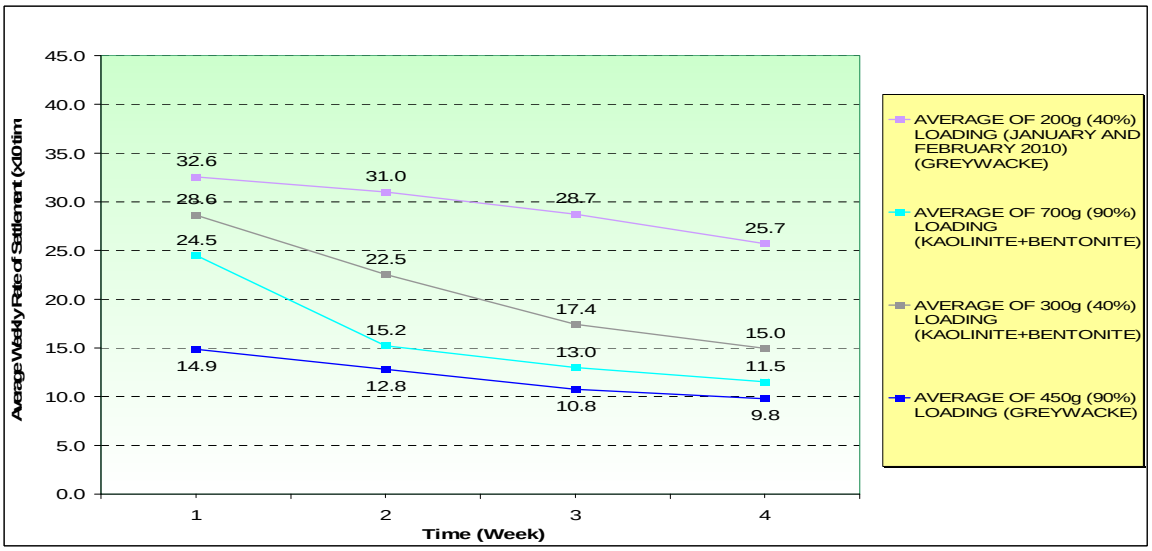

Figure 6.36. Comparing weekly rate of settlements of high plasticity clays with greywackes under 90% and 40% of their failure loads

To compare the behaviour of greywackes with kaolinites, their average weekly settlement rates are plotted together on the same graph as shown in Figure 6.37.

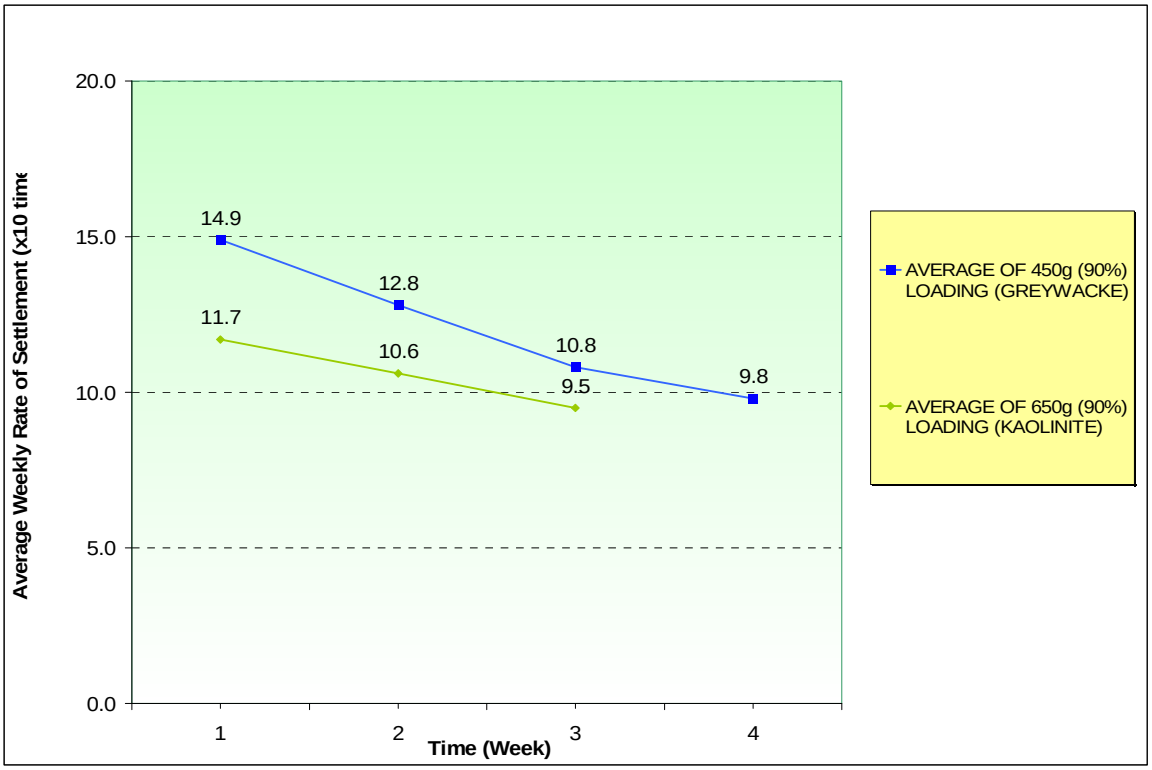

Figure 6.37. Comparing low plasticity clays (kaolinite) with greywackes under 90% of their failure loads

We can say that low plastic clays have a linear rate of settlement, as weeks passed kaolinite samples do settle almost at the same amounts, where this does not apply for bentonite and kaolinite mixture. High plastic clays' initial settlement rates are greater than the ongoing weekly rate values.

The relation between highly plastic clays and greywackes are much more complex, as Figure 6.36 indicates, at low loads greywackes have a settlement rate greater than bentonite and kaolinite mixture, but at high loads their settlement rates becomes lesser.

As seen from Figure 6.37. kaolinite samples have similar rate of settlement values with greywacke samples under 90% of their failure loading. The difference is that greywackes settle more initially and their settlement rate decreases as the weeks passed.

Figure 6.38. shown below is for the comparison of all samples used in the tests, average weekly rate of settlement values for kaolinite samples, bentonite-kaolinite mixture samples and greywacke samples is plotted on the same graph.

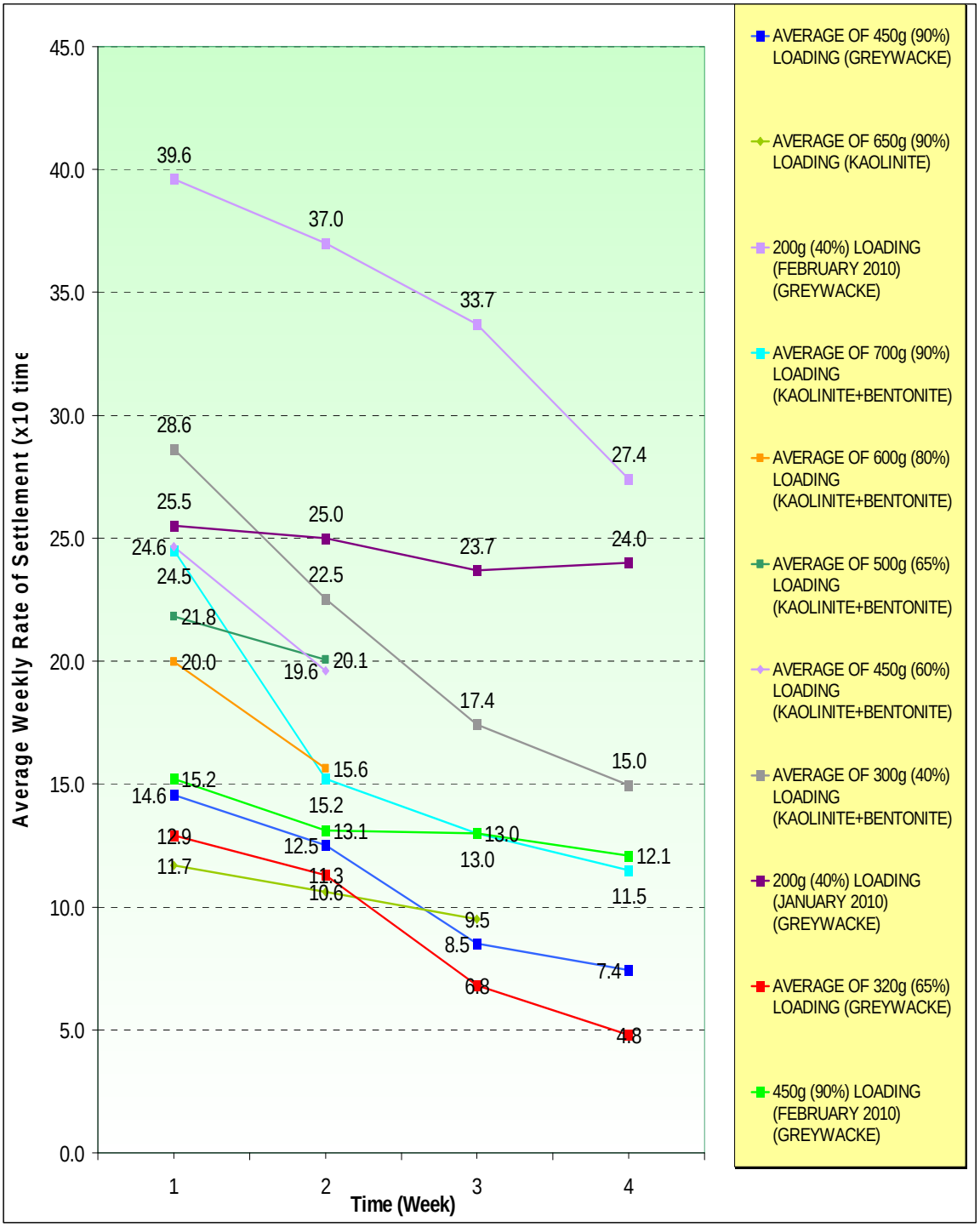

Figure 6.38. Comparing weekly settlement rates of all three types of soils under all of the used test loads

7. CONCLUSION

The main purpose of this research was to determine the creep properties of soils with different plasticity to be used as fill materials at geosynthetic reinforced walls. For this purpose 2 different clays with high and low plasticity and 1 type of greywacke are prepared and tested in an oedometer apparatus to observe the long term creep effects, and creep rupture under various loading. Creep rupture was not observed in any of the tests, where even after 28 days all samples have a tendency to continue settlement, but with a slower rate.

Failure loads evaluated for the 3 soil types are 725gr (85kPa) - 800gr (90kPa) and 500gr (55kPa) for kaolinite samples, bentonite-kaolinite mixture samples and greywacke samples respectively. These are average values obtained by breaking 15-20 samples of each kind on the same testing device.

We can say that loading directly affects vertical deformations for clay and greywacke samples with lower loads gives lower initial (first 24hours) and ending deformations. When we compare the weekly rate of settlement values of greywacke samples we can say that loading does not effect much on their first 7 days values but there's again a certain drop on the 28 days values on all loads.

From the comparison graphs, it can be seen that high plasticity clays have a greater range of settlement drop with a concave curve, with tendency to drop less on the onward weeks, than low plastic clays and greywackes, and they settle much more even on less loading than 40% of failure loads than low plastic clays, which have lower and linear rate of settlement on their 90% of failure loading.

The relationship between high plastic clays and greywackes are much different. Where under low loads, like 40% of their failure loads, greywackes have the greatest rate of settlement values with a convex curve, a tendency to drop more on the onward weeks, than the concave curves of high plastic clays with lesser rate of settlement, and under higher loads like 40% of failure loads, clays with high plasticity have greater rate of settlement values than greywackes.

When we compare low plastic clays with greywackes under 90% of their failure loading, we can say that their weekly rate of settlement averages are similar, but greywackes have a tendency to drop more on the onward weeks, where clays with low plasticity have linear drop in the rate of settlement values.

Table 7.1. Comparing testing results of all types of soils covered in this study

SOIL TYPES	GREYWACKE	KAOLINITE	50%KAOLINITE-50%BENTONITE
LIQUID LIMIT VALUE	25	29	56
PLASTIC LIMIT VALUE	NA	20	22
PLASTICITY INDEX	NA	9	34
UNIT WEIGHT (TON/M3)	1.78	1.65	1.33
EVALUATED FAILURE LOAD (kPa)	55-60	85-90	90
INITIAL DEFORMATION AVERAGES AT 90% OF FAILURE LOAD (1st DAY-1/100MM)	1,333	150	322
VERTICAL DEFORMATIONS AT 90% OF FAILURE LOAD (28th DAY-1/100MM)	1,360	180	367
RATE OF SETTLEMENT VALUES (14-DAYS)	12.48	10.33	15.22
RATE OF SETTLEMENT VALUES (28-DAYS)	7.42	9.25	11.50

Seen on Table 7.1 are the tests results of all types of soils used in the tests. Under the light of the data shown, we can say that with high PI, resistance to pressures become higher and failure loads increases respectively. Also the increase rate of initial consolidation decreases which reflects an increase in secondary consolidation slope values.

APPENDIX A: D4405 – 04 STANDARD TEST METHOD FOR CREEP OF SOFT ROCK CORE SPECIMENS IN UNIAXIAL COMPRESSION AT AMBIENT OR ELEVATED TEMPERATURE

A.1. Scope

A.1.1 This test method covers the creep behavior of intact cylindrical soft rock core specimens in uniaxial compression. It specifies the apparatus, instrumentation, and procedures for determining the strain as a function of time under sustained load. Soft rocks include such materials as salt and potash, which often exhibit very large strain at failure.

A.1.2 All observed and calculated values shall conform to the guidelines for significant digits and rounding established in Practice D 6026.

A.1.2.1 The method used to specify how data are collected, calculated, or recorded in this standard is not directly related to the accuracy to which the data can be applied in design or other uses, or both. How one applies the results obtained using this standard is beyond its scope.

A.1.3 The values stated SI units are to be regarded as the standard.

A.1.4 This standard does not purport to address all of the safety concerns, if any, associated with its use. It is the responsibility of the user of this standard to establish appropriate safety and health practices and determine the applicability of regulatory limitations prior to use.

A.2. Referenced Documents

A.2.1 ASTM Standards:

D 653 Terminology Relating to Soil, Rock, and Contained Fluids
D 2113 Practice for Diamond Core Drilling for Site Investigation
D 2216 Test Method for Laboratory Determination of Water Content of Soil and Rock

D 3740 Practice for Minimum Requirements for Agencies Engaged in the Testing and/or Inspection of Soil and Rock as Used in Engineering Design and Construction
D 4543 Practice for Preparing Rock Core Specimens and Determining Dimensional and Shape Tolerances
D 5079 Practices for Preserving and Transporting Rock Core Samples
D 6026 Practice for Using Significant Digits in Geotechnical Data
E 4 Practices for Load Verification of Testing Machines
E 122 Practice for Choice of Sample Size to Estimate a Measure of Quality for a Lot or Process

A.3. Terminology

A.3.1 Refer to Terminology D 653 for specific definitions.

A.4. Summary of Test Method

A.4.1 A section of rock core is cut to length and the ends are machined at to produce a cylindrical test specimen. The specimen is placed in a loading frame and, if required, heated to the desired test temperature. Axial load is rapidly applied to the specimen and sustained. Deformation is monitored as a function of elapsed time.

A.5. Significance and Use

A.5.1 There are many underground structures that are created for permanent or long-term use. Often these structures are subjected to an approximately constant load. Creep tests provide quantitative parameters for the stability analysis of these structures.

A.5.2 The deformation and strength properties of rock cores measured in the laboratory usually do not accurately reflect large-scale in situ properties, because the latter are strongly influenced by joints, faults, inhomogeneities, weakness planes, and other factors. Therefore, laboratory values for intact specimens must be employed with proper judgment in engineering applications.

NOTE 1—Notwithstanding the statements on precision and bias contained in this test method; the precision of this test method is dependent on the competence of the personnel performing it, and the suitability of the equipment and facilities used. Agencies that meet the criteria of Practice D 3740 are generally considered capable of competent and objective testing. Users of this test method are cautioned that compliance with Practice D 3740 does not in itself assure reliable testing. Reliable testing depends on many factors; Practice D 3740 provides a means of evaluating some of these factors.

A.6. Apparatus

A.6.1 Loading Device —The loading device shall be of sufficient capacity to apply load at a rate conforming to the requirements specified in 10.5 and shall be able to maintain the specified load within 2 %. It shall be verified at suitable time intervals in accordance with the procedures given in Practices E 4 and comply with the requirements prescribed in this test method.

NOTE 2—By definition, creep is the time-dependent deformation under constant stress. The loading device is specified to maintain constant axial load, and therefore, constant engineering stress. The true stress, however, decreases as the specimen deforms and the cross-sectional area increases. Because of the associated experimental ease, constant load testing is recommended. However, the procedure permits constant true-stress testing, provided that the applied load is increased with specimen deformation so that true stress is constant within 2 %.

A.6.2 Elevated-Temperature Enclosure —The elevated temperature enclosure may be either an enclosure that fits in the loading apparatus or an external system encompassing the complete test apparatus. The enclosure may be equipped with humidity control for testing specimens in which the moisture content is to be controlled. For high temperatures a system of heaters, insulation, and temperature measuring devices are normally required to maintain the specified temperature. Temperature shall be measured at three locations, with one sensor near the top, one at midheight, and one near the bottom of the specimen. The average specimen temperature based on the midheight sensor shall be maintained to within ±1°C of the required test temperature. The maximum temperature difference between the midheight

sensor and either end sensor shall not exceed 3°C.

NOTE 3—An alternative to measuring the temperature at three locations along the specimen during the test is to determine the temperature distribution in a dummy specimen that has temperature sensors located in drill holes at a minimum of six positions: along both the centerline and specimen periphery at midheight and each end of the specimen. The temperature controller set point shall be adjusted to obtain steady-state temperatures in the dummy specimen that meet the temperature requirements at each test temperature (the centerline temperature at midheight shall be within ±1°C of the required test temperature, and all other specimen temperatures shall not deviate from this temperature by more than 3°C). The relationship between controller set point and dummy specimen temperature can be used to determine the specimen temperature during testing, provided that the output of the temperature feedback sensor (or other fixed-location temperature sensor in the triaxial apparatus) is maintained constant within ±1°C of the required test temperature. The relationship between temperature controller set point and steady-state specimen temperature shall be verified periodically. The dummy specimen is used solely to determine the temperature distribution in a specimen in the elevated temperature enclosure; it is not to be used to determine creep behaviour.

A.6.3 Temperature Measuring Device—Special limits-of-error thermocouples or platinum resistance thermometers (RTDs) having accuracies of at least ±1.0°C with a resolution of 0.1°C.

A.6.4 Platens—Two steel platens are used to transmit the axial load to the ends of the specimen. They shall have a hardness of not less than 58 HRC. One of the platens should be spherically seated and the other a plain rigid platen. The bearing faces shall not depart from a plane by more than 0.015 mm when the platens are new and shall be maintained within a permissible variation of 0.025 mm. The diameter of the spherical seat shall be at least as large as that of the test specimen but shall not exceed twice the diameter of the test specimen. The center of the sphere in the spherical seat shall coincide with that of the bearing face of the specimen. The spherical seat shall be properly lubricated to assure free movement. The movable portion of the platen shall be held closely in the spherical seat, but the design shall be such that the bearing face can be rotated and tilted through small angles

in any direction. If a spherical seat is not used, the bearing faces of the platens shall be parallel to 0.0005 mm/mm of platen diameter. The platen diameter shall be at least as great as the specimen but shall not exceed the specimen diameter by more than 10 % of the specimen diameter.

NOTE 4—Because soft rocks can deform significantly in creep tests it is important to reduce friction in the platen-specimen interfaces to facilitate relative slip between the specimen ends and the platens. Effective friction-reducing precautions include polishing the platen surfaces to a mirror finish and attaching a thin, 0.15-mm thick te on sheet to the platen surfaces.

A.6.5 Strain/Deformation Measuring Devices—The strain/ deformation measuring system shall measure the strain with a resolution of at least 25 X 10^{-6} strain and an accuracy within 2 % of the value of readings above 25 X 10^{-6} strain and an accuracy and resolution within 5 X 10^{-6} for readings lower than 250 X 10^{-6} strain, including errors introduced by excitation and readout equipment. The system shall be free from noncharacterizable long-term instability (drift) that results in an apparent strain of 10^{-8} per second.

A.6.5.1 Axial Strain Determination —The axial deformations or strains may be determined from data obtained by electrical strain gages, compressometers, linear variable differential transformers (LVDTs), or other suitable means. The design of the measuring device shall be such that the average of at least two axial strain measurements can be determined. Measuring positions shall be equally spaced around the circumference of the specimen close to midheight. The gage length over which the axial strains are determined shall be at least ten grain diameters in magnitude

A.6.5.2 Lateral Strain Determination —The lateral deformations or strains may be measured by any of the methods mentioned in 6.5.1. Either circumferential or diametrical deformations (or strains) may be measured. A single transducer that wraps around the specimen can be used to measure the change in circumference. At least two diametric deformation sensors shall be used if diametric deformations are measured These sensors shall be equally spaced around the circumference of the specimen close to midheight. The average deformation (or strain) from the diametric sensors shall be recorded.

Note 5—The use of strain gage adhesives requiring cure temperatures above 65°C is not allowed unless it is known that microfractures do not develop at the cure temperature.

A.7. Safety Precautions

A.7.1 Many rock types fail in a violent manner when loaded to failure in compression. A protective shield should be placed around the test specimen to prevent injury from flying rock fragments.

A.7.2 Elevated temperatures increase the risks of electrical shorts, fire, and burns.

A.8. Sampling

A.8.1 Samples can be either drill cores obtain directly from the in situ rock or obtained from block samples cored in the field or in the laboratory.

A.8.2 Moisture condition can have a significant effect upon the deformation of the rock. Test samples must meet any requirements determined in section 9.2. Therefore, it follows that the field moisture condition of the samples may need protection during and after sampling. This may require special collection and handling techniques such as those outlined in Practices D 2113 and D 5079.

A.8.3 The location of the specimens for each test sample shall be selected from the cores to represent a valid average of the type of rock under consideration. This can be achieved by visual observations of mineral constituents, grain sizes and shape, partings and defects such as pores and fissures, or by other methods such as ultrasonic velocity measurements.

A.8.4 The number of specimens required to obtain a specific level of statistically valid results may be determined using Practice E 122. However, it may not be economically possible to achieve a specific confidence levels and professional judgment may be required too.

A.9. Test Specimens

A.9.1 Preparation —Prepare test specimens from the drill core samples in accordance with Practice D 4543 and sections 8.3 and 9.2.

A.9.2 Moisture condition of the specimen at the time of test can have a significant effect upon the deformation of the rock. Good practice generally dictates that laboratory tests be made upon specimens representative of field conditions. Thus, it follows that the field moisture condition of the specimen should be preserved until the time of test. On the other hand, there may be reasons for testing specimens at other moisture contents, including zero. In any case, the moisture content of the test specimen should be tailored to the problem at hand and reported in accordance with 12.1.3. If the moisture content of the specimen is to be determined, follow the procedures given in Test Method D 2216.

A.9.3 If moisture content is to be maintained, and the elevated temperature enclosure is not equipped with humidity control, seal the specimen using a flexible membrane or apply a plastic or silicone rubber coating to the specimen sides.

A.10. Procedure

A.10.1 Check the ability of the spherical seat to rotate freely in its socket before each test.

A.10.2 Place the lower platen on the base or actuator rod of the loading device. Wipe clean the bearing faces of the upper and lower platens and of the test specimen, and place the test specimen on the lower platen. Place the upper platen on the specimen and align properly. A small axial load, approximately 100 N, may be applied to the specimen by means of the loading device to properly seat the bearing parts of the apparatus.

A.10.3 When appropriate, install elevated-temperature enclosure and deformation transducers for the apparatus and sensors used.

A.10.4 If testing at elevated temperature, raise the temperature at a rate not exceeding 2°C/min until the required temperature is reached (see Note 6). The test specimen shall be

considered to have reached temperature equilibrium when all deformation transducer outputs are stable for at least three readings taken at equal intervals over a period of no less than 30 min (3 min for tests performed at room temperature). Stability is defined as a constant reading showing only the effects of normal instrument and heater unit fluctuations. Record the initial deformation readings. Consider this to be the zero for the test.

Note: 6—It has been observed that for some rock types microcracking will occur for heating rates above 1°C/min. The operator is cautioned to select a heating rate such that microcracking is not significant.

A.10.5 Apply the axial load continuously and without shock to the required test load within 20 s. Thereafter, the test load shall be held constant for the remainder of the test for constant load testing or increased with specimen deformation for constant true stress testing.

A.10.6 Record the strain or deformation immediately after the required test load has been applied. Thereafter, record the strain or deformation at suitable time intervals. During the early rapid transient straining, readings shall be taken every few minutes to few hours until the deformation rate slows and becomes relatively constant. Readings shall be taken at least twice daily until the test is terminated. If the strain rate accelerates as failure is approached, increase the frequency of readings appropriately.

A.10.7 Record the load and specimen temperature either continuously or each time the strain or deformation is read.

A.11. Calculation

A.11.1 The axial strain, ε_a, and lateral strain, ε_l, may be obtained directly from strain-indicating equipment, or may be calculated from deformation readings, depending on the type of apparatus or instrumentation employed.

A.11.1.1 Calculate the axial strain, ε_a, as follows:

$$\varepsilon_a = \Delta L / L \qquad \text{(A.1)}$$

where:

L = original undeformed axial gage length, and
ΔL = change in measured axial length (negative for decrease in length).

Note: 7—Tensile stresses and strains are used as being positive herein. A consistent application of a compression-positive sign convention may be employed if desired. The sign convention adopted needs to be stated explicitly in the report. The formulas given are for engineering stresses and strains. True stresses and strains may be used if desired.

Note: 8—If the deformation recorded during the test includes deformation of the apparatus, suitable calibration for apparatus deformation must be made. This may be accomplished by inserting into the apparatus a steel cylinder having known elastic properties and observing differences in deformation between the assembly and steel cylinder throughout the loading range. The apparatus deformation is then subtracted from the total deformation at each increment of load to arrive at specimen deformation from which the axial strain of the specimen is computed. The accuracy of this correction should be verified by measuring the elastic deformation of a cylinder of material having known elastic properties (other than steel) and comparing the measured and computed deformations.

A.11.1.2 Calculate the lateral strain, ε_l, as follows

$$\varepsilon_l = \Delta D / D \qquad \text{(A.2)}$$

where:

D = original undeformed diameter, and
ΔD = change in diameter (positive for increase in diameter).

Note: 9—Many circumferential transducers measure change in chord length and not change in arc length (circumference). The geometrically nonlinear relationship between change in chord length and change in diameter must be used to obtain accurate values of lateral strain.

A.11.2 Calculate the compressive stress in the test specimen from the compressive loadon the specimen and the initial computed cross-sectional area as follows:

$$\sigma = P/ A \qquad (A.3)$$

where:

σ = stress

P = load, and

A = area

A.11.3 Plot the strain-versus-time curves for the axial and lateral directions (Figure A.1).

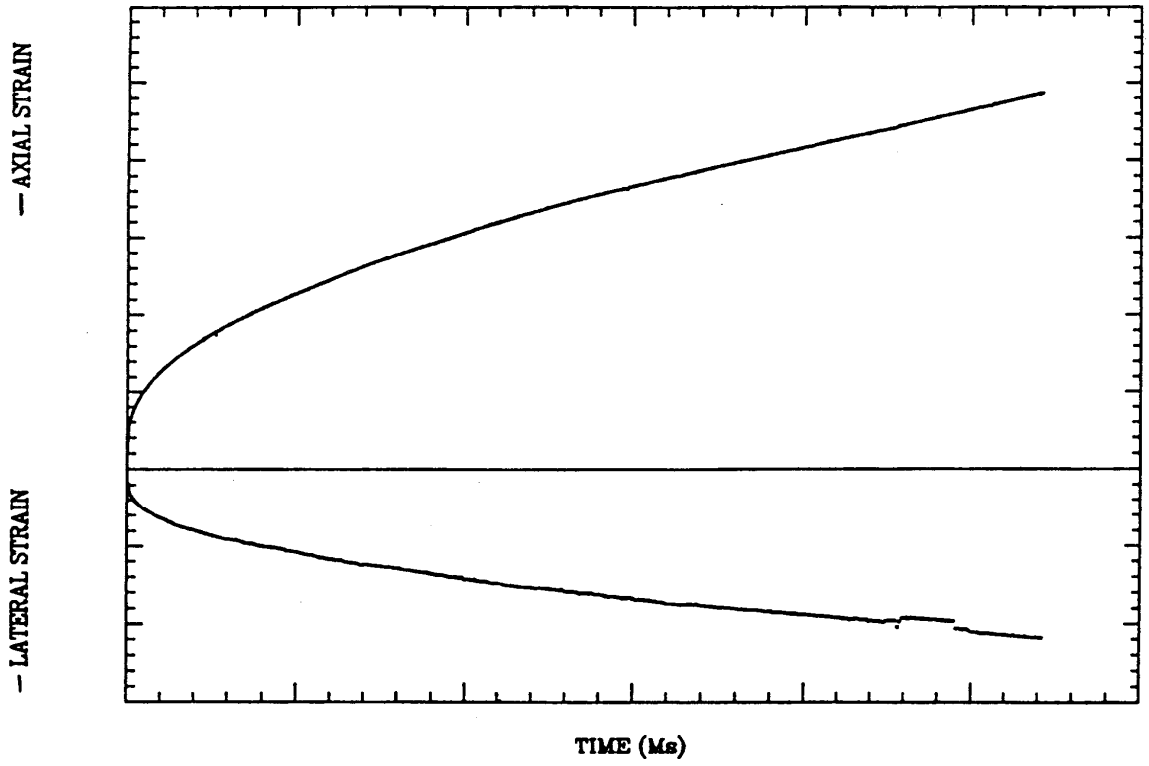

Figure A.1. Typical Strain-Versus-Time Curves

A.12. Report

A.12.1 Report the following :

A.12.1.1 Source of sample, including project name and location (the location is specified in terms of the drill hole number and depth of specimen from the collar of the hole),

A.12.1.2 Lithologic description of the rock, formation name, and load direction with respect to lithology,

A.12.1.3 Moisture condition of specimen before test,

A.12.1.4 Specimen diameter and height, conformance with dimensional requirements,

A.12.1.5 Stress level at which test was performed. Indicate whether engineering or true stress was held constant,

A.12.1.6 Temperature at which test was performed,

A.12.1.7 Plot of the strain versus time curve (Figure A.1),

A.12.1.8 Tabulation of selected strain and time data,

A.12.1.9 A description of physical appearance of specimen after test, including visible end effects such as cracking, spalling, or shearing at the platen-specimen interfaces, and

A.12.1.10 If the actual equipment or procedure has varied from the requirements contained in this test method, each variation and the reasons for it shall be discussed.

A.13. Precision and Bias

A.13.1 Precision —Due to the nature of rock materials tested by this test method, it is either not feasible or too costly at this time to produce multiple specimens that have uniform mechanical properties. Any variation observed in the data is just as likely to result from specimen variation as from operator or laboratory testing variation. Subcommittee D18.12 welcomes proposals that would allow for development of a valid precision statement.

A.13.2 Bias —Bias cannot be determined since there is no standard creep deformation that can be used to compare with values determined using this test method.

A.14. Keywords

14.1 compression testing; creep; deformation; loading tests; rock

Summary of Changes

In accordance with Committee D18 policy, this section identifies the location of the changes to this standard since the last edition 1998 that may impact the use of this standard.

(1) Revised title of standard to include elevated temperature deleted “cylindrical”, and made “compressions” singular.
(2) Inserted missing caveat in Section 1 on significant figures.
(3) Corrected section 1.3 from inch-pound to SI units.
(4) Inserted missing and new references to standards D 653, D 2113, D 3740, D 5079, and D 6026, and E 122 under item 2.
(5) Section 4.1 Changed “sample” to “specimen.”
(6) Inserted Item 4 Terminology and renumbered all subsequent items.
(7) Inserted Note 1 D 3740 caveat and renumbered all subsequent Notes.
(8) Section 7.1, added safey precaution for burns.
(9) Changed section 8.1 to 8.3 and changed emphasis from specimen to test sample.
(10) Section 8.1 and 8.2 to include the importance of collection and curatorial care of the samples from the point of origin to the laboratory.
(11) Added section 8.4 to reference E 122 and to the number of specimens required.
(12) Section 9.1 added that the specimens are prepared from the drill core sample and to be prepared in accordance with the requirements in sections 8.3 and 9.2 which covers the moisture content of test specimens.
(13) Inserted Summary of Changes section.

APPENDIX B: D4406 – 04 STANDARD TEST METHOD FOR CREEP OF ROCK CORE SPECIMENS IN TRIAXIAL COMPRESSION AT AMBIENT OR ELEVATED TEMPERATURE

B.1. Scope

B.1.1 This test method covers the creep behavior of intact cylindrical soft rock core specimens in uniaxial compression. It specifies the apparatus, instrumentation, and procedures for determining the strain as a function of time under sustained load.

B.1.2 All observed and calculated values shall conform to the guidelines for significant digits and rounding established in Practice D 6026.

B.1.2.1 The method used to specify how data are collected, calculated, or recorded in this standard is not directly related to the accuracy to which the data can be applied in design or other uses, or both. How one applies the results obtained using this standard is beyond its scope.

B.1.3 The values stated SI units are to be regarded as the standard.

B.1.4 This standard does not purport to address all of the safety concerns, if any, associated with its use. It is the responsibility of the user of this standard to establish appropriate safety and health practices and determine the applicability of regulatory limitations prior to use. For specific precautionary statements, see Section 7.

B.2. Referenced Documents

B.2.1 ASTM Standards:

D 653 Terminology Relating to Soil, Rock, and Contained Fluids
D 2113 Practice for Diamond Core Drilling for Site Investigation

D 2216 Test Method for Laboratory Determination of Water (Moisture) Content of Soil and Rock
D 3740 Practice for Minimum Requirements for Agencies Engaged in the Testing and/or Inspection of Soil and Rock as Used in Engineering Design and Construction
D 4341 Test Method for Creep of Cylindrical Hard Rock Core Specimens in Uniaxial Compression
D 4543 Practice for Preparing Rock Core Specimens and Determining Dimensional and Shape Tolerances
D 5079 Practices for Preserving and Transporting Rock Core Samples
D 6026 Practice for Using Significant Digits in Geotechnical Data
E 4 Practices for Load Verification of Testing Machines
E 122 Practice for Choice of Sample Size to Estimate a Measure of Quality for a Lot or Process

B.3. Terminology

B.3.1 Refer to Terminology D 653 for specific definitions.

B.4. Summary of Test Method

B.4.1 A section of rock core is cut to length and the ends are machined at to produce a cylindrical test specimen. The specimen is placed in a triaxial loading chamber, subjected to confining pressure, and, if required, heated to the desired test temperature. Axial load is rapidly applied to the specimen and sustained. Deformation is monitored as a function of elapsed time. Specimen deformation is monitored periodically.

B.5. Significance and Use

B.5.1 There are many underground structures that are created for permanent or long-term use. Often these structures are subjected to an approximately constant load. Creep tests provide quantitative parameters for the stability analysis of these structures.

B.5.2 The deformation and strength properties of rock cores measured in the laboratory

usually do not accurately reflect large-scale in situ properties, because the latter are strongly influenced by joints, faults, inhomogeneities, weakness planes, and other factors. Therefore, laboratory values for intact specimens must be employed with proper judgment in engineering applications.

NOTE 1—Notwithstanding the statements on precision and bias contained in this test method; the precision of this test method is dependent on the competence of the personnel performing it, and the suitability of the equipment and facilities used. Agencies that meet the criteria of Practice D 3740 are generally considered capable of competent and objective testing. Users of this test method are cautioned that compliance with Practice D 3740 does not in itself assure reliable testing. Reliable testing depends on many factors; Practice D 3740 provides a means of evaluating some of these factors.

B.6. Apparatus

B.6.1 Loading Device —The loading device shall be of sufficient capacity to apply load at a rate conforming to the requirements specified in 10.5 and shall be able to maintain the specified load within 2 %. It shall be verified at suitable time intervals in accordance with the procedures given in Practices E 4 and comply with the requirements prescribed in this test method.

NOTE 2—By definition, creep is the time-dependent deformation under constant stress. The loading device is specified to maintain constant axial load, and therefore, constant engineering stress. The true stress, however, decreases as the specimen deforms and the cross-sectional area increases. Because of the associated experimental ease, constant load testing is recommended. However, the procedure permits constant true-stress testing, provided that the applied load is increased with specimen deformation so that true stress is constant within 2 %.

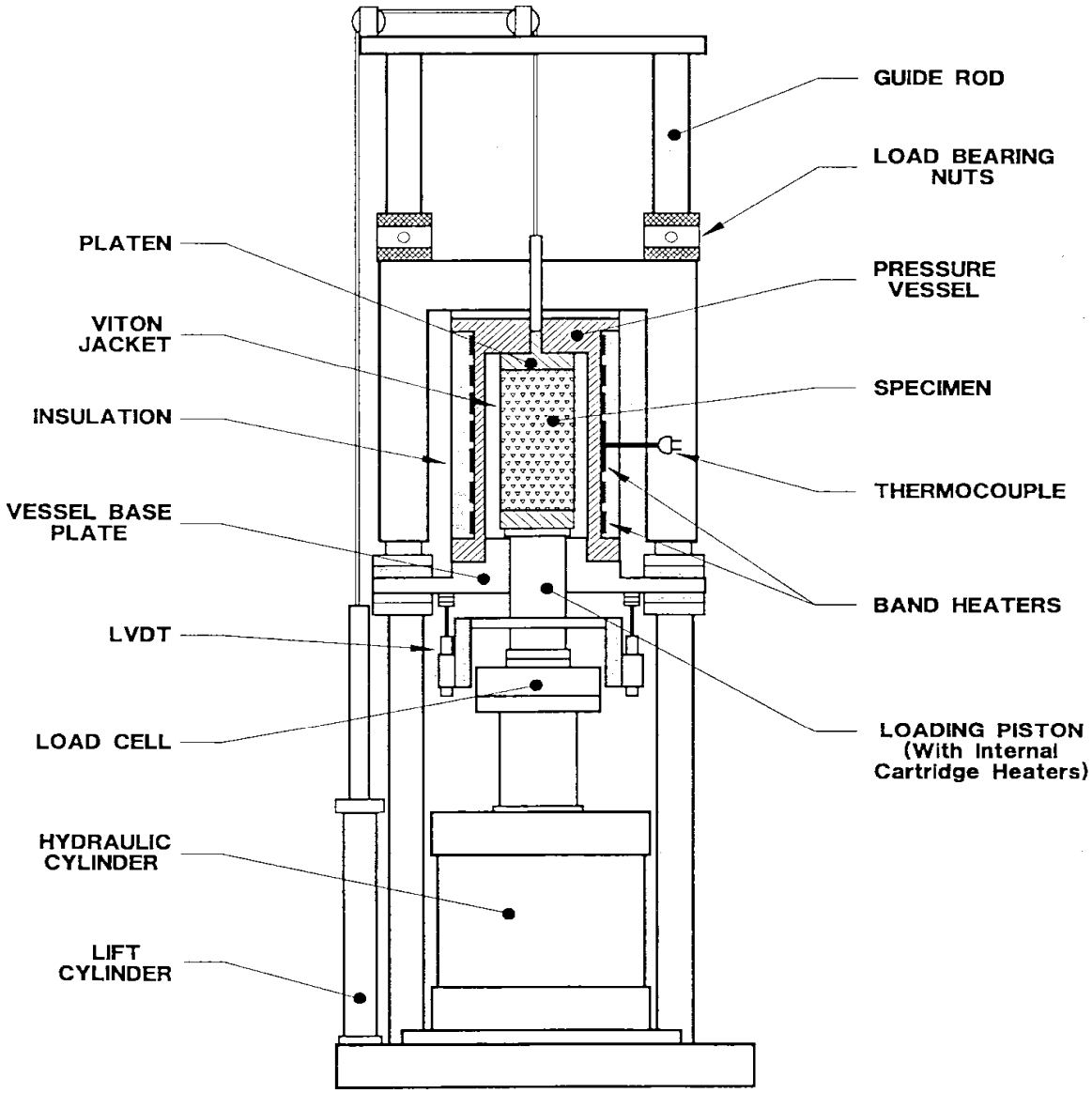

Figure B.1. Test Apparatus

B.6.2 Triaxial Apparatus —The triaxial apparatus shall consist of a chamber in which the test specimen may be subjected to a constant lateral fluid pressure and the required axial load. The apparatus shall have safety valves, suitable entry ports for filling the chamber, and associated hoses, gages, and valves as needed. Figure B.1 shows a typical test apparatus and associated equipment.

B.6.3 Flexible Membrane—This membrane encloses the rock specimen and extends over the platens to prevent penetration by the confining fluid. Asleeve of natural or synthetic rubber or plastic is satisfactory for room temperature tests; however, metal or high-

temperature rubber jackets are usually required for elevated temperature tests. The membrane shall be inert relative to the confining fluid and shall cover small pores in the sample without rupturing when confining pressure is applied. Plastic or silicone rubber coatings may be applied directly to the sample, provided these materials do not penetrate and strengthen the specimen. Care must be taken to form an effective seal where the platen and specimen meet. Membranes formed by coatings shall be subject to the same performance requirements as elastic sleeve membranes.

B.6.4 Pressure-Maintaining Device —A hydraulic pump, pres sure intensifier, or other system of sufficient capacity to maintain constant the desired lateral pressure. The pressurization system shall be capable of maintaining the confining pressure constant to within ±1 % throughout the test. The confining pressure shall be measured with a hydraulic pressure gage or electronic transducer having an accuracy of at least ±1 % of the confining pressure, including errors due to readout equipment, and a resolution of at least 0.5 % of the confining pressure.

B.6.5 Confining-Pressure Fluids—For room temperature tests, hydraulic fluids compatible with the pressure-maintaining device should be used. For elevated temperature tests the fluid must remain stable at the temperature and pressure levels designated for the test.

B.6.6 Elevated-Temperature Enclosure —The elevated temperature enclosure may be either an enclosure that fits in the loading apparatus or an external system encompassing the complete test apparatus. The enclosure may be equipped with humidity control for testing specimens in which the moisture content is to be controlled. For high temperatures a system of heaters, insulation, and temperature measuring devices are normally required to maintain the specified temperature. Temperature shall be measured at three locations, with one sensor near the top, one at midheight, and one near the bottom of the specimen. The average specimen temperature based on the midheight sensor shall be maintained to within ±1°C of the required test temperature. The maximum temperature difference between the midheight sensor and either end sensor shall not exceed 3°C.

NOTE 3—An alternative to measuring the temperature at three locations along the specimen during the test is to determine the temperature distribution in a dummy specimen

that has temperature sensors located in drill holes at a minimum of six positions: along both the centerline and specimen periphery at midheight and each end of the specimen. The temperature controller set point shall be adjusted to obtain steady-state temperatures in the dummy specimen that meet the temperature requirements at each test temperature (the centerline temperature at midheight shall be within ±1°C of the required test temperature, and all other specimen temperatures shall not deviate from this temperature by more than 3°C). The relationship between controller set point and dummy specimen temperature can be used to determine the specimen temperature during testing, provided that the output of the temperature feedback sensor (or other fixed-location temperature sensor in the triaxial apparatus) is maintained constant within ±1°C of the required test temperature. The relationship between temperature controller set point and steady-state specimen temperature shall be verified periodically. The dummy specimen is used solely to determine the temperature distribution in a specimen in the triaxial apparatus; it is not to be used to determine creep behaviour.

B.6.7 Temperature Measuring Device—Special limits-of-error thermocouples or platinum resistance thermometers (RTDs) having accuracies of at least ±1.0°C with a resolution of 0.1°C.

B.6.8 Platens—Two steel platens are used to transmit the axial load to the ends of the specimen. They shall have a hardness of not less than 58 HRC. One of the platens should be spherically seated and the other a plain rigid platen. The bearing faces shall not depart from a plane by more than 0.015 mm when the platens are new and shall be maintained within a permissible variation of 0.025 mm. The diameter of the spherical seat shall be at least as large as that of the test specimen but shall not exceed twice the diameter of the test specimen. The center of the sphere in the spherical seat shall coincide with that of the bearing face of the specimen. The spherical seat shall be properly lubricated to assure free movement. The movable portion of the platen shall be held closely in the spherical seat, but the design shall be such that the bearing face can be rotated and tilted through small angles in any direction. If a spherical seat is not used, the bearing faces of the platens shall be parallel to 0.0005 mm/mm of platen diameter.

B.6.8.1 Hard Rock Specimens —The platen diameter shall be at least as great as the

specimen but shall not exceed the specimen diameter by more than 1.50 mm. This platen diameter shall be retained for a length of at least one-half the specimen diameter.

B.6.8.2 Soft Rock Specimens —The platen diameter shall be at least as great as the specimen but shall not exceed the specimen diameter by more than 10 % of the specimen diameter. Because soft rocks can deform significantly in creep tests, it is important to reduce friction in the platen-specimen interfaces to facilitate relative slip between the specimen ends and the platens. Effective friction-reducing precautions include polishing the platen surfaces to a mirror finish and attaching a thin, 0.15- mm-thick teflon sheet to the platen surfaces.

B.6.9 Strain/Deformation Measuring Devices—The strain/ deformation measuring system shall measure the strain with a resolution of at least 25 X 10^{-6} strain and an accuracy within 2 % of the value of readings above 25 X 10^{-6} strain and an accuracy and resolution within 5 X 10^{-6} for readings lower than 250 X 10^{-6} strain, including errors introduced by excitation and readout equipment. The system shall be free from noncharacterizable long-term instability (drift) that results in an apparent strain of 10^{-8} per second.

NOTE 4—The user is cautioned about the in uence of pressure and temperature on the output of strain and deformation sensors located within the triaxial environment.

B.6.9.1 Axial Strain Determination —The axial deformations or strains may be determined from data obtained by electrical resistance strain gages, compressometers, linear variable differential transformers (LVDTs), or other suitable means. The design of the measuring device shall be such that the average of at least two axial strain measurements can be determined. Measuring positions shall be equally spaced around the circumference of the specimen close to midheight. The gage length over which the axial strains are determined shall be at least ten grain diameters in magnitude

B.6.9.2 Lateral Strain Determination —The lateral deformations or strains may be measured by any of the methods mentioned in 6.9.1. Either circumferential or diametrical deformations (or strains) may be measured. A single transducer that wraps around the specimen can be used to measure the change in circumference. At least two diametric

deformation sensors shall be used if diametric deformations are measured These sensors shall be equally spaced around the circumference of the specimen close to midheight. The average deformation (or strain) from the diametric sensors shall be recorded.

NOTE 5—The use of strain gage adhesives requiring cure temperatures above 65°C is not allowed unless it is known that microfractures do not develop at the cure temperature.

B.7. Safety Hazards

B.7.1 Danger exists near triaxial testing equipment because of the high pressures and loads developed within the system. Elevated temperatures increase the risks of electrical shorts, burns, and fire. The flash point of the confining pressure fluid should be above the operating temperatures during the test.

B.7.2 Test systems must be designed and constructed with adequate safety factors, assembled with properly rated fittings and provided with protective shields to protect people in the area from unexpected system failure.

B.7.3 The use of a gas as the confining pressure fluid introduces potential for extreme violence in the event of a system failure.

B.8. Sampling

B.8.1 Samples can be either drill cores obtain directly from the in situ rock or obtained from block samples cored in the field or in the laboratory.

B.8.2 Moisture condition can have a significant effect upon the deformation of the rock. Test samples must meet any requirements determined in section 9.2. Therefore, it follows that the field moisture condition of the samples may need protection during and after sampling. This may require special collection and handling techniques such as those outlined in Practices D 2113 and D 5079.

B.8.3 The location of the specimens for each test sample shall be selected from the cores to

represent a valid average of the type of rock under consideration. This can be achieved by visual observations of mineral constituents, grain sizes and shape, partings and defects such as pores and fissures, or by other methods such as ultrasonic velocity measurements.

B.8.4 The number of specimens required to obtain a specific level of statistically results may be determined using Practice E 122. However, it may not be economically possible to achieve a specific confidence levels and professional judgment may be required too.

B.9. Test Specimens

B.9.1 Preparation —Prepare test specimens from the drill core samples in accordance with Practice D 4543 and sections 8.3 and 9.2.

B.9.2 Moisture condition of the specimen at the time of test can have a significant effect upon the deformation of the rock. Good practice generally dictates that laboratory tests be made upon specimens representative of field conditions. Thus, it follows that the field moisture condition of the specimen should be preserved until the time of test. On the other hand, there may be reasons for testing specimens at other moisture contents, including zero. In any case, the moisture content of the test specimen should be tailored to the problem at hand and reported in accordance with 12.1.3. If the moisture content of the specimen is to be determined, follow the procedures given in Test Method D 2216.

B.10. Procedure

B.10.1 Check the ability of the spherical seat to rotate freely in its socket before each test.

B.10.2 Place the lower platen on the base or actuator rod of the loading device. Wipe clean the bearing faces of the upper and lower platens and of the test specimen, and place the test specimen on the lower platen. Place the upper platen on the specimen and align properly. Fit the membrane over the specimen and platens to seal the specimen from the confining fluid. Place the specimen in the test chamber, ensuring proper seal with the base and connect the confining pressure lines. A small axial load, approximately 100 N, may be applied to the triaxial compression chamber by means of the loading device in order to

properly seat the bearing parts of the apparatus.

B.10.3 When appropriate, install elevated-temperature enclosure and deformation transducers for the apparatus and sensors used.

B.10.4 Put the confining fluid in the chamber and raise the confining stress uniformly to the specified level within 5 min. Do not allow the lateral and axial components of the confining stress to differ by more than 5 % of the instantaneous pressure at any time.

B.10.5 If testing at elevated temperature, raise the temperature at a rate not exceeding 2°C/min until the required temperature is reached (Note 6). The test specimen shall be considered to have reached pressure and thermal equilibrium when all deformation transducer outputs are stable for at least three readings taken at equal intervals over a period of no less than 30 min (3 min for tests performed at room temperature). Stability is defined as a constant reading showing only the effects of normal instrument and heater unit fluctuations. Record the initial deformation readings. Consider this to be the zero for the test.

NOTE: 6—It has been observed that for some rock types microcracking will occur for heating rates above 1°C/min. The operator is cautioned to select a heating rate such that microcracking is not significant.

B.10.6 Apply the axial load continuously and without shock to the required test load within 20s. Thereafter, the test load shall be held constant for the remainder of the test for constant load testing or increased with specimen deformation for constant true stress testing.

B.10.7 Record the strain or deformation immediately after the required test load has been applied. Thereafter, record the strain or deformation at suitable time intervals. During the transient straining, readings shall be taken every few minutes to few hours until the deformation rate slows and becomes relatively constant. Readings shall be taken at least twice daily until the test is terminated. If the strain rate accelerates as failure is approached, increase the frequency of readings appropriately.

B.10.8 Record the load and specimen temperature either continuously or each time the strain or deformation is read.

B.10.9 To make sure that no testing fluid has penetrated into the specimen, the specimen membrane shall be carefully checked for fissures or punctures at the completion of each triaxial test.

B.11. Calculation

B.11.1 The axial strain, ε_a, and lateral strain, ε_l, may be obtained directly from strain-indicating equipment, or may be calculated from deformation readings, depending on the type of apparatus or instrumentation employed.

B.11.1.1 Calculate the axial strain, ε_a, as follows:

$$\varepsilon_a = \Delta L / L \qquad \text{(B.1)}$$

where:

L = original undeformed axial gage length, and
ΔL = change in measured axial length (negative for decrease in length).

NOTE: 7—Tensile stresses and strains are used as being positive herein. A consistent application of a compression-positive sign convention may be employed if desired. The sign convention adopted needs to be stated explicitly in the report. The formulas given are for engineering stresses and strains. True stresses and strains may be used if desired.

NOTE: 8—If the deformation recorded during the test includes deformation of the apparatus, suitable calibration for apparatus deformation must be made. This may be accomplished by inserting into the apparatus a steel cylinder having known elastic properties and observing differences in deformation between the assembly and steel cylinder throughout the loading range. The apparatus deformation is then subtracted from the total deformation at each increment of load to arrive at specimen deformation from

which the axial strain of the specimen is computed. The accuracy of this correction should be verified by measuring the elastic deformation of a cylinder of material having known elastic properties (other than steel) and comparing the measured and computed deformations.

B.11.1.2 Calculate the lateral strain, ε_l, as follows

$$\varepsilon_l = \Delta D / D \qquad \text{(B.2)}$$

where:

D = original undeformed diameter, and
ΔD = change in diameter (positive for increase in diameter).

NOTE: 9—Many circumferential transducers measure change in chord length and not change in arc length (circumference). The geometrically nonlinear relationship between change in chord length and change in diameter must be used to obtain accurate values of lateral strain.

B.11.2 Calculate the compressive stress in the test specimen from the compressive load on the specimen and the initial computed cross-sectional area as follows:

$$\sigma = P / A \qquad \text{(B.3)}$$

where:
σ = stress
P = load, and
A = area

NOTE 10—If the specimen diameter is not the same as the piston diameter through the triaxial apparatus, a correction must be applied to the measured load to account for the confining pressure acting on the difference in area between the specimen and the loading piston where it passes through the seals into the triaxial apparatus.

B.11.3 Plot the strain-versus-time curves for the axial and lateral directions (Figure B.2).

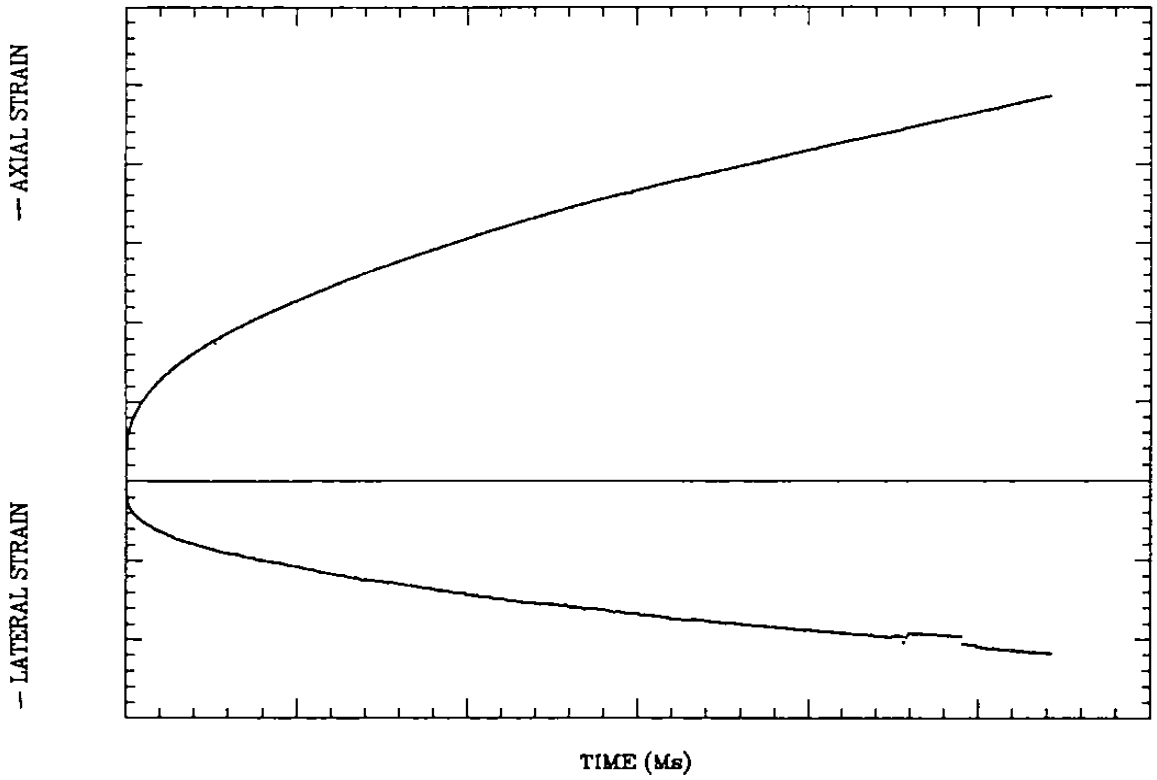

Figure B.2. Typical Strain-Versus-Time Curves

B.12. Report

B.12.1 Report the following information :

B.12.1.1 Source of sample, including project name and location (often the location is specified in terms of the drill hole number and depth of specimen from the collar of the hole),

B.12.1.2 Lithologic description of the rock, formation name, and load direction with respect to lithology,

B.12.1.3 Moisture condition of specimen before test,

B.12.1.4 Specimen diameter and height, conformance with dimensional requirements,

B.12.1.5 Confining stress level at which test was performed

B.12.1.6 Temperature at which test was performed,

B.12.1.7 Stress level at which test was performed. Indicate whether engineering or true stress was held constant,

B.12.1.8 Plot of the strain versus time curve (Figure B.2),

B.12.1.9 Tabulation of selected strain and time data,

B.12.1.10 A description of physical appearance of specimen after test, including visible end effects such as cracking, spalling, or shearing at the platen-specimen interfaces, and

B.12.1.11 If the actual equipment or procedure has varied from the requirements contained in this test method, each variation and the reasons for it shall be discussed.

B.13. Precision and Bias

B.13.1 Precision —Due to the nature of rock materials tested by this test method, it is either not feasible or too costly at this time to produce multiple specimens that have uniform mechanical properties. Any variation observed in the data is just as likely to result from specimen variation as from operator or laboratory testing variation. Subcommittee D18.12 welcomes proposals that would allow for development of a valid precision statement.

B.13.2 Bias —Bias cannot be determined since there is no standard creep deformation that can be used to compare with values determined using this test method.

B.14. Keywords

B.14.1 compression testing; creep; deformation; loading tests; rock

Summary of Changes

In accordance with Committee D18 policy, this section identifies the location of the changes to this standard since the last edition 1998 that may impact the use of this standard.

(1) Revised title of standard to include elevated temperature and took out cylindrical.
(2) Inserted missing caveat in Section 1 on significant figures.
(3) Added missing statement in Section 1 regarding the type of numeric units.
(4) Inserted missing referenced standards D 653, D 3740, and D 6026 under item 2.
(5) Section 3.1 Changed “sample” to “specimen.”
(6) Inserted Item 4 Terminology and renumbered all subsequent items.
(7) Inserted Note 2 D 3740 caveat and renumbered all subsequent Notes.
(8) Section 7.1, added safety precaution for burns.
(9) Changed first sentence in Section 8, Sampling, to differentiate between specimen and sample.
(10) Added section 8.1 and 8.2 to include the importance of collection and curatorial care of the samples from the point of origin to the laboratory.
(11) Added section 8.4 to reference E 122 and to the number of specimens required.
(12) Section 9.1 added that the specimens are prepared from the drill core sample and to be prepared in accordance with the requirements in sections 8.3 and 9.2 which covers the moisture content of test specimens.
(13) Inserted Summary of Changes section.

REFERENCES

Abdel-Hady, M. and M. Herrin, 1966, "Characteristics of Soil-Asphalt as a Rate Process", *Journal of the Highway Division, ASCE.*

Bishop, A. W., 1966, "The Strength of Soils as Engineering Materials", *Sixth Rankine Lecture, Geotechnique*, Vol. 16, No. 2, pp. 112–126.

Bromhead, E. N., 1992, "The Stability of Slopes", *Blackie Academic and Proffessional*, Boston.

Christensen, R. W. and T. H. Wu, 1964, "Analysis of Clay Deformation as a Rate Process", *Journal of Soil Mechanics and Foundation Eng. Division, ASCE*, Proceedings Paper 4147, pp. 125–157.

Çevikbilen, G., 1999, *Yumuşak Kil Zeminlerin İkincil Konsolidasyonu*, M.S. Thesis, İstanbul Technical University, İstanbul.

Çevikbilen, G. and A. Sağlamer, 2008, *Samsun – Çarşamba Mavi Kilinin Sıkışma Davranışına Örselenmenin Etkisi*, İ.T.Ü. Müh. Dergisi, Vol. 7, No. 5, pp. 79-88.

De Wit, C. T. and P. L. Arens, 1991, "Moisture Content and Density of Home Clay Minerals and Some Remarks on the Hydration Patterns of Clay", *Trans. 4th International Congress of Soil Sci.*, Vol. 2, pp. 59-62.

Eroskay, S. O., 1985, "Greywackes of İstanbul Region", *Proceedings of International Symposium on Design of Supports to Deep Excavations*, pp. 41-44, İstanbul.

Forslind, E., 1948, "The Crystal Structure and Water Absorption of the Clay Minerals", *Trans. 1st International Ceramic Congress*, pp. 98–110.

Glasstone, S., K. Laidler and H. Eyring, 1941, "The Theory of Rate of Process", *McGraw-Hill*.

Hendricks, S. B. and M. E. Jefferson, 1938, "Structure of Kaolin and Talc-Pyrophylite Hydrates and Their Bearing on Water Sorption of Clays", *American Mineralogy*, Vol. 23, pp. 135-145.

Horn, D. L., Y. O. Chang and C. W. Chien, 2002, "Time Dependent Displacement of Diaphgram Wall Induced by Soil Creep", *Journal of the Chinese Institute of Engineers*, Vol. 25, No. 2, pp. 223-231.

Keskin, H. B., 2008, *Analysis of the Performance of Retaining Systems in Deep Excavations in Greywackes*, Ph. D. Thesis, Boğaziçi University, İstanbul.

Kırım, G., 2006, *Investigation of Shear Strength of Prefailed Overconsolidated High and Low Plastic Clayey Slopes with Fast Shearing*, M.S. Thesis, Boğaziçi University, İstanbul.

Macey, H. H., 1941, "Clay-Water Relationships and Internal Mechanism of Drying", *Trans. Ceramic. Soc.*, Vol. 41, pp. 73-121.

Mitchell, J. K., 1964, "Shearing Resistance of Soils as a Rate Process", *Journal of Soil Mechanics and Foundation Eng. Division, ASCE*, Vol. 90, No. SMI, Proceedings Paper 3773, pp. 29–61.

Mitchell, J. K. and R. G. Campanella, 1964, "Creep Studies on Saturated Clays", Symposium on Laboratory Shear Testing of Soils, ASTM-NRC, Ottawa, Canada, *ASTM Special Tech. Publication*, No. 361, Sept. 1963.

Mitchell, J. K. and R. G. Campanella, 1967, "Temperature Effects on Volume Changes and Pore Pressures in Soils".

Mitchell, J. K., A. Singh and R. G. Campanella, 1967, "Bonding Effective Stress and Strength of Soils as Revealed by Creep Behaviour".

Mitchell, J. K., 1993, "Fundementals of Soil Behaviour", *Second Edition,* pp. 383–392.

Murayama, S. and T. Shibata, 1958, "On the Rheological Characteristic of Clay", Part 1, Bulletin No.26, *Disaster Prevention Research Institute*, Kyoto University.

Murayama, S. and T. Shibata, 1961, "Rheological Properties of Clays" *Proceedings – 5th International Congress Soil Mech. and Foundation Eng.*, pp. 269–273.

Murayama, S. and Shibata, T., 1966, "Flow and Stress Relaxation of Clays (Theoretical Studies on the Rheological Properties of Clay – Part 1)", *Rheology and Soil Mech. Symposium of the Int. Union of Rheoretical and Applied Mechanics, in Grenoble*

Nanda, S., M. L. Sadana and C. Pradhan, 2005, "Creep Behaviour of Varanasi Soil with Chemical", *International Geotech. Congress 2005*, pp. 161-164, Ahmedabad, India.

Özüer, A. B., 1975, *Çatlaklı Grovak ve Killi Şistlerin Mühendislik Özellikleri*, Ph. D. Thesis, İstanbul Technical University, İstanbul.

Ralph E. G., 1953, "Clay Mineralogy", *McGraw-Hill Book Co*, pp. 1-5, 161-168.

Singh, A. and J. K. Mitchell, 1967, "A General Stress-Strain Time Function for Soils".

Tietz, T. and J. Dorn, 1956, "Creep of Copper at Intermediate Temperatures", Transactions, *American Institute of Mech. Eng.,* Vol. 206, pp. 156.

Tuğrul, A. and Ö. Ündül, 2006, "Engineering Geological Characteristics of İstanbul Greywackes, Turkey", *Proceedings of the Tenth IAEG Congress*, Paper No. 395, Nottingham.

Yılmaz, E., 2000, *Samsun – Çarşamba Mavi Kilinin İkincil ve Üçüncül Sıkışma Davranışı*, Ph. D. Thesis, İstanbul Technical University, İstanbul.